68-66

Copy 1

WOODS HOLE OCEANOGRAPHIC INSTITUTION

REFERENCE NO. 68-66

A REPORT ON ATLANTIS II CRUISE 22
JUNE, JULY, AND AUGUST 1966

PART I - THE DYNAMICS OF OCEAN MOVEMENTS IN THE
SARGASSO SEA REVEALED BY SOUND
VELOCITY AND TEMPERATURE
MEASUREMENTS

John C. Beckerle

This document has been approved for public release and sale; its distribution is unlimited.

WOODS HOLE, MASSACHUSETTS

WOODS HOLE OCEANOGRAPHIC INSTITUTION
Woods Hole, Massachusetts

REFERENCE NO. 68-66

A REPORT ON ATLANTIS II CRUISE 22
JUNE, JULY, AND AUGUST 1966

PART I - The Dynamics of Ocean Movements in the
Sargasso Sea Revealed by Sound Velocity
and Temperature Measurements
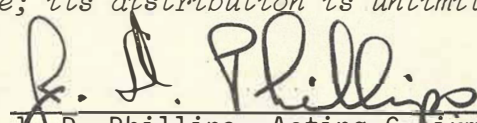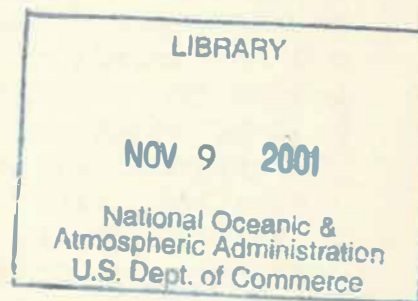
by

John C. Beckerle

October 1970

TECHNICAL REPORT

Approved for Distribution _____
J. D. Phillips, Acting Chairman
Department of Geology & Geophysics

ABSTRACT

On Cruise #22 of R/V ATLANTIS II from June 10 to August 4, 1966, 115 sound velocity profiles WHOI SVP #371 - SVP #485, were measured with a sound velocity profiling system that incorporated an on-line PDP-5 computer. The cruise covered approximately 356,000 square miles of water between Bermuda and the Antilles. The main purpose of the cruise was to look for long-period internal Rossby waves expected from earlier cruises, ATLANTIS II #11 and CHAIN #47, and to improve our techniques in gathering oceanographic data. Part I of this report presents the observations of ATLANTIS II Cruise #22 with possible interpretations. On the way to the Sargasso Sea ATLANTIS II traversed the eye of hurricane ALMA and we obtained new information on the air-sea interaction. In the Sargasso Sea the temperature data and the sound velocity data suggest that the circulation is complicated with eddies of large size. Part II is separately bound and consists of figures of the sound velocity profiles with comments concerning their reliability where necessary.

TABLE OF CONTENTS

REPORT ON ATLANTIS II CRUISE #22

Table of Contents   iii

                                                                    Page

LIST OF FIGURES

LIST OF FIGURES
SECTION III - SOUND VELOCITY MEASUREMENTS (Continued)

SECTION I - INTRODUCTION

In any effort to understand the fluctuation of sound
signals propagating through the ocean, it is necessary to
learn about the spatial and temporal variability of the
transmission medium. The design of meaningful acoustical
experiments depends on such information, and for this reason,
several cruises have been undertaken to measure the sound
speed in the Sargasso Sea area. ATLANTIS II Cruise #22 was
the fourth of these studies. Earlier W.H.O.I. cruises to this
area were made by ATLANTIS in July 1962, by ATLANTIS II in
July 1964 (Cruise #11) and by CHAIN (Cruise #47) in April
1965.

ATLANTIS II Cruise #22 left Woods Hole on June 10 and
ended in Bermuda on August 4, 1966 with port stops in Bermuda
and Puerto Rico. An overall track chart of this expedition
is shown in Figure I-1, while Figure I-2 shows in more detail
the long line of sound velocity profile locations southwest
of Bermuda.

The objectives of ATLANTIS II Cruise #22 were technical
as well as scientific. On the scientific side, the cruise
was designed to determine the existence of large-scale hori-
zontal variations in the sound velocity which are believed
to reveal the existence of internal Rossby waves in the
ocean. The sound velocity observations of the earlier cruises
had uncovered a horizontal wave pattern having a scale of
about 240 nautical miles. Therefore this region was
of special interest to be studied using a towed instrument
as well as by taking sound velocity profile stations. A
test experiment was also planned to measure the presence
of internal ocean waves in the seasonal and main thermo-
cline by repeatedly lowering and raising the sound velocity
profiling equipment. This experiment was carried out close
to Bermuda to allow for radar fixes on Argus Island.

On the technical side of the cruise, we planned to demonstrate the feasibility of obtaining sound velocity profiles using an on-line computer with the W.H.O.I. sound velocity profiling system.* This system measures the sound speed each second as the instrument is lowered and raised through the water, and also the travel time of a sound pulse transmitted from the instrument to the sea surface and back. The depth of the instrument is calculated as an integral of the sound speed over the acoustic travel time by the on-line computer (PDP-5). A plot of the profile is then presented in real time (M. Press et al, 1966).

Emphasis was given to the on-line computer system during the cruise for two reasons. One, to provide an accurate analysis of sound velocity profiling data while the cruise was underway, and two, to allow for interpretation and presentation of the observations shortly following the cruise. Both of these objectives were met.

Although an on-line presentation of the measurements was available much of the time aboard the ship, the digital magnetic tape recordings were reprocessed on the computer at W.H.O.I. to insure correction of minor errors that had developed at sea with the system. This post-cruise analysis was particularly time consuming, but was a necessary delay to check out observations from a data collecting system that was undergoing design modifications. Shortly following the cruise a number of lectures were given presenting portions of the observations.**

----
*A cooperative developmental effort for the on-line system was undertaken by staff members of the Applied Research Laboratory of the Sylvania Electronic Products Corp. in Waltham, Massachusetts, at their own cost.

**USW Research and Development Planning Council Meeting, October 11-13, 1966 at Woods Hole, Massachusetts.

We believe that measurement of the sound speed in the ocean
and a study of sound propagation through the ocean will prove
to be very valuable for oceanographers. Only after a demonstra-
tion that the monitoring of sound signals permits a useful
description of the motions of the oceans continuously, will
the full impact of acoustical oceanography be appreciated.
Prior to such an effort, however, we present here the measure-
ments of sound speed and temperature obtained during ATLANTIS
II Cruise #22, 1966, that reveal the aspects of the dynamic
behavior of the Sargasso Sea. A serious effort is made to
avoid letting preconceived notions as to what should happen
influence the objective presentation.

This report is in the form of a total cruise analysis
and includes the major events during the work, but the analysis
is still far from complete. We have made an effort to let
the data presentation in Sections II, III, and IV reveal
ocean processes and to limit ourselves to tentative interpre-
tations until Section V, where a theoretical discussion gives
some justification for the interpretations used.

The highlights of ATLANTIS II Cruise #22 to the waters south
of Bermuda during the summer of 1966 are described in Part I
of this report. A number of contour charts both in the hori-
zontal and vertical dimensions are presented as different ways
of exhibiting the measurements. Part II of this report is
separately bound and contains plots of the sound velocity
profiles (W.H.O.I. Ref. No. 68-67, Beckerle, 1968b).

The cruise results are grouped according to the ocean
process being measured, the sea-hurricane interaction, the
sound velocity measurements, and the temperature measurements.
In Section II, measurements of sea and air temperature in
traversing the eye of hurricane ALMA are offered as unique
data pertinent to air-sea interaction research. The sea
temperature variations suggest an interpretation in terms
of regions of upwelling associated with unstable baroclinic waves.

In Section III, we present the sound velocity measurements.
First we describe the thermocline variations observed in a
300-mile long line of sound velocity profiles southwest of
Bermuda that were obtained in a few days. These data appear

to be related to temporal variations measured in one location
near Bermuda over a number of years (PANULIRUS data). Next a
short time series of internal waves in the depth interval of
60 to 260 meters are described. They were obtained during a
test using the technique of repeatedly raising and lowering
a sound velocity measuring system, the "Yo-Yo" technique.
Some features that can be seen in the data are interpreted
as resulting from the superposition of an upgoing and down-
going internal wave group. Changes in the period of some
small-amplitude oscillations appear to be the result of the
interference (or scattering interaction) of a larger trochoid-
like internal wave.

The major portion of the sound velocity data was collected
in the rhombic grid pattern seen in Figure I-1. In analyzing
these data various forms are presented, i.e., horizontal and
vertical contour charts, with interpretations. The horizontal
contours at several depths are interpreted as providing
information about average current flow directions. The
pattern of contours appears to indicate that large eddies
exist in the Sargasso Sea. Some have intensities that vary
in depth as well as location. There is evidence that near
the depths of 1800 and 4000 meters, horizontal variations
of sound speed are at a minimum, along some tracks. This
leads to speculations about the vertical distribution of
turbulence. The contour charts suggest that flows are toward
the west at 800 meters but toward the east at 200 meters,
in the region of the thermal front near 28°N. Considerable
discussion is given to temporal variations of the sound velo-
city measurements in order to establish the meaningfulness
of the measurements. For instance, measurements are presented
that indicate that the contour patterns obtained were reasonably
steady during the cruise.

Independent measurements using standard bathythermograph
(BT) observations and a towed temperature sensor throughout
the cruise are described in Section IV. These observations
were used to obtain depth variations of the 20°C isothermal
surface for the area. The resulting pattern is consistent with

the sound velocity measurements and suggests a circulation
for the Sargasso Sea that can be characterized by a system
of eddies. Some support for the hypothesis that the pattern
relates to the direction of water flow is presented. Next,
the pattern of eddies is shown to have visual correlations
with the shape of the ocean bottom. A speculation is offered
that relates the pattern of eddies to prominent features of
the sediment distribution on the ocean floor.

Section V contains a theoretical account of the observa-
tions based on the assumption that the flow in the Sargasso
Sea is isentropic. This allows the use of Ertel's theorem
(1942) which relates vorticity to vertical temperature gradients
on surfaces of constant temperature. The observations are
shown to be in agreement with the above hypothesis but in
view of the lack of extensive current measurements a thorough
evaluation of the hypothesis is not possible. In Section VI
the report concludes with recommendations for research into
acoustically monitoring large ocean areas for information
about oceanographic variations as well as further study into
the circulation of the Sargasso Sea.

List of Figures

Fig. I-1   Overall Track Chart - ATLANTIS II Cruise #22 (1966).

ATLANTIS II-22
CHART II
BERMUDA LEG

LINE OF SOUND VELOCITY PROFILES
15-22 JUNE 1966

BERMUDA

66°

32°

396 ●
394 ● ● /395
393 ●

● 397

392 ●

391 ●

387 ●● 390
388

31° N

386 ●

65° W

385 ●

384 ●

67° W

383 ●
389 ●

30° 382 ●● 380

30° N

381 ●
379 ●

378 ●

377 ●

68° W

376 ●

29° N
66° W

375 ●

374 ●

373 ●

372 ●

28° N

371 ●

67° W
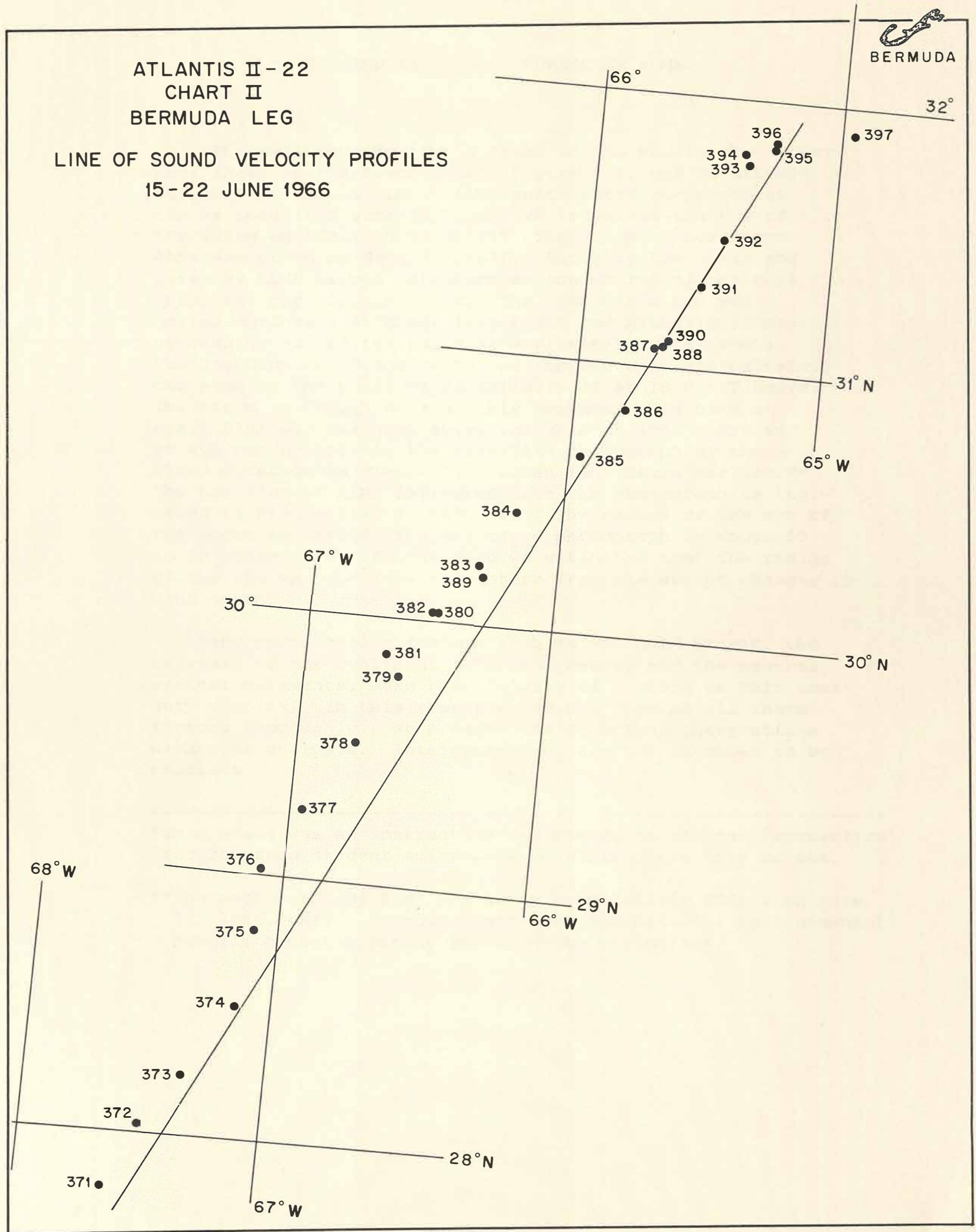
Fig. I-2   Sound Velocity Profile Locations from Bermuda Leg.

SECTION II   -   HURRICANE ALMA

The westerly jog in the track on the way to the survey
area shown in the Track Chart, Figure I-1, was an attempt
to avoid hurricane ALMA. ALMA anticipated our moves as
can be seen in Figure II-1, and we traversed the eye of
the storm on the 12th of June.* The track of hurricane
ALMA was given by Hubert (1967). Actually the winds and
waves of ALMA helped to determine the course of the ship
into, and out of, the storm. The weakened storm was
moving northerly at about five knots and ATLANTIS II was
proceeding toward the south at approximately ten knots.
The coordinates of the center of the eye were approximately
the same as the position of ATLANTIS II at 1830 EDT hours.
The storm, although considerably weakened, did have an
eye. Blue sky was seen above the ship at 1830 hours and
an eye can be seen in the satellite photograph of the
cloud coverage in Figure II-2 taken four hours earlier.**
The position of ALMA estimated from the photograph is indi-
cated in Figure II-1 at 1430 EDT. The radius of the eye of
the storm estimated from the cloud photograph is about 50
to 60 kilometers. On the ship we estimated that the radius
of the eye was about 54 kilometers from the abrupt changes in
wind speed.

Many contributing factors such as the Gulf Stream, the
nearness to the continent, the bathymetry, and the general
weather movements, make the analysis of a storm in this area
very complex. In this report we do not examine all these
factors thoroughly. We present the principal observations
with some analysis. Interpretations are not intended to be
complete.

----
*This event was an instructive experience in air-sea interaction
 for fourteen student scientists on their first trip to sea.

**The photograph of ALMA was taken by Satellite ESSA I on June
 12, 1966. Mr. J. Gordon Vaeth from the National Environmental
 Satellite Center kindly provided the photograph.

During the traversal, we recorded the sea temperature
with a quartz thermometer that was mounted on the bow at a
depth of four meters on a digital magnetic tape recorder
and an eight-channel Sanborn Recorder. In addition, several
other physical quantitites were recorded on the Sanborn
Recorder: air temperature from a quartz thermometer mounted
four meters above the water at the stern; the barometric
pressure; the ocean wave heights using a wave recorder that
approximately compensated for the roll of the ship; the
ship's speed; the ship's heading; and the time. A sample
record is included as Figure II-3. These data are considered
to be unique and are of value in air-sea interaction studies.
Figure II-4 contains a plot of the barometric pressure, air
temperature and the sea temperature during the passage
through ALMA.

Discussion of the Air Temperature

The eye of the weak hurricane is readily located between
times 1530 and 2130 hours EDT by the minimum of the baro-
metric pressure (the bottom curve in Figure II-4) and with
high air temperatures as seen in the middle curve of Figure
II-4. The cool air aloft descends down the eye and is
warmed in the process by dry adiabatic compression, (Haurwitz,
1935; Godske et al, 1957, p. 574). This accounts for the
relatively high air temperatures in the center of the eye.
It is interesting that the air temperature in the eye of the
hurricane at sea level is about one-half degree Centigrade
colder than the sea-surface temperature.

The rise in temperature of the central region of
the air-temperature curve in the eye of the storm might be
related to an anticyclonic circulation of the water that
exists near the center according to theoretical calculations
(O'Brien and Reid, 1967), or to a similar vorticity in the air.
This possibility needs study.

We expect the air temperature to decrease abruptly as the
ship passes out of the eye of the storm. This appears in
Figure II-4 at a time shortly after 2030 hours on June 12.

Most of the temperature data obtained in hurricanes
from aircraft are limited to no closer than 300 meters above
the ocean for safety during flight. Consequently, inferences
about air-sea interaction from aircraft temperature measure-
ments remain vague. In this connection, it seems significant
that the air temperature recording at four meters above the
sea surface in ALMA is similar in shape to temperature recordings
obtained by an aircraft in traversing hurricane CLEO (1958)
at an altitude of 300 meters. Since we suspect that the air
temperature recordings by an aircraft are related to the
absolute vorticity under the assumption of nearly layer-wise
isentropic flow, it is surprising to find a close similarity
to the recordings so near to the sea surface (Figure II, 4a).

In his discussion about hurricane CLEO, LaSeur (1962)
presented a vertical cross section of the temperature anomaly
from mean tropical conditions measured in the hurricane, August
18, 1958 at 35°N. CLEO appears to have very similar character-
istics (size of eye, windspeed, etc.) to hurricane ALMA. LaSeur
suggested that the anomaly in temperature is evidence that
convective processes play a primary role in determining the
structure and formation of hurricanes and also in their movement.
Riehl (1963) developed arguments explaining the radial air
temperature distrbution in hurricanes that ought to apply to
intense hurricanes and found that his model did not explain
the temperature structure of hurricane CLEO, a weak hurricane
having a large eye with winds around 60 knots. This difficulty
surely results in part from the need to take into account more
carefully the air-sea interaction for which measurements are
needed.

Discussion of the Sea Temperature Record

The observations in Figure II-4 indicate that warm sea-
surface temperatures exist in the eye where upwelling should
be greatest, whereas much colder sea temperatures occur some
distance outside of the eye of the hurricane. Although these
observations are apparently in conflict with the observations

of cold water found along the track of hurricane HILDA
(Leipper, 1967) that are explained by upwelling in the
region of the eye (O'Brien and Reid, 1967), we may avoid
the conflict if we suppose that the cold, upwelling central
region of the ocean under ALMA did not penetrate the iso-
thermal surface layer. Also note from Figure II-1 the
complication evidently introduced by the Gulf Stream.

The surface isothermal layer was measured in the eye
near the eyewall by a bathythermograph to extend 45 meters.
According to O'Brien and Reid's calculations, this layer
should become thicker in the radial direction away from the
central region for a stationary hurricane. Unfortunately it
was too hazardous to obtain bathythermograph recordings while
in the storm to verify this directly. Moreover, one needs
to take into account the influence of the Gulf Stream in the
analysis.

The sea-surface temperature record for hurricane ALMA
in Figure II-4 exhibits a sequence of intense cusp-like
variations that increase in spacing in the radially outward
direction. We suggest that the cusps are regions of intense
upwelling of cold water brought about by the response of
the ocean to the moving storm or a modification by the storm
of a pre-existing sea temperature condition. To clarify this
suggestion we will discuss both inertial gravity waves and
longer period baroclinic waves with respect to the observa-
tions. However, we will omit introducing at this point
complexity of the Gulf Stream influence.

Internal gravity waves with a period slightly shorter
than the inertial period are continually stimulated by in-
stabilities generated by the storm center. They should exhibit
a nearly standing wave pattern with respect to the storm center
since the group velocity for inertial-period gravity waves is
near zero. The spacing between successive waves of this pattern
should change depending on the phase speed of internal gravity
waves which varies with the layer depth. The upper-layer depth
in the water, according to theory, varies radially from the
storm center because of the main upwelling process. It is

thinner toward the center of the disturbance. The layer
thickness reaches a nearly equilibrium shape after twelve
hours of a stationary storm according to O'Brien and Reid
(1967).

The phase velocity of an internal gravity wave*, at the
interface of a less-dense $\rho - \Delta\rho$ upper layer of thickness
h, overlying a thick, lower layer H is given approximately
by

$$\sqrt{\frac{\Delta\rho}{\rho} g \frac{hH}{H+h}} \sim \sqrt{\frac{\Delta\rho}{\rho} gh} \ .$$

For an isothermal upper layer of 100 meters' thickness, this
could reach three knots. Close to the storm center, where
upwelling possibly reduces the layer thickness substantially,
the wave speed might be as low as one-half knot. The wave-
length of an internal gravity wave at the inertial period of
twenty hours (which corresponds to the latitude of the storm)
depends on the phase speed of the waves. Since this wave
speed increases with radial distance from the storm, from
one-half knot to possibly three knots, the wavelength should
vary from ten miles at a short distance from the storm center
to sixty miles at a large distance. The spatial separations
of the major sea-surface temperature drops shown in Figure II-4
at 1800, 1930, 2200, 0100, and 0600 hours, can be obtained by
multiplying the ship's speed relative to the storm by the time
intervals for the above times. These separations vary from
about 15 miles to sixty miles. This wavelength interpretation

----

*We restrict the discussion to a two-layered ocean recognizing
 that it is only an approximation to the continuously stratified
 ocean. The upper, thin layer is taken to be an isothermal,
 mixed layer with an abrupt lower boundary and therefore very
 long wavelength, inertial gravity waves should be possible as
 a two-layered oscillation.

of the spacings between the cusp-shapes indirectly supports
the theory for the existence of an increase in the average
thickness of the isothermal layer along a radius from the
storm center. We use the word indirectly here to suggest
that other factors may also play an important role in the
observations, i.e., change in the depth of the water and
the presence of the Gulf Stream.

We suspect that the large temperature dips may be evidence
of unstable baroclinic long waves. The depth of an isotherm
(or a layer) might have a marked rise toward the surface at
the places where the temperature drops in Figure II-4. This
would indicate intense upwelling and counterclockwise circul-
ation. It is easy to visualize the existence of these waves
since we are primarily interested in the southern side of a
hurricane and in this region there is an eastward component
to the current flow produced by the storm. Accordingly, we
can imagine Rossby waves and unstable long waves being held
stationary in this region since these waves can have a
westward component to their phase velocity that may just equal
the eastward current. Moreover, the minimum wavelength for
baroclinic waves is given by 2π times the internal gravity
wave speed divided by the Coriolis parameter (Longuet-Higgins,
1965). This is the same wavelength relationship just described
for inertial-period, internal gravity waves that was related
to the spacings of the large temperature dips in the sea tempera-
ture recording.

Discussion of the Sea-Air Temperature Difference

The radial air-sea temperature difference is surely an
important measurement relating to the thermodynamics of the
interaction of the sea and the hurricane. There are three
distinct regions of the storm to be considered as is clearly
shown in Figure II-4. The first region is that portion of
the eye of the storm where the sea-air temperature difference
is essentially constant. The next region from about 2030 to
0100 shows that the sea-air temperature difference increases.

This is followed by a region after 0100 where this difference decreases. If we ignore for the moment the large dips in the sea-temperature record of Figure II-4 and plot the sea-air temperature difference against time on a log-log plot, we obtain the results shown in Figure II-5. Time is approximately proportional to the range of the ship from the center of the storm. These measurements are relative to the ship, and could be difficult to interpret if the storm in this region were moving northward rapidly. However, this is not necessarily the situation in the region south of the storm center.

In Figure II-5, the first two and one-half hours are still within the eye of the storm. The second region of the storm is characterized by an increase in the temperature difference. In Figure II-5, two lines are drawn through the points, the solid line shows an increase proportional to the square of the distance and the dashed line shows an increase proportional to the three-halves power of the distance. In an oral presentation of these data*, the measured sea-air temperature difference was reported as closer to the three-halves power. Upon re-examination of the measurements and with the requirement that the line be outside the eye of the storm (the point at 2.5 hours in Figure II-5), the line proportional to the square of the distance seems more appropriate.

The third zone is also shown in Figure II-5 where the temperature is inversely proportional to the distance. The low values of the air-water temperature difference in this outer region were not used in estimating the 1/r slope since they are regions where the sea temperature goes through large anomalous temperature dips which will be discussed later. Unfortunately, instrumentation to measure wind speed accurately was not available and estimates were crude. Nevertheless, the maximum wind speeds in the storm probably occurred at the location of maximum air-sea temperature difference indicated in this figure. An abrupt increase in wind speeds occurred 3 hours from storm center.

----

*Sixth Technical Conference on Hurricanes, Dec. 2-4, 1969
 Miami, Florida.

Often data about hurricanes concerns the power law for
the dependence on radial distance from the center of the
wind speed at an altitude of 300 or more meters. Riehl
(1963) examined the radial dependence of wind speeds
obtained from aircraft in several hurricanes and found
that in the outer field the tangential component
of wind velocity decreases with the radius as $r^{-1/2}$. He
pointed out that this implies conservation of potential
vorticity. He also found that the wind speed closer to
the eye usually increases as the first power of the radius,
although there are exceptions. The observations presented
in Figure II-5 give indirect support to the hypothesis that
the air-sea temperature difference is proportional to the
square of the wind speed in the outer zone and also in the
inner zone.

Malkus and Riehl in 1960 presented arguments that the
air-sea temperature difference might be related to the square
of the wind speed. They assumed that heat-transfer from the
ocean to the air occurs isothermally while the air in a layer
close to the sea expands as the air converges inward toward
lower pressures. Thus the added heat from the sea is thought
to balance the drop in temperature that comes about due to
expansion. This is the reason given for the constant tempera-
ture inflow region frequently found far from the central region
of a hurricane. This also is presented as the heat supply
mechanism to explain why hurricanes can intensify at sea but
not over land (this notion was suggested by Byers in 1944).
The underlying reasons why an isothermal mechanism such as
this should take place are not well understood. However,
Malkus and Riehl show that an isothermal process would maximize
an assumed analytical expression for the kinetic energy that
contained terms for the production and dissipation process.
They argued that stability should be associated with a minimum
of kinetic energy, and therefore a process which maximized
kinetic energy over other possible processes would become
dominant at the fastest rate and be the observed process.
The main question is surely whether there is adequate time
available through turbulent motions in a hurricane in the layer
close to the sea for heat energy to be added or subtracted from
all parts of the working fluid that is primarily responsible

for a process being isothermal. Otherwise, the process
would tend to be adiabatic. It is interesting that the
range of observed barometric pressure variations shown
in Figure II-4 is comparable to the magnitude of the
saturation vapor pressure change that would correspond
to the observed air temperature variations (considered
as wet bulb temperatures).

Discussion of the Variations in the Set of the Ship.

There are observations that tend to confirm the existence
of the intense circulations associated with the temperature dip
in the record. We observed effects on the ability to steer the
ship and the intensity of ocean surface waves in these regions.
A plot of the ship's Loran positions and the ship's headings
shows definite variations in the set of the ship that relate
sensibly to the interpretation of the sea conditions discussed
earlier. These data are shown in Figure II-6. The set of
the ship (in degrees) and the direction indicated along the
track are considered to be meaningful in view of the experience
of the ship's crew in navigation and in view of the continuous
recordings of the ship's heading and speed (see the example of
the Sanborn recordings in Fig. II-3). The average of the
estimated sets in Figure II-6 was 7° to port. This was
subtracted from the numerical values giving the set variations
around the mean shown in the figure. A gyrocompass correction
of 2° to starboard should be subtracted from the mean value
of 7° to port making a mean set to port of 9°. Consequently,
only in the narrow region 0500 to 0600 EDT was ATLANTIS II set
to the southwest. The oscillating solid line drawn along the
track representing the variations in set suggests a meandering
flow path for the water (see small arrowhead drawn on curve).

The flow line is based on the large variations of the set
in the ship's course created primarily by the direction of
water flow, wind and waves. The sets are to the northeast
as expected for the general circulation of water brought about
by the hurricane. From the sketch of the meandering flow line

in Figure II-6 we infer the existence of marked counter-
clockwise circulations that occur close to the locations
of the main sea-temperature dips shown in Figure II-4.
The estimated southeasterly direction and character of the
water streaming in Figure II-6 are in qualitative agreement
with the theory of unstable baroclinic long waves that may
be propagating to the northwest on the southern side of the
storm center. The flow pattern suggested in Figure II-6
is complicated by a narrow zone between the times 0100 and 0200
where a large set deviation is indicated. This zone might
be a region of strong streaming (a jet). The jet region
may be represented approximately by two oppositely circulating
eddies located on either side of it. The large dips in
temperature of Figure II-4 occur on the southeastern part
of smaller scale counterclockwise circulations and on the
northwestern part of larger scale clockwise circulations
(as indicated by the arrows). This characteristic suggests
a familiar counterpart in the distribution of vorticity in
vortex pairs on a rotating earth. A clockwise vortex intensi-
fies on its western side in the northern hemisphere because
the northward flowing water gains negative relative vorticity.
Just the opposite is expected for a counterclockwise vortex.
Thus we infer from the variations in the ship's set that a
strong jet to the northeast occurs at the ship's position
around 0100, ship's time, and that current streams from the
north and from the south of this position combine to form
the jet.

Final Remarks

The brief account above does not include discussion of
other important considerations such as the role of the Gulf
Stream in the observation or the fact that the storm was moving.
The omission only means that we do not intend that the observa-
tions and interpretations offered at this writing are to be
considered complete. Moreover, a considerable development of
the mathematical side of the problem based on an extension of
the work of Kuo (1949) has been done that is not presented here.
This work included both free baroclinic waves in a region of a
north-south shear in the mean eastward flow as well as a special
case for these waves augumented by the wind.

Hurricane air-sea interaction is obviously very compli-
cated and observations that can shed some light on the relative
importance of some of the processes that can take place are
scarce. Further study is essential, and some questions are
raised here for this purpose. One concerns the mechanism of
air-sea coupling when winds are high and when winds make up
a vortex. Another concerns tracks of hurricanes and a possible
influence of the variation in depth of the ocean.

1) Vorticity is transferred to the ocean when ocean
waves break and non-linear effects are present. Phillips
(1966, p. 88) points out that turbulence is particularly
important in estimating induced pressures when the wind speed
is close to wave speed. Turbulence is also present when
transfer of energy per unit time is most efficient. Phillips
(p. 129) describes peaks in an energy spectrogram at low wave
numbers for the data he presents of Barnett and Wilkerson
where the wave speeds for short fetches matched wind speeds.
In the case of hurricane winds the ocean waves generated will
be inclined to the wind since they radiate away from the
center. In this case even short-wavelength waves may have a
phase speed that is as large as the wind speed along the nearly-
circular course of the wind path. It even seems possible for
wave phase speeds to exceed wind speeds and transfer wave
energy to the air. This region where wind speed and wave
phase speeds are near each other implies effective turbulent
wind-to-sea coupling that should be important in the calculations
of the rate of increase of ocean circulation beneath the storm.
If the response time is short enough then the system of vortex
flows developed in the ocean near the sea surface and the wave
response to the winds may lead to an important interaction
in the dynamics of the hurricane itself.

2) Some speculative questions suggested for further study
arose from an examination of the gross behavior of hurricane
ALMA during its trip and demise in the Atlantic Ocean.

A track of the storm presented by Hubert (1967) indicates
that ALMA moved eastward from Georgia along latitude 33°N to
73°W longitude where it veered northward. Its intensity grew
during its eastward motion as it crossed the Gulf Stream and

the continental shelf and moved out over the continental
slope to deep water. In its trip northward, the ocean depth
decreased and the hurricane center came into the Gulf Stream
region again. Its northward trip stopped at the edge of the
continental shelf, 38°N, where the storm's track turned and
followed the edge of the shelf northeasterly. During this
portion of the trip ALMA decayed rapidly into a diffuse
extra-tropical storm. Some of the dissipation results from
the influence of the colder water north of the Gulf Stream.
We speculate that this behavior of hurricane ALMA also
supports the possibility that the distribution of vorticity
in the ocean may influence the motion of a hurricane and
that the edge of the continental shelf and the shallow depth
of the shelf may be connected with rapid dissipation. Certainly,
the phase speed of sea surface waves traveling in the direction
of the wind is limited by water depth over the shelf. Thus
the edge of the shelf should mark the location of a change
in wind-wave interaction. In addition we speculate that as
the storm reached latitude 38°N the growing vortex system
in the water began to carom into the edge of the shelf causing
rapid shedding of underwater eddies. The winds of the storm
may then regenerate the vorticity in the sea. In this manner
the storm may have drained large amounts of its energy into
ocean vortices which were rapidly shed as the storm moved
slowly parallel to the shelf edge. Not all hurricanes, in
view of the variations in their northward speeds and intensities,
could be expected to behave in this manner.

No estimates of angular momentum and energy exchange were
made for this supposed process, nor were the possible compli-
cations of such a speculation examined to take into account
the effects of the Gulf Stream. Nevertheless, there are
tracks of a number of hurricanes that seem also to suggest
a possible dependence of dissipation and trajectory on the
water depth, the edge of the continental shelf and vorticity
distribution in the water. Some of these are:

CLEO 1960 Traveling northwest, at 42°N, 66°W she became
a tropical storm and veered eastward to travel along the edge
of the shelf as she dissipated.

ESTHER 1961   This hurricane traveled northward from 35°N, 73.5°W to 41°N, 71°W which is near the edge of the continental shelf.   There she veered eastward, weakened and made a large clockwise-looping trajectory.

GERDA 1961   Moving northward, she changed from a tropical storm to a weaker, extra-tropical storm at 42°N, 65°W (the edge of the shelf) where her path turned to a more easterly direction.

FRANCES 1961   Moving northwesterly, changed from a hurricane to a tropical storm near 42°N, 67°W and moved over the shallow water.   She then veered sharply to the east as she became an extra-tropical storm.

ALMA 1962   Moving northeasterly, weakened at 41°N, 69°W and then at 42°N, 68°W, while over shallow water, she veered eastward over the southeast channel.

GINNY 1963   This storm performed several loops in the region of the Blake Plateau and the Outer Ridge.

GLADYS 1964 and 1968   These hurricanes weakened near 44°N, 63°W which is close to the continental shelf edge.

These observations, in the author's view are enough to encourage an investigation of the above speculation even though other factors also influence the direction and dissipation of hurricanes.

LIST OF FIGURES

SECTION II - Hurricane ALMA

<u>Figure</u>

Fig. II-1   Tracks of ATLANTIS II and Hurricane ALMA and the
North Wall of the Gulf Stream.
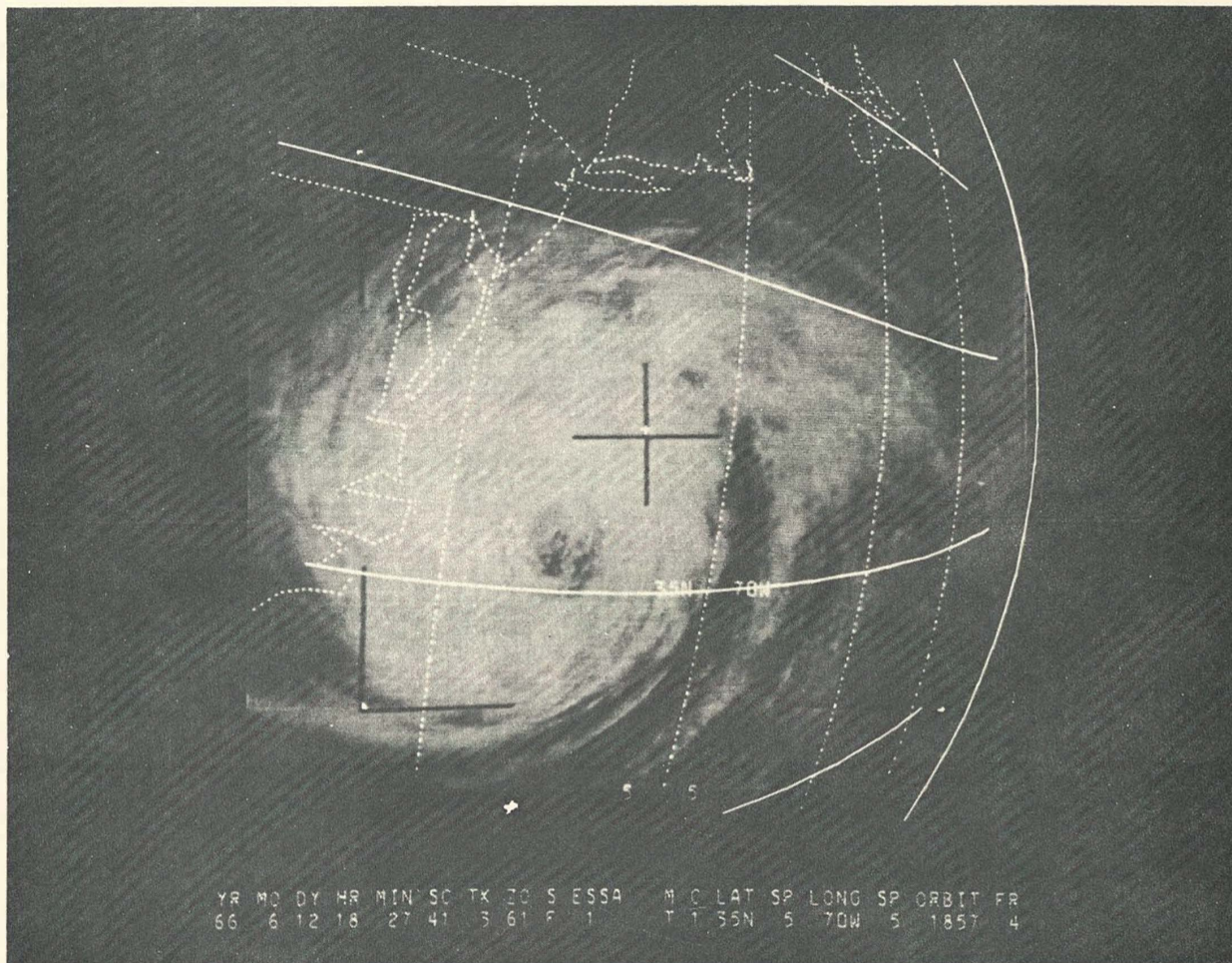
Fig. II-2   Satellite Photograph of Hurricane ALMA at
            1430 EDT on June 12, 1966.
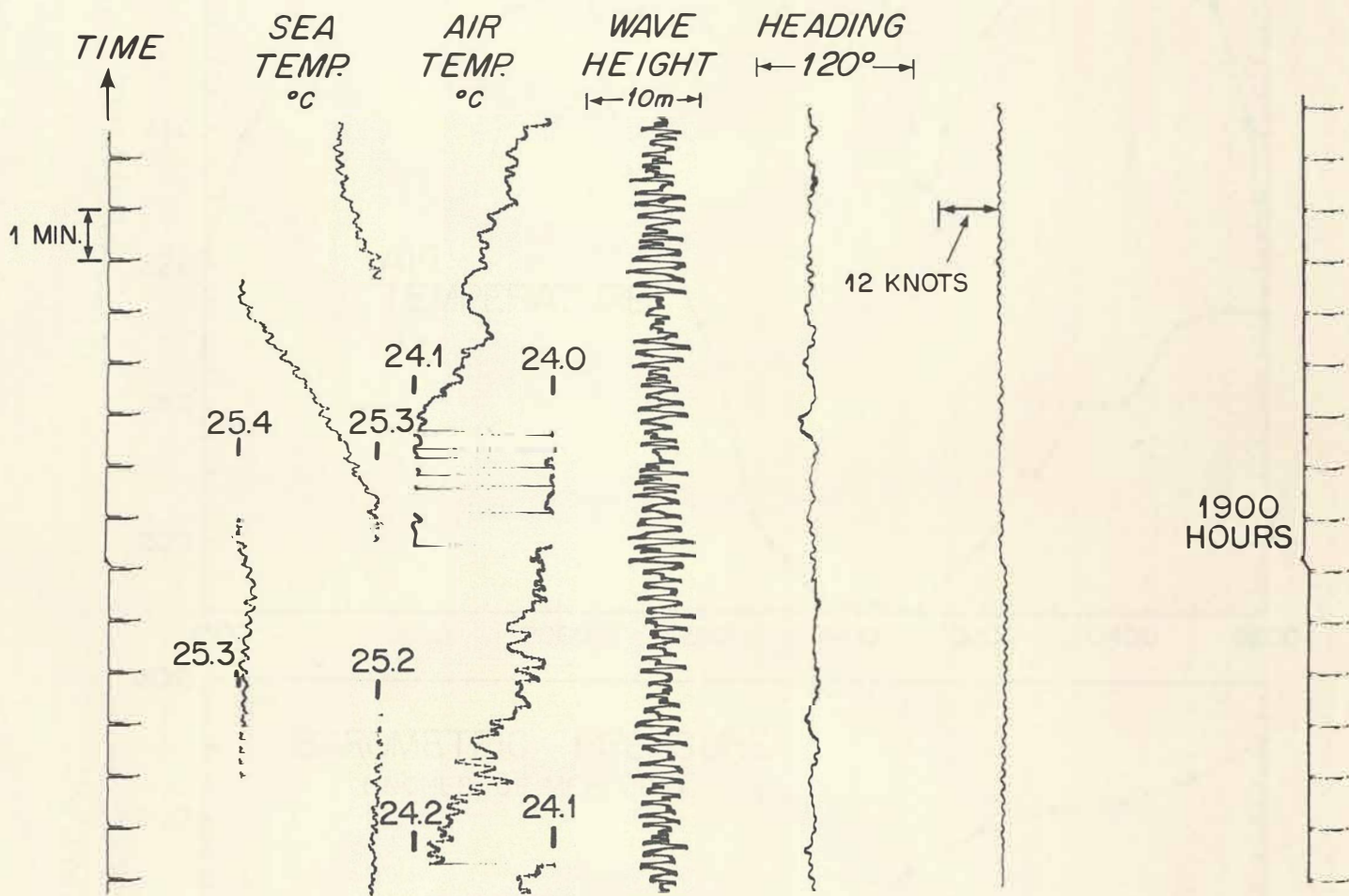
Fig. II-3   Sample Sanborn Recording of Data Taken While Traversing ALMA.
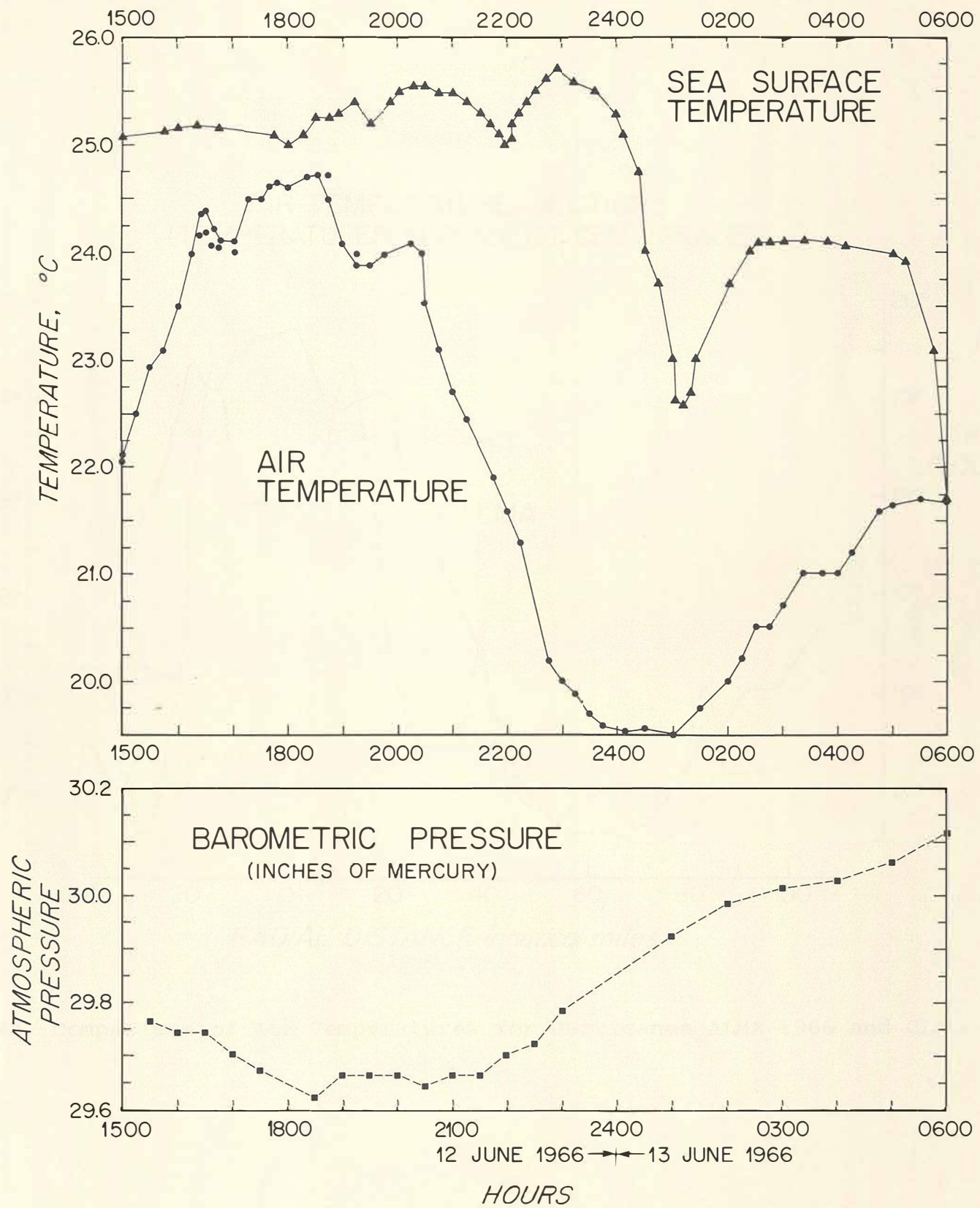
Fig. II-4   Barometric Pressure, Sea and Air Temperatures
During Passage through Storm.

AIR-TEMPERATURE SECTIONS
(TEMPERATURES IN DEGREES CENTIGRADE)
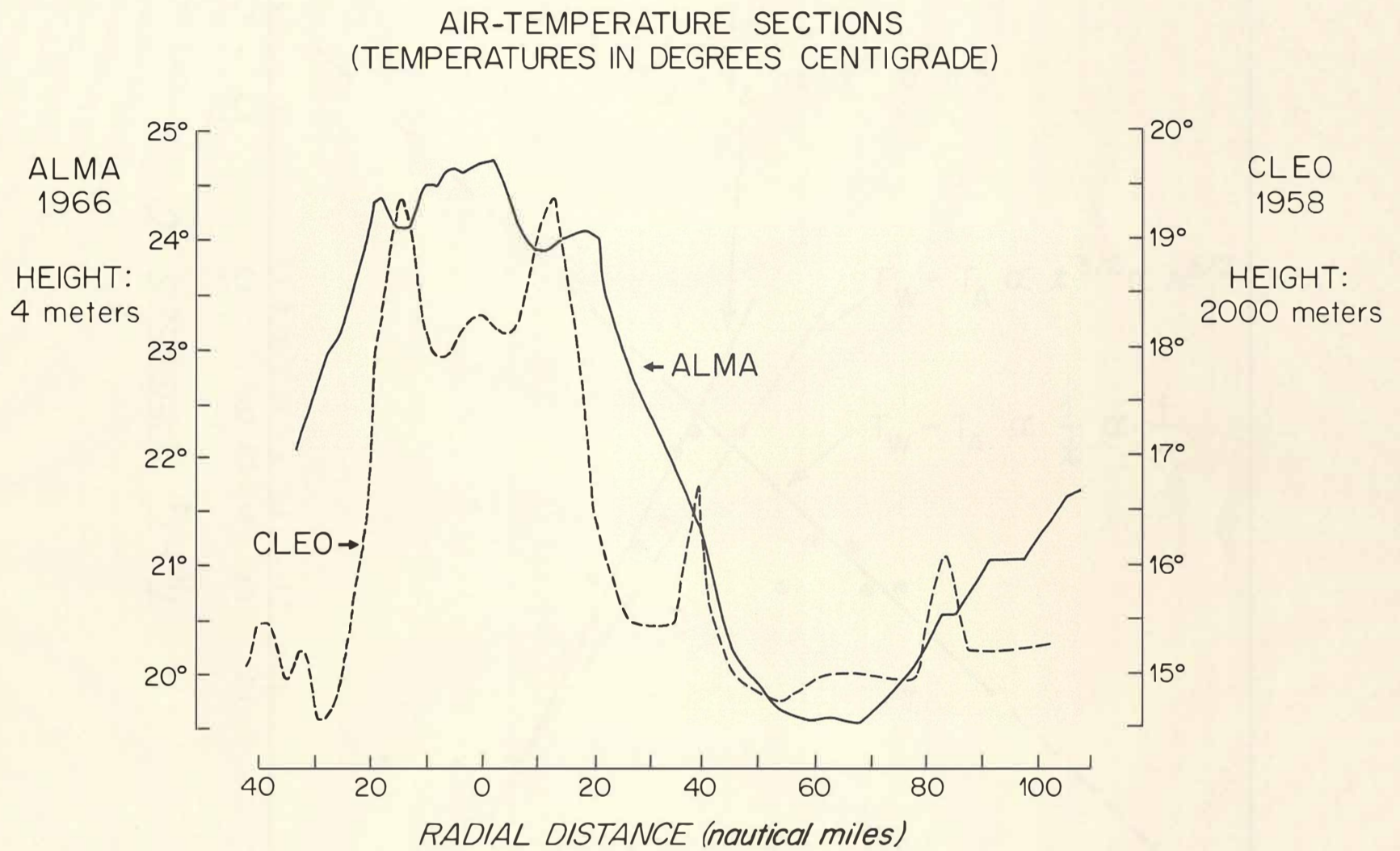
Fig. II-4a Comparison of Air Temperatures for Hurricanes ALMA 1966 and CLEO 1958.

SEA-AIR TEMPERATURE DIFFERENCE
HURRICANE ALMA (1966)
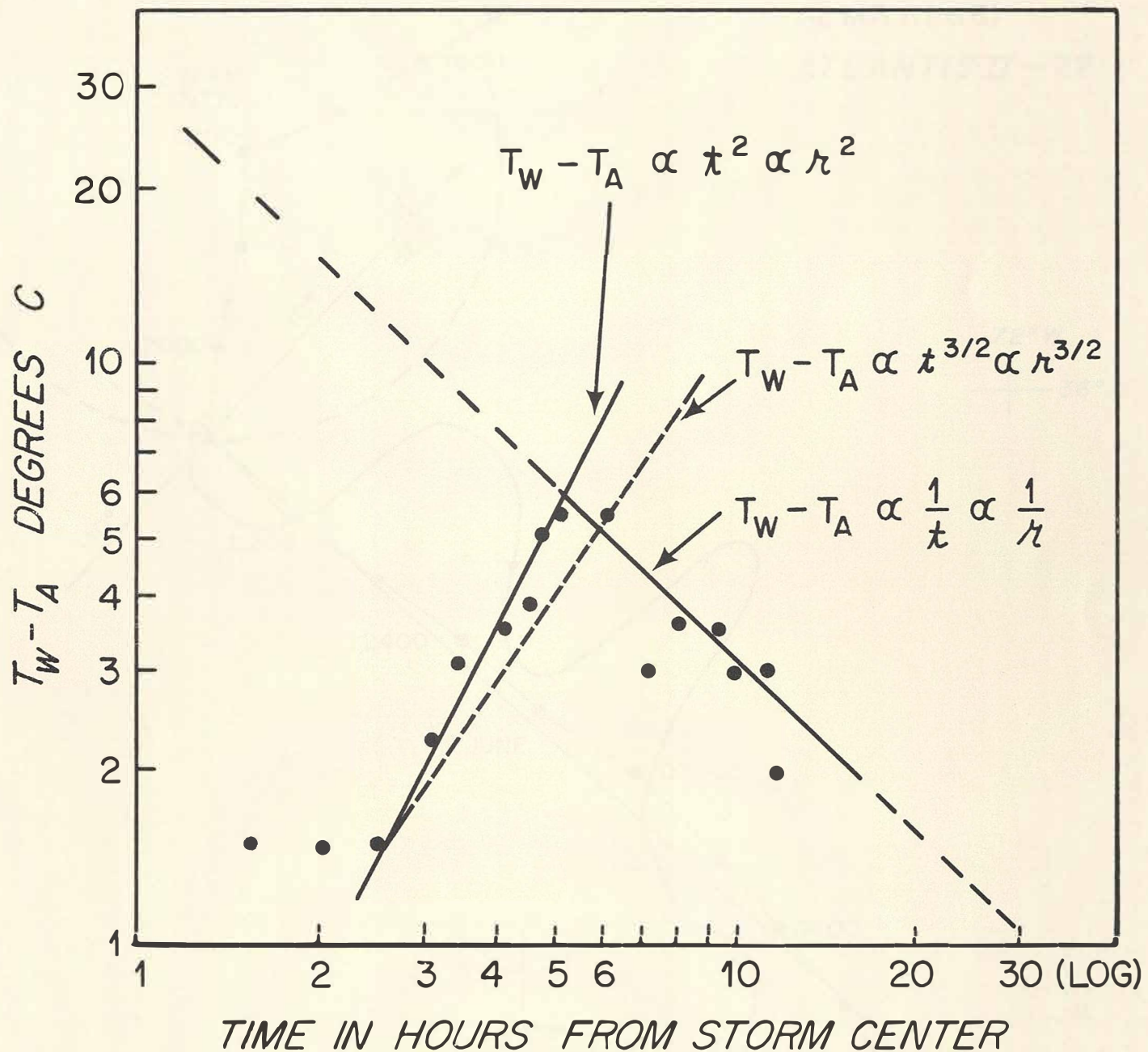
Fig. II-5   Sea-Air Temperature Difference during
Traversal of Hurricane ALMA.
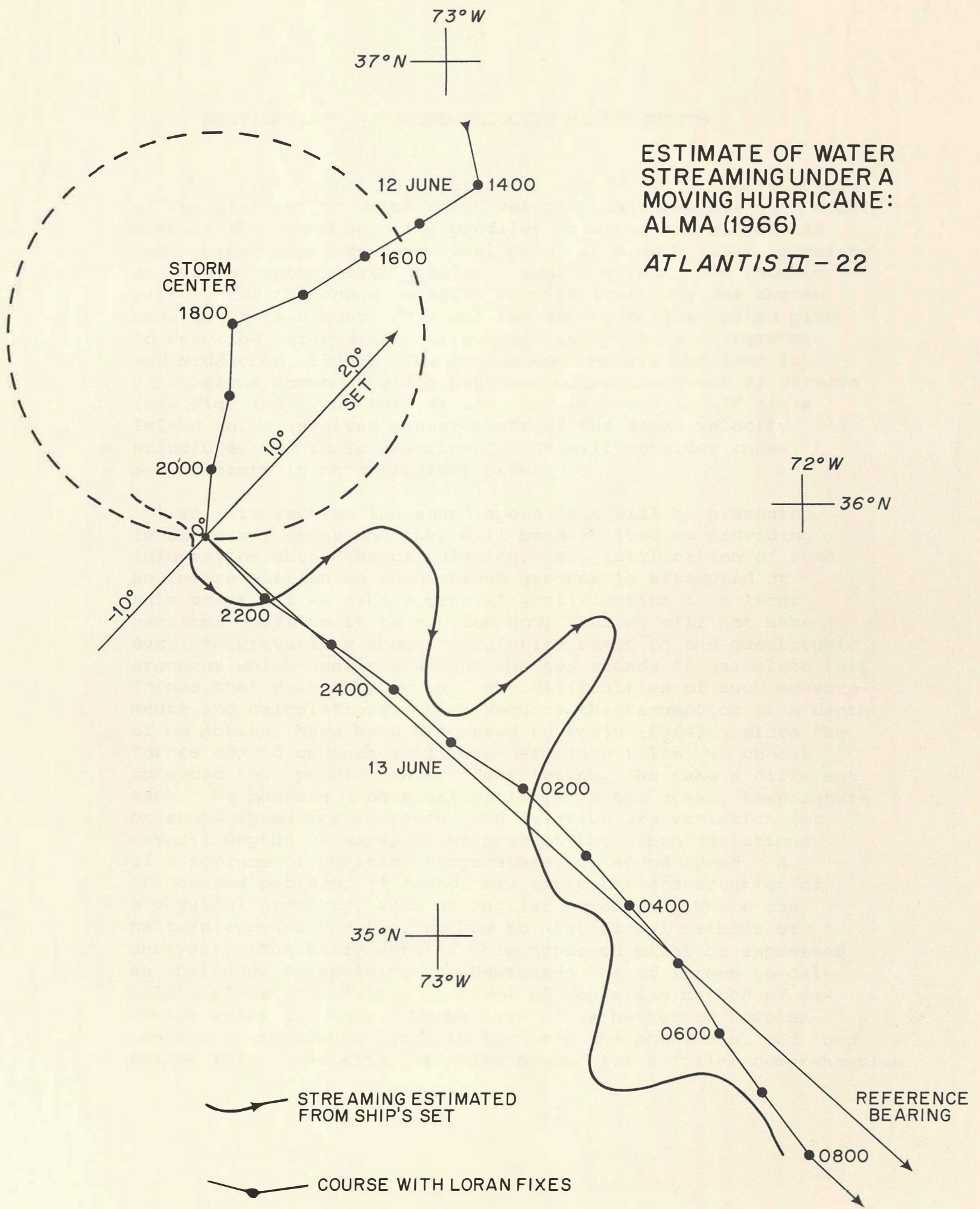
Fig. II-6   Variations in Set of Ship about a Mean Set of 9° to Port.

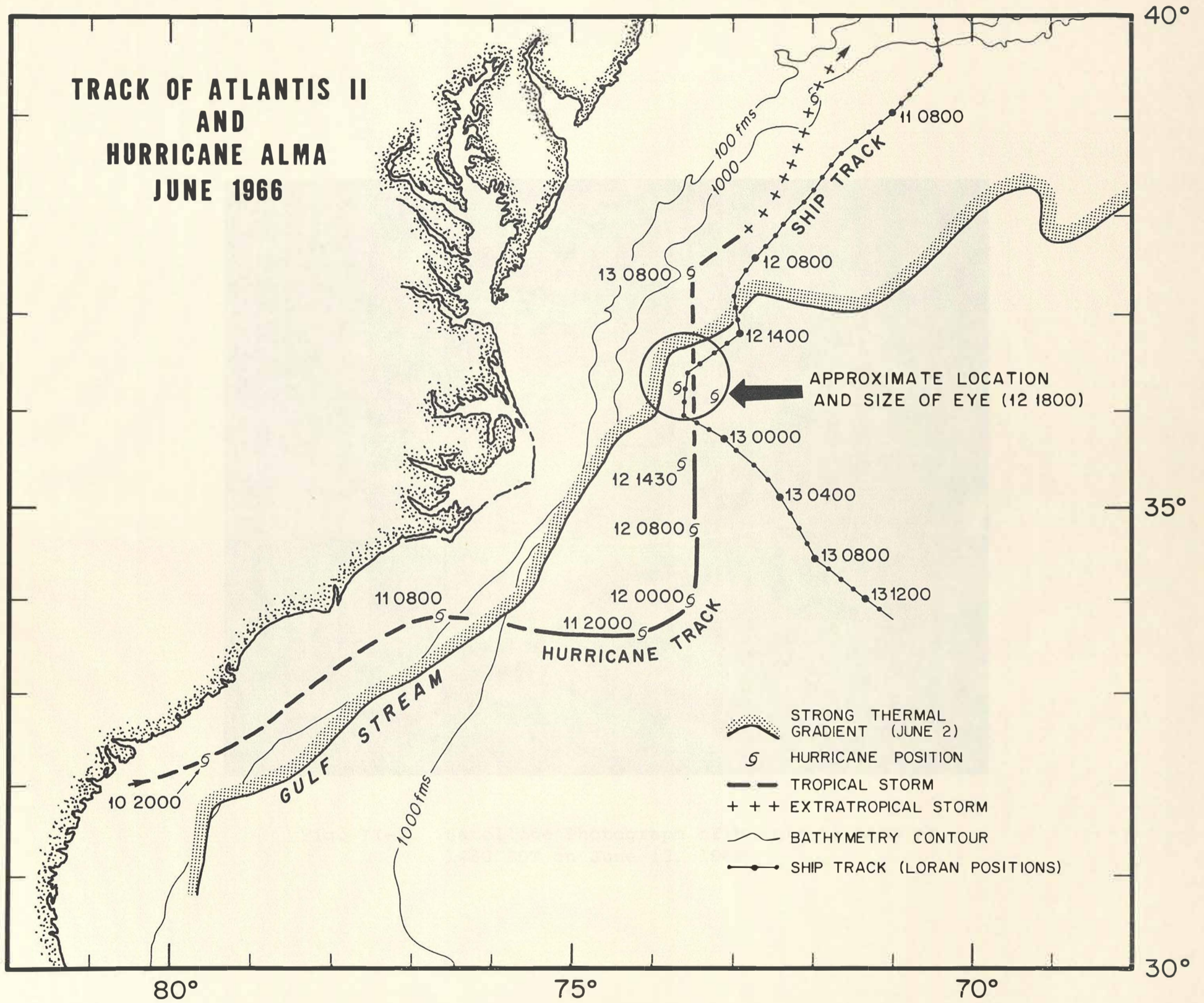SECTION III - SOUND VELOCITY MEASUREMENTS

     The track charts in Figures I-1 and I-2 show the locations
of the stations at which sound velocity measurements were made.
Most of the sound velocity profiles obtained on this cruise
were spaced sixty-five nautical miles from each other, covering
an area of approximately 356,000 square miles. The rhombic
pattern for the sound velocity profile locations was chosen
because it is a most efficient two-dimensional sampling plan
to describe large-scale horizontal wave phenomena (Petersen
and Middleton, 1962). The two exceptions are the long line
of stations commencing 290 nautical miles southwest of Bermuda
(see Fig. I-2), the Bermuda Leg, and the station off Argus
Island which involved measurements of the sound velocity
structure, the Yo-Yo experiment. We will consider these
measurements in chronological order.

     In this section the sound speed data will be presented
in different forms and they will be described as providing
information about the circulation. No justification of such
an interpretation on theoretical grounds is attempted at
this point but we make a general justification in a later
section. Suffice it to say for now, that we will not make
our interpretations about circulation based on the geostrophic
argument which uses the height the sea stands to calculate the
forces that drive the ocean. The difficulties of such measure-
ments and calculations, which require the assumption of a depth
of no motion, have been discussed by Fomin (1964). Since the
forces depend on such small ocean-surface tilts, we choose
to avoid this problem in our description. We take a different
tack. We measure a physical variable in the ocean, temperature
or sound speed for instance, and describe its variation for
several depths on maps, or we present the depth variations
of a surface of constant temperature, or sound speed. A
structured pattern, if found, may imply the conservation of
a physical property, such as angular momentum. Where the
pattern appears chaotic, we bow to statistical methods of
analysis. The difference of this approach might be expressed
as analogous to avoiding the Newtonian use of forces to cal-
culate planetary orbits, in favor of Keplerian method of de-
fining rules for them. We believe it is better to have ex-
tensive measurements first to lay bare the phenomena, and then
follow this by looking for rules needed for a fuller comprehension.

Instrumentation

Most of the observations that will be presented here involve the measurement of sound speed in sea water as a function of depth. In sea water the sound speed depends mainly on temperature and slightly on pressure and salinity. The reliability of the depth measurement is critical when our purpose is to compare the depth variations of sound speed at different times at the same station and also over widely spaced stations. Therefore, the sound velocity profiles were calculated from measurements made by an improved version of a sing-around velocimeter that was originally developed by Greenspan and Tschiegg (1957), and an inverted echo sounder.

The sound velocimeter* consists of an ultrasonic trans- ducer and a reflective plate about 10 cm distance apart. The transducer emits a signal which is reflected from the plate and received near the source. This pulse generates another pulse of sound which accounts for the descriptive name "Sing-around". The sing-around frequency is propor- tional to the local sound speed. Calibration of the instru- ments in distilled water over the temperature range of interest can yield values accurate to between 0.02 to 0.06 meters/sec. for the root mean square deviation from the standard values of sound speed versus temperature. However, there is considerable variation in absolute accuracy of the instrument because of the uncertainty between standard measurements of sound speed in water as function of temperature (McSkimin, 1965; Carnvale et al, 1968). Until further work is well established, we do not assign an absolute accuracy to sound speed measurements in the sea of better than 0.15 meters/second in 1500 meters/ second.

The inverted echo sounder (Dow and Stillman, 1961) operates in a similar fashion since an acoustical pulse is reflected from the sea surface and its time of arrival back at the instrument that is being lowered into the sea is measured.

----

*NUS Corporation, Paramus, New Jersey, U.S.A.

With our present system, the round-trip acoustic travel time, measured every second or two, is telemetered to the ship along with the sound velocimeter signal where a computer calculates the integral of the measured sound speed over the travel time to determine the instrument depth. The basic technique has been improved on gradually since 1962, and the system has achieved an estimated depth accuracy in a calm sea of better than 2 meters at a depth of 5000 meters. The instrument frame that is lowered into the sea now contains a number of additional instruments (pressure, temperature and salinity). A final plot of the measurements is available aboard ship.

The individual sound velocity profiles for the Bermuda Leg of which SVP #383 in Figure III-1 is a typical example are presented in Part II together with comments on them. These sound velocity profile plots were obtained from the computer at W.H.O.I. using the digitized magnetic tape data from the cruise. Only the descent was plotted although measurements were taken during ascent also. The computer was programmed to plot sound velocity values at depths greater than 3000 meters by shifting the 3000-meter depth to the position of the 1000-meter depth and continuing the plot down the paper. Also notice that at approximately 750 meters, 1500 meters, 2250 meters and 3000 meters there are short gaps in the data. These gaps in the plots result from questionable travel-time measurements of the echo from the ocean surface that occurred during the time of the outgoing signal from the transmitter. (See description of measurement technique in Part II for more details).

The Bermuda Leg

The long line of SVP's (Fig. I-2) is designated the Bermuda Leg. Similar sound velocity sections were obtained on earlier cruises. They cross the thermal front zone at 30°N latitude and lie along a path convenient for sound transmission studies. These data were intended to supplement a transmission experiment which was not completed.

(a) Observations

From the information obtained in the sound velocity
profiles (Part II of this report), the contoured chart of
sound velocity along this vertical section, shown in Figure
III-2, was constructed. The contours reveal a pronounced
upward shift of over 200 meters in the region of the main
thermocline, starting with SVP #373 through SVP #377. This
shift was located just north of latitude 28°N which is known
to be the latitude of a thermal front zone in this season
(Voorhis and Hersey, 1964). Moreover, there is evidence
that this transition zone separates two large regions of
markedly different amounts of marine life, productivity
being much greater to the north (Backus et al., 1969).
Sound velocity contours drawn for a similar line of stations
(Beckerle, 1965) from ATLANTIS II Cruise #11 also revealed
a transition zone at depths much greater than the original
near-surface measurements that uncovered the thermal front.

Another rise of the thermocline in Figure III-2 occurs
at SVP #388, a distance about 240 nautical miles from SVP
#375. This rise appears prominent in the broad area sound
velocity patterns obtained during the latter portion of this
cruise (Section III).   Its existence here supports reports
of a 240-mile wavelength on earlier cruises (Beckerle, 1965
and 1966a).

(b) Comparison with PANULIRUS Data

There exists additional data in Nansen cast measurements
made from PANULIRUS to the south of Bermuda. There were only
a few alterations in the two-week sampling schedule over the
11 year period June 1954 to June 1965. Some analysis of
these data was reported by Schroeder and Stommel (1969).
Here we present in Figure III-3 some additional analysis
since these data appear to be related to the contour pattern
in Figure III-2.

Sound velocities calculated from the Nansen cast data yielded several time series corresponding to depths of 200, 500, 800, 1000, 1300, and 1600 meters. In Figure III-3 the mean sound velocity and variance of these series are presented. The variance (solid curve), as expected, is nearly symmetrical and has a maximum at 800 meters, the middle of the thermocline. The distribution of the sound velocity fluctuations about the mean also is shown in several dotted curves in Figure III-3. The distribution is symmetrical at 800 meters, but has a pronounced skew at 500 meters and an opposite skew at 1000 meters. The skew in the distributions can be understood if one imagines that the internal trochoid-like vertical displacements of water shown on the left-hand side of the figure are associated with the internal Rossby waves. (Observations made in 1964 indicated that a depth variation was associated with a large-scale 240-nautical mile horizontal internal Rossby wave.) One expects that a random sampling of the wave at 500 meters and 1000 meters would lead to skewed distributions since more observations would take place in a trough than in a crest. Since sound velocity decreases with depth in the thermocline one expects the skew in the distribution at 500 meters to be reversed from that found at 1000 meters where velocity increases with depth. The skew distribution in sound velocity obtained at 200 meters in Figure III-3 would result if a wave motion in the ocean at this depth had cusps pointed downward. The assumed water displacements in the main thermocline, shown on the left-hand side of Figure III-3 are strikingly similar to the contour pattern variations observed in the cross-section of Figure III-2.

A distribution of the period in days between maxima in the samples of sound velocity with time for 800 meters in the PANULIRUS data shows a broad mode centered around 110 days, and other sharper modes occurring at 56 days and 30 days. These latter are roughly one-half and one-fourth of the 110-day period and this gives emphasis to the 110-day period even though it shows up as a much broader mode. These periods are also approximately multiples of the lunar fortnightly tide. The probable importance of the fortnightly tidal period in

the dynamics of large-scale ocean movements would place considerable doubt on the validity of a spectral analysis of these data because of the choice of sampling period (two weeks). One cannot rule out aliasing* effects. The brief modal analysis described above suggests aliasing most likely is present. The presence of aliasing in spectral analysis, nevertheless, does not invalidate the statistical study of the distribution of the measurement described in Figure III-3.

(c) Interpretation of Sound Velocity Contours

In the range between SVP #378 and SVP #384 (Fig. III-2) there is a pronounced rise of the contour lines below the channel axis (at 1400 meters). This large-scale spatial variation of sound velocity contours in a region as deep as the main sound channel is a characteristic feature of the vertical cross sections of many series of sound velocity profiles measured on this cruise. It indicates that move-ments of the water column extend very deep in the Sargasso Sea area. A similar deep anomaly in the sound velocity along this line was obtained in June 1954 on ATLANTIS II Cruise #11 (Beckerle, 1965).

This variation in the sound velocity contours near the sound channel axis is located below a warm-range interval nearer the surface in Figure III-2, suggesting possibly both downward displacement of water and increased downward heat flux. Near SVP #380, where the contours of sound velocity above the sound channel dip down toward the axis (1200 meters) and the contours below the axis rise up, we might at first think that water above the sound-channel axis is descending and water below the axis is rising, but the

----
*Aliasing is the technical word used in reference to the difficulty of not being able to distinguish in widely spaced samples whether or not the value of the samples is due to variations that occur in the physical variable at shorter intervals than the sampling interval. This is particularly serious in spectral analysis.

latter may not be a correct interpretation. The behavior
of sound velocity contours near the sound-channel axis
results from a sensitive balance between the temperature
dependence and the pressure dependence. Thus warm water
that may be descending can produce a rise in the contours
of equal sound velocity below the sound-channel axis.

This contour pattern can be described analytically
quite easily by approximating a typical sound velocity
profile in the deep ocean by

$$c(z) = c_o + bz + \Delta c \left[1 - \tanh \frac{2}{h} (z - z_o) \right] ,$$

in which b is a positive coefficient for the change in
sound velocity with depth (z) due to increasing pressure,
and the parameters Δc, h, and z_o in the last term are
adjusted to allow the expression to represent the sound
velocity that results from other factors, such as tempera-
ture and salinity, that may vary with geographical location
and/or time.

This equation has a gradient, negative in the main thermo-
cline and positive below the sound-channel axis, given by

$$G(z) = dc/dz = (b - 2 \Delta c)/(h \cosh^2 (\frac{2}{h} (z - z_o))).$$

Since cosh(o) is 1, the gradient is a maximum at $z = z_o$, which
gives one relation among the parameters.

Now let us consider the change in depth of the sound
velocity contour as the range changes. We have already assumed
that the speed of sound, c, is an explicit function of the
four variables z, z_o, h, and Δc. Each of these variables
may depend on the range, R. Thus, the change with range of
the depth of a sound velocity contour can be obtained by
setting dc/dR = 0, where

$$\frac{dc}{dR} = \left(\frac{\partial c}{\partial z}\right)\frac{dz}{dR} + \left(\frac{\partial c}{\partial z_0}\right)\frac{dz_0}{dR} + \left(\frac{\partial c}{\partial h}\right)\frac{dh}{dR} + \left(\frac{\partial c}{\partial(\Delta c)}\right)\frac{d(\Delta c)}{dR}.$$

The coefficient of dz/dR is of course just the gradient, $G(z)$. Now we can set dc/dR = 0 and solve for dz/dR, which will tell how the depth of a particular contour changes with range in terms of the parameter changes. Thus we have

$$\frac{dz}{dR} = \frac{-1}{G(z)}\left\{\left[\frac{2\Delta c}{h \cosh^2 \frac{2}{h}(z-z_0)}\right]\left(\frac{dz_0}{dR} + \frac{z-z_0}{h}\frac{dh}{dR}\right) + \left[1 - \tanh\frac{2}{h}(z-z_0)\right]\left(\frac{d(\Delta c)}{dR}\right)\right\}.$$

If we consider for a special case a thermocline variation such that $\frac{d(\Delta c)}{dR} = 0$, we can describe a change in the thermocline with range by a descent of z_0 accompanied by a steepening of the gradient at z_0 by a decrease in h. This choice would not be expected for a temperature diffusion process but could occur for a downward displacement of the water layer. In this case, for z greater than z_0 all the terms in dz/dR are positive and we find the sign of dz/dR depends only on the sign of $G(z)$. Therefore the contour of constant c should rise for depths just below the sound-channel axis wherever a contour just above the axis descends, as exhibited in Figure III-2 near SVP #380.

If at some depth below the sound-channel axis dz/dR = 0 for all ranges, then for the above type of thermocline motion we would have the condition that

$$\frac{dz_0}{dR} = -(z-z_0)\frac{dh}{h\,dR}.$$

Solving for this depth, we get $z = z_0 - h\frac{dz_0}{dh}$ in which we put $z_0 \simeq 800$ meters, $h \simeq 800$ meters and $\frac{dz_0}{dh} \simeq -1$, all of which are reasonable for the middle Atlantic Ocean. This

indicates that for thermocline changes with range of this type,
there should be a depth below the sound channel (1600 meters)
that will have a minimum fluctuation. This condition occurs
in the data reported later (in Section III)   around 1800
meters and it has been noted in earlier measurements (Beckerle,
1965).

The Yo-Yo Experiment

In this section measurements of the fluctuations of sound
velocity while the ship kept a fixed location off Argus
Island are presented. The measurements were obtained during
a test of a new technique, that of raising and lowering our
sound velocity profiling instrument repeatedly.* The measure-
ments were not taken over a long period of time since this
was merely a test of the technique. However, we admit having
had a sense of technical achievement as the on-line computer
presented us with a plot clearly showing the two-hour period
variations of the sound velocity structure that results
from internal waves. Included in this section is a recomputed
graph of the fluctuations of sound velocity, which should
give some appreciation of the temporal inhomogeneities that
scatter sound in this depth interval.

Previously, records of sound-scattering inhomogeneities
in the upper ocean were available from thermistor chain
measurements. (The thermistor chain technique was developed
at W.H.O.I. and early work was reported by R.M. Snyder (1961)
and Hubbard and Richardson (1959) of W.H.O.I. and later
the technique was used to advantage by the LaFonds (1966).)
The "Yo-Yo" technique has an advantage of providing continuous
measurements in depth, covering any interval of 500 meters in
a time-period comparable with almost all of the most rapid
internal-wave oscillation that occurs in the ocean. These
two methods present complementary aspects of the fluctuations,
one more spatial and the other more temporal in character.
Although these sound velocity series were too short a sample
to justify any extended analysis (five hours), they did

----

*Since these measurements, this method has been used extensively
 by other researchers independently.

stimulate some questions that are presented briefly below
along with some attempts at answers and some speculations.
These are offered to encourage experimental work in this
area. But first we point out that in measurements of
internal waves from ships there are difficulties in holding
the ship in position. Moreover, the question of whether
the data would be more suitable for analysis if the
recording system drifted with the water rather than
maintaining as fixed a position as possible, is far from
settled.

(a)   Observations

Continuous sound speed measurements were made at a
position about eight miles south of Argus Island by lowering
and raising the sound velocity profiling system between 50
meters and 260 meters in so-called Yo-Yo fashion (June 22,
1966). The period of the cycling was 4.7 minutes (top to
bottom) and the sequence continued for five hours. An on-line
computer display of the sound velocity variations was obtained
during the operation and internal-wave fluctuations were
observed in these records. The data were also recorded on
digital magnetic tape and contours of equal sound velocity
were recalculated and plotted using the W.H.O.I. computer
facility. The measurements obtained while raising the
instrument were omitted because the instrument frame carried
some water along with it that effected the sound velocity
measurements slightly. Figure III-4 presents the variation
of the depth of the sound velocity isolines as a function
of time.

(b)   Some Comments on these Observations

The variations observed in Figure III-4 depend on the
influence of turbulence (or internal waves), but the changes
of sound velocity with depth depend on the pressure. This
effect amounts to about one meter per second in a depth of
sixty meters. It is not insignificant in comparison to the
variations in Figure III-4. For instance, the vertical
separation between the 1524- and 1523-m/sec isolines at
one hour is about sixty meters. Accordingly, the change

indicated might be explained as due to a temperature decrease
with depth of nearly one-half degree C neglecting salinity
effects. The corresponding temperature change at the top
of the record, between 1529 and 1528 m/sec is nearer a one-
quarter degree C change.

There are several specific interpretations to be made
with respect to the data shown in Figure III-4:

1) The depth fluctuations of the sound velocity isolines
with time show a peak-like character facing upward and a
smooth character on the underside in many instances (see for
example the contour of 1528 m/sec.). Since the sound speed
decreases with depth, such fluctuations correspond to vertical
water displacements that are in the opposite direction. A
trochoidal wave has a similar shape.

2) Portions of internal gravity waves of several hours'
period are revealed by changes in the vertical spacing of
the isolines as for example between the 1527 and 1526 m/sec
isolines. In the depth interval near 180 meters where the
sound velocity gradient is small there are patches where the
speed is slightly greater than 1523 m/sec. Two such regions,
at one hour, and two and one-third hours, after start time,
suggest a period of about eighty minutes in these fluctuations.
Periods that are close to being integral fractions of this
are readily observed as smaller-scale fluctuations in the
several contours.

3) Larger amplitude fluctuations occur in regions where
the sound velocity gradient is weaker. This is expected
from internal wave theory (Eckart, 1961) and has significance
in sound scattering.

4) A hint of an interesting wave interaction is indicated
in the region of the dashed curve A, B, C, D (in Fig. III-4).
Observe the change in the period between AB and BC. A curve
A, B, C, D was drawn through the apex of the points so labeled.
The downward and upward movement of water estimated by
measuring the slopes of this curve at A, B C, and D are
related to the actual water movement just before and following
each point given by the slopes of the 1529-m/sec sound velocity
isoline.

Despite the graphical approximations made, it appears from the estimates of water motion in Table III-1 that the observed motion is influenced by the presence of a larger internal wave (the dashed curve). Accordingly, the upward speed before point A is smaller in magnitude than the observed downward speed following point A by approximately twice the downward speed of a larger scale water movement. This kind of observation should be expected with simple superposition of trochoid-like waves.

TABLE III-1   ESTIMATED WATER MOTIONS

Point	Upward Speed Before Point m/hr	Dashed Curve Speed at Point m/hr	Downward Speed After Point m/hr	Calculated Downward Water Speed m/hr
A	28	- 19	- 64	-28+2(-19)= -66
B	30	- 8	- 51	-30+2(-8)= -46
C	29	+ 1	- 25	-29+2(+1)= -27
D	47	+ 6	- 33	-47+2(+6)= -35

The period of time between crests of the 1529 m/sec isoline given by AB, BC, and CD decreases during the portion where the dashed wave is descending, revealing a kind of scattering of longer period waves into shorter period waves. There is some suggestion that this is followed by the reverse sequence. Something like these fluctuations in the depth-time isolines has been observed in depth-distance contours of temperatures obtained with towed thermistor chain measurements from CHAIN Cruise #17 (Fig. III-5). A scattering process like this has been described theoretically by Eckart (1961) and Phillips (1966) as a resonance interaction process, however, our data are too limited to establish a definite connection.

Several large dashed curves, such as AA', have been sketched through the observations in Figure III-4 and these also suggest that the small-scale fluctuations are the result of an interference of much larger-scale waves. The dashed curve AA' was drawn in the direction of the slopes of some of the sound velocity isolines but can be seen to cross others, namely, the 1528-and 1525-m/sec isolines. These and similar correlations found elsewhere in the observations, stimulated consideration of an idealized model of the interaction of two internal wave groups. Such a model is helpful in understanding the complexity of thermocline motions.

The property of nearly alternate crossing of isolines that can be seen in Figure III-4 can be explained qualitatively by supposing a linear superposition of upgoing and downgoing internal wave groups in a depth versus range plot. In Figure III-6 we present an idealized picture of these internal waves. Figure III-6 (a) shows an upgoing internal wave group where the phase of the waves propagates at right angles to the direction the group moves. The angle θ indicates the direction the group propagates from the horizontal. It varies as $\sin \theta = \dfrac{\omega}{N}$, where ω is the circular frequency of the waves and N is the stability frequency of the water column. The frequency N increases as the group moves upward and therefore the trajectory for the group is curved. A near-surface reflected group returns with its group and phase propagation directions changed as in Figure III-6(b). The alternate flow of water in these groups therefore adds and subtracts to form cells as in Figure III-6(c). The direction of the net flow pattern in Figure III-6(d) exhibits an apparent alternate crossing of flow lines if one draws a path through several contours. A similar variation in appearance would be expected in a depth-time recording of this spatial pattern as it crossed a given position, as can be seen in Figure III-4. Much larger downward-dipping dashed curves have been sketched through the isolines in Figure III-4, suggesting the possible interference of large waves.

In summary, the analysis of the Yo-Yo data has led
to some interesting conjectures about wave processes in the
ocean. It appears that the layers in the ocean are continually
in a near-breaking internal-wave state, giving rise to a zone
of near isothermal water separated vertically and horizontally
by zones of strong vertical temperature gradients. The pheno-
menon has a distribution dependent on the interference and
possibly non-linear interaction of internal wave groups.

The Broad-Area SVP Investigation

ATLANTIS II made a stop at Bermuda on June 23, departing
on June 26 to commence the second phase of the sound velocity
profiling work, as shown on the Track Chart (Fig. I-1). This
phase of the work was interrupted by a short stop at San Juan
from July 15 through July 18 and was terminated on August 4
at Bermuda.

The Sound Velocity Profiles obtained during this phase
of the cruise are spaced 65 nautical miles apart on the rhombic
grid pattern. The individual SVP's are collected in Part II
of this report. Here we relate this data to our study of the
ocean.

The ocean is a three-dimensional space whose properties
are changing in time. The expectation is that the major
properties of this area do not change much during the duration
of the cruise (7 weeks). In order to help in the interpretation
of the sound velocity data, it is examined in different ways.
First we can plot contours of equal sound velocity at several
depths. Then the vertical variation in sound velocity is
examined for each leg of the cruise.

(a) Spatial Variation

One way of presenting these data is to examine the
sound velocity in a horizontal plane at a fixed depth. For
the depths of 200, 600, and 800 meters, the sound velocity
contours for the area covered in this cruise are shown in
Figures III-7, III-8, and III-9. These depths are above the

main thermocline (200 m) and near the top (600 m) and near the bottom (800 m) of the main thermocline. If a depression in the thermocline region is associated with a circular flow in the clockwise direction (Defant, 1961) the pattern of contours can be interpreted as large circulating masses of water with both clockwise and counterclockwise rotations which vary with depth. These figures show that the motion in this region of the Sargasso Sea is quite complicated.

The contour chart for a depth of 800 meters, Figure III-9, indicates a large-scale north-south oscillation or meander of the main thermocline just south of 30°N latitude. High and low regions of sound velocity are indicated in the figure. The separations between "high's and low's" indicate a spatial wavelength of about 240 nautical miles (Beckerle, 1966b)

A comparison of these sound velocity contours at 800 meters' depth with mean surface temperature contours reported in "The Gulf Stream" (Monthly Summary of the U.S. Naval Oceanographic Office) for August 1966, reveals a similarity. In a figure in that report there are large meanders (four degrees of latitude) in the 82°F mean temperature contour having an estimated wavelength around 240 nautical miles. This surface temperature pattern is shifted somewhat north of the sound velocity meander pattern at 800 meters in Figure III-9. A considerable effort went into near-surface temperature measurements during cruise ATLANTIS II #22, and a comparison of deep, sound velocity measurements and shallow temperature measurements are made later on in this report.

The contours in the 800-meter sound velocity pattern are assumed to be parallel to the direction of current flow under the assumption of near-geostrophic balance. The arrows indicate clockwise circulation around areas of high sound velocity. Arrows were also inserted on a similar contour plot from the June 1964 data obtained during ATLANTIS II Cruise #11 for which there was some confirmation from current measurements using moored buoys (Beckerle, Reitzel, et al, 1966) The justification

at this point for treating contours of sound velocity as
indicating near-geostrophic flow directions is weak and
merely follows from the fact that sound velocity in sea
water increases with temperature. Temperature contours
have been used by oceanographers in the past to indicate
flow directions when measurements leading to density or
pressure were not available.

An average westward direction of flow is suggested
by the arrows for the 800-meter depth chart for the region
of the 240-nautical mile wave near 28°N latitude although
the flow line undergoes considerable north-south meander.
There are indications of this also in the 600-meter depth
chart, Figure III-8, although the contour reaches south as
far as 25°N latitude.

In this same latitude region, the contour pattern for
the sound velocity nearer the surface (at 200 meters) that is
shown in Figure III-7 suggests a nearly geostrophic flow in
an eastward direction (see the oscillation of the 1523-m/sec.
contour east of 70°W longitude). Further on in this report
we will interpret an isothermal surface obtained from numerous
BT's as indicating an eastward flowing current in the thermal
front zone (latitude 28°N). In several near-surface studies
of this thermal front region the meandering current directions
were, on the average, eastward (see Voorhis, 1965; Beckerle,
1968a; Katz, 1969) in agreement with Rossby wave theory.

Some additional support for a counterflow at greater
depth below the thermal front zone is suggested by the line
of sound velocity profiles obtained across this zone in ATLANTIS
II Cruise #11 in 1964 reported by Beckerle (1966b). In these
data it was observed that the water was colder on the southern
side of the thermal front at a depth of 400-600 meters.
Measurements obtained near the surface across the thermal
front have usually reported warmer water located on the southern
side of the frontal zone (Voorhis, 1965; and Katz, 1969).

The eastward flow direction indicated by the contour
patterns in the upper layer at 200 meters' depth and the westward
direction for the lower layer at 800 meters' depth can be
described conveniently in terms of an alternating double vortex
row. Barkley (1968) recently advanced a similar viewpoint with
regard to the Kuroshio-Oyashio Front. He points out a well-
recognized failure of the model in that the vortex array
propagates to the east, whereas the movement of the front
ought to be westward according to Rossby wave theory. However,
without addressing ourselves to this question and without
introducing any mechanism for the generation of the thermal
front zone (such as wind stress curl at the boundary between
the trade winds and westerlies) consider an alternating array
of vortices (Figure III-10(a)) with clockwise vortices located
on the southern side. There are two flow directions compatible
with the array of vortices. An eastward-flowing jet is drawn
as the solid wavy curve and a westward flow with a large north-
south meander is indicated by the dashed curve. In Figure
III-10(b) we have drawn these two flows above and below an
oscillating isothermal surface considered as separating the
ocean into two depth intervals. This picture is consistent with
our discussions concerning the contour patterns of sound velocity,
but it has several shortcomings.

(b) An Intense, Deep Anticyclonic Eddy

In Figure III-9 the relatively intense "high" (value of
sound velocity) located at approximately 28°N, 66°W was contoured
with dashed lines in order to indicate that the data supporting
the contours and the contour-spacing chosen depend to a great
extent on SVP #438. Therefore, we examined carefully the
reliability of this sound velocity profile. We have found no
reason to suspect the data, although it is very different from
other sound velocity profiles. Some description of the evidence
follows.

Supporting the reliability of SVP #438 is the fact that
the sound velocity profile made during descent of the instru-
ment compares closely with the measurement obtained during its
ascent. These two measurements are independent. The plots of
SVP #438 up and down that were obtained aboard ATLANTIS II from

the on-line computer system are shown in Figure III-11. They
are essentially the same within the resolution of the scale of
the plot. Moreover, since instrument depth is obtained from
a measurement of acoustic travel time to the ocean surface,
there is no possibility of having a serious error in depth that
could not be readily recognized. For this reason the reliability
of the measurement technique is superior to that of the present
state of the art that depend solely on pressure sensors.

The relationship between SVP #438 and neighboring sound
velocity profiles can be observed in Figure III-12. In
particular, notice the relationship of SVP #437 and SVP #438,
above and below the 320-meter depth. The sound velocity
profiles to the east and west and south of SVP #438 in Figure
III-12 exhibit a more typical character for the Sargasso Sea
water.

The depression of the thermocline in SVP #438 extends
over 100 meters deeper than that observed in SVP #437 which
was located about 65 miles north of it. The increase in the
value of the sound velocity at the knee near the depth of
650 meters over that in the other profiles, and the greater
depth at which this knee occurs in SVP #438 can be shown to
be due to the influence of the dependence of the sound velocity
on water pressure and to the effects associated with a marked
depression of the water mass. Moreover, the minimum sound
velocity which occurs on SVP #438 at 320 meters also has the
same value and depth in SVP #437. The large descent and the
steepening of the main thermocline should be expected in a
large, intense, anticyclonic eddy for a stratified ocean,
as was pointed out by Defant (1961).

A simple qualitative sketch appropriate to a clock-
wise vortex in a two-layered ocean is shown in Figure III-13.
The interface shows a depression when the rotational velocity
in the upper layer is greater than that in the lower, more
dense layer. In the event that the vortex motion in the lower
layer near the core has a greater rotational flow than the liquid
in the upper layer, then the interface would be deformed upward
as shown (Neumann and Pierson, 1966).

(c) Variations of Eddy Circulations with Depth in the Ocean

We continue our examination of the 800-meter sound
velocity contour chart, Figure III-9, using the interpretation
concerning the direction of circulation of water described
previously. We will make a judgment that greater circulation
(intensity of an eddy) is indicated when there are more contours
encircling a region.

Just south of the 1504-m/sec closed contour for the
800-meter depth in the center of the survey, there exists a
region of low sound velocity (four closed contours) where the
direction of flow is suggested to be counterclockwise. To
the east of this circulation there appears to be a weaker
clockwise circulation consisting of a single closed contour
of 1502 m/sec. The contours of sound velocity at 200 meters
are shown in Figure III-7. In this chart the clockwise and
counterclockwise circulations at latitude 24°N that correspond
to the closed contours just described with regard to the 800-
meter depth are markedly changed in intensity. The counter-
clockwise circulation is relatively weak (consisting of only
one closed contour, 1524-m/sec) while the clockwise circulation
consists of many closed contours. This striking variation of
the intensity of eddies with depth can be observed in many of
the eddies in the Sargasso Sea.

The intensity suggested for the eddy at approximately
24°N 66°W in the 200-meter depth chart, depends critically
on the correctness of the 1533-m/sec sound velocity measure-
ment indicated. For this reason a discussion of this measure-
ment and the surrounding observations will be offered later
(see "Temporal Variations"). On comparison, the intense eddy
at 800 meters located at 28°N 66°W described earlier appears
very weak on the 200-meter depth chart (a single contour of
1524 m/sec). This appearance is in part due to the existence
of the well-known thick layer (or lens) of nearly isothermal
water that occurs near this latitude. The isothermal layer
thickness is almost 400 meters at 28°N, but is much thinner
to the south around 24°N.

(d) The Relationship of Sound Velocity Contours and Bottom
     Topography

     Some contours at 800 meters in Figure III-9 appear to
be related to the passages through the Bahama Bank, namely
those contours near Mayaguana Passage, Caicos Passage and
Mouchoir Passage. In particular, notice the 1496-m/sec
contour near Silver Bank Passage. These contours were
drawn from the data before the island passages and Silver
Bank were indicated. This kind of comparison with bottom
contours was made earlier of measurements from ATLANTIS
obtained in 1962 and from ATLANTIS II Cruise #11 obtained
in 1964 (Wilson and Beckerle, 1965), although there was
need for additional supporting evidence.

     In the horizontal contour charts for 200 meters and
600 meters (Fig. III-7 and III-8) the relationship to the
passages appears more striking. For example, the 1527-m/sec
contour at Mouchoir Passage in the 200-meter depth chart
suggests that at this level flow is out of this passage
and circulates clockwise around an intense eddy at 24°N
66°W eventually to flow toward Puerto Rico. In the corresponding
areas of the 600-meter depth chart the contours suggest a flow
(see 1512-m/sec contour) that is southwesterly around the clock-
wise eddy at 24°N 66°W, then counterclockwise around the eddy
at 27°N 68°W before flowing southward into Mouchoir Passage.
That the sound velocity contour patterns should suggest nearly
opposite flow directions at two different levels in the ocean
and through the same passage is quite significant. There is
evidence for different flow directions for different depths in
the ocean as indicated from these sound velocity contours and
from current meters on ATLANTIS II Cruise #11. Unfortunately,
we were unable to make current measurements during ATLANTIS
II Cruise #22. The 600-meter depth chart also suggests that
flow is out of Caicos Passage northward and that it eventually
turns around and returns to Crooked Passage. A similar pattern
is suggested by the 800-meter chart.

The flow pattern suggested by the shallower 200-meter chart is out of Mayaguana Passage and Caicos Passage and northward, becoming part of the eastward-flowing water in the thermal front zone around 28°N latitude.

Lamb (1932, p. 333) gave mathematical solutions for free steady fluid motions that indicate the flow tends to be directed along bottom contours. Others since 1932 have explained flow along contours using conservation of potential vorticity, a concept introduced into oceanography by Rossby (1939) and recently reviewed by Platzman (1968). Warren (1963) applied this theory of the conservation of vorticity in connection with the Gulf Stream meanders and bottom topography. Welander (1968) used conservation of potential vorticity in studying deep-water circulation around the Mid-Atlantic Ridge. Rhines (1968) has described theoretically the various influences of large and small topographical changes on steady and transient circulation patterns. Rhines (1968) points out that very small topographic features on the ocean bottom can have effects on flow patterns since the size of the relative depth change is proportional to the ratio of the frequency of a vorticity wave to the Coriolis parameter. Thus, long-period Rossby waves will be influenced by small and gradual variations in the ocean depth.

When streaming is nearly geostrophic then the flow direction along a line of constant f/H should be such as to keep smaller values of f/H to the right, in the northern hemisphere. Here by f we mean the Coriolis parameter and by H the water depth. Thus circulation tends to be clockwise around a depression in the bottom and counterclockwise around a mound (when the change of f is small compared to the changes in H).

A simple rationale for the influence of a seamount or a bottom depression follows from the heuristic argument that as water moves toward a region of shallower depth, the flow speed tends to increase in order to keep the same total momentum transport. The Coriolis deflection of the flow to the right is increased because of the higher speed of flow. The deflection to the right decreases when the flow is slowed

as the water deepens on the other side of the seamount or as the water flows over a depression in the bottom. Streamline patterns similar to the illustration for a depression in the bottom (Fig. III-14) should be expected and the pattern orientation depends on the flow direction. The partial deflection of a streamline such as AA' results from the change in depth under the path.

The pattern of flow in the area 20°-25°N and 65-70°W at 200 meters (Fig. III-7) would be expected for an eastward movement of water, given the ocean depth variations in this area. A similar statement can be made about the contour pattern for the 600-meter depth (Fig. III-8) with a general flow direction toward the southwest. Specifically, the center of the clockwise eddy (labeled 1533 m/sec in the 200-meter chart) at 24°N 66°W is located at the western boundary of the deep 5800-meter depth contour in Pratt's chart (Pratt, 1968) (Fig. III-15). This is just to the east of the Vema Gap. In addition, the low value in sound velocity (counterclockwise flow) near 24°N 68.5°W is located in the region of a broad mound according to Pratt's chart. The 1512-m/sec contour around this low in the 600-meter chart might well be related to the rise in the bottom defined by the 5400-meter depth contour. We suspect that the circulation has an important influence on the bathymetry and deposition of sediments, as well as the converse, that bathymetry influence circulation.

There are numerous other places where the contour patterns of sound velocity obtained from the cruises ATLANTIS II #11 and #22 can be brought into somewhat convincing corre-lation with bottom contours. In some instances however, the contour gradients are abrupt so that non-geostrophic flow (i.e. flow crossing the contours) takes place. This com-plicates the interpretation of flow directions (see Welander, 1968). We will consider the effect of topography on flow of water again when we describe the isothermal surface obtained from BT measurements throughout the cruise (Section IV).

Some data suggest that features of the horizontal sound velocity pattern might have considerable permanence. As pointed out before, the intense counterclockwise eddy suggested by the low in sound velocity of 1494-m/sec in Figure III-9 (the 800-meter chart) is approximately located over an extensive sea mound at 23°N 68°W. This eddy might have a tendence to stay in that location since a pronounced low in sound velocity at this same location was reported from the ATLANTIS II Cruise #11 observations in June 1964 (Beckerle, Reitzel, et al., 1966). In addition, a temperature-contour pattern obtained for the depth of 500 feet (150 meters) from extensive BT measurements with stations as close as thirty miles made in February 1964 and reported by B. Thompson (1965) is similar in shape to our June 1966 sound velocity contour chart at 200 meters (Figure III*7)in certain areas. In particular, a comparison of the results of measurements 2 1/2 years apart is shown in Figure III-16 of the contour shapes for sound speed and for temperature in the vicinity of 24°N 67°W and to the south and southeast, that suggest approximately the same flow pattern. The February, 1964 temperature pattern, if shifted northwestward for best pattern fit to the sound velocity contours, appears to relate also to Silver Bank. Moreover, the range of temperature change and sound speed changes as well as their values are in close agreement. Neglecting salinity corrections, the conversions that should help comparison are: 1520 m/s $\equiv$ 69.9°F$\equiv$21°C; 1530 m/s $\equiv$ 75.2°F $\equiv$ 24°C; 1540 m/s $\equiv$ 80.6°F $\equiv$ 27°C. Notice the temperature change from 76°F in the center of the temperature pattern to 66°F north of it relates approximately to a corresponding change of 1533 meters/sec. to 1522 meters/sec on the sound velocity chart. These several agreements suggest long persistence and that bottom topography tends to influence the circulation although the patterns undergo lateral displacement in position with season. Perhaps the great inertia of rotation of the circulation pattern once established, causes it to "remember" its shape even after it has been translated a considerable distance.

(e) Comparison of Collected Sound Velocity Profiles for Each Leg.

An appreciation of the spatial variations in the sound velocity as a function of depth can also be obtained by comparing collections of sound velocity profiles for each leg in the Track Chart, Figure I-1. The collected profiles are presented in Figures III-17, Leg 1 through Leg 10. A few remarks about the reliability of the data presented in these figures are appropriate here.

The data in the set of Figures III-17 represent those measurements made during the descent of the instrument package. Many sound velocity profiles were repeated as the instrument returned to the surface and the measurements on the way up agree substantially with the measurements on the way down. Accordingly, the variations indicated on the set of graphs are considered real in most instances. A few obvious exceptions occur. In Figure III-17 for Leg 6 the computer plotted a curve in error. The error is in the region above 500 meters, and it occurred in the computation of SVP #473. In Figure III-17 for Leg 7, the computer plotted the lower half of SVP #476 in the wrong position. In Figure III-17 for Leg 8, SVP's #456 and #458 were corrected in the upper region indicated, using some of the measurements obtained during ascent of the instrument. In view of the large amount of data presented in this set of figures, remarks will be made only about major features.

In the region above the main thermocline in Figure III-17, Leg 1, the profiles tend to form two groups. The group showing the secondary sound channel at 100 meters occurs on the northern side of the thermal front zone at 28°N latitude. This group also has the greatest descent of the main thermocline region for this leg giving rise to a large isothermal layer. Such a layer exhibits a gradual increase in sound velocity with pressure. Similar splitting into groups for the upper-ocean region can be observed in the collected sound velocity profiles for the other legs, see for instance, Figures III-17, Leg 2 and Leg 3.

The thermal front zone which extends about two degrees of latitude, seems to contain a layer of nearly constant sound velocity between 200 and 500 meters.

There are considerable variations in the set of profiles from one leg to another; for instance, compare the variations in the main thermocline that occur on Leg 1 with those that occur on Leg 3 and Leg 5. The variation in the depth of the main thermocline in the Sargasso Sea is well over 300 meters.

There are several sets of profiles, for example, for Leg 2, Leg 3, and Leg 7, in which there is a pinching or convergence of the profiles around the depth of 1800 meters since below this depth the scatter in the sound velocity profiles increases again for several hundred meters. A node at 1800 meters was observed in the line of sound velocity profiles obtained on CHAIN Cruise #47 in April 1965 (Beckerle and Bergstrom, 1967). The minimum variation at 1800 meters occurs in those collections of sound velocity profiles that do not exhibit large variations in the main thermocline, whereas the collections for Leg 1, Leg 5 and Leg 6, where the variation observed in the main thermo- cline along the leg is considerably larger than on the other legs, do not show this pinching or node point at 1800 meters in the profiles.

An explanation for the node at 1800 meters stems from the upward and downward movement of the main thermocline along the track coupled with a tendency for the gradient in the thermocline to become larger as the thermocline descends. This is a type of variation observed in large-amplitude thermocline motions as can be seen in the contour of Figure III-2 for the Bermuda Leg. In Figure III-2, in the main thermocline region, the spacing of the contours in this section is wider when the contours are shallower and conversely. When the magnitude of the descent of the main thermocline becomes too large, the effect of the steepening of the vertical gradient cannot compen- sate for the downward movement and the node at 1800 meters does not occur. Large vertical downward movements might be expected in a region where anticyclonic rotation is present.

Below the 1800-meter depth some of the sound velocity profiles show wide deviations from the rest of the collection. Notice in Leg 2 of III-17 that a particular profile namely SVP #411 deviates from the rest by two meters per second at depths between 2000 and 4000 meters. In Leg 3 another profile, SVP #424, deviates from the collection in the opposite way. In Leg 7 it is SVP #475, the southernmost profile on the leg, that has lower sound velocity values than the rest at depth around 3000 meters. The nearness of steep boundaries such as the Bahama Bank in the vicinity of SVP's #410, 411, 424, 425, and

426 is an important factor affecting the sound velocity deep
in the ocean. On Leg 10 (Figure III-17) SVP #447 is shifted
considerably toward lower sound velocity values from the others.
This profile is located over the Puerto Rico Trench. We have
not been able to attribute this anomolous profile to malfunction
of the instrument. At 620 meters in SVP #447, there is a large
decrease in sound velocity with depth.

Variations near the Bahama Bank and near the edge of the
Puerto Rico Trench appear in the hydrocast observations of
temperature reported in Fuglister's Atlas (1960, p. 33) at
24°N and 74°W to 65°W. In addition, Fuglister's Figure 51
shows a marked variation at 3000 meters in the north-south
line near the Puerto Rico Trench at 20°N to 21°N. Wüst (1963)
reported Antarctic bottom water in the Puerto Rico Trench.
More measurements are needed to relate properly water motion
and these changes in temperature and, of course, sound velocity
to their location near boundaries and in deeper water.

Several of the collections of sound velocity profiles
exhibit a node at 4200 meters; that is, the profiles seem to
pinch together and then diverge again. This pinching together
near 4200 meters occurs in Figure III-17 for Leg 5 and also
in some of the other scatter plots. The explanation for this
coming together of the group of profiles at as great a depth as
4200 meters is not known. It is probably not an effect of
the measuring instrument, although this cannot be entirely
ruled out at this time. An earlier version of the sound velo-
cimeter which had its transducers mounted on a thick metal
plate did undergo a bending under great pressures which altered
the sound speed measurement. The present instrument, a TR-4
manufactured by the NUS Corporation, does not have this limitation
although the effect of the pressure on the other instrument
design can be taken into account by calibration.

The node at 4200 meters may have something to do with
an adiabatic temperature increase that is known to exist in
very deep water where the up and down motion of the water is
small enough not to disturb the effect. For example, measurements
from hydrostation #419* on ATLANTIS II Cruise #11 in 1964 in the

---

*Obtained by R. Stanley

Puerto Rico Trench down to 8000 meters with Nansen bottles indicated a temperature increase with depth from 1.97°C at 5500 meters, to 2.4°C at 8000 meters. Although the adiabatic temperature increase resulting from compression of salt water at these depths seems to be a possible explanation for the node at 4200 meters, it does not account for the wide variation in the sound velocities at depths greater than 4200 meters which is exhibited particularly in the data of Leg 2 and Leg 5, and to a smaller extent on Leg 9 of Figure III-17. This variation in the sound velocity at great depth suggests that the density layers throughout the entire ocean column can at times undergo vertical motions of considerable magnitude. It is tempting to assume that the scatter obtained from the comparison of spatially separated sound velocity profiles relates to the temporal scatter one might expect to find at one location. Thus the increase in scatter of sound velocity variations as the depth increases from 4200 meters to the bottom may be due to turbulence (overturning) in the water close to the bottom that results from heat transfer from the bottom, or from a horizontal shearing instability caused by variations of the bottom depth and its physical properties as water slowly flows over it. Where the turbulence is least, around 4200 meters, one might expect the least amount of sediment and organic material since turbulent diffusion would be needed to balance out the settling. Consequently, one should expect an increase in particulate material in suspension as one approaches the bottom from 4200 meters. Eittreim, Ewing and Thorndike (1969) recently reported a nepheloid layer near the bottom in the western North Atlantic with a minimum of parti- culate material occurring near 4200 meters.

The collected sound velocity profiles do not show the spatial variation north to south. Consequently these data for the vertical section are presented in Figures III-18 for Leg 1 through Leg 10 as contoured sections. The data in this form will not be discussed in detail.

The vertical cross-section contours show the dip and rise occurring in the sound velocity contours in the sound channel region that was discussed in connection with the

Bermuda Leg. The contours for Leg 5 (Fig. III-18) show the pronounced dip in the main thermocline of SVP #438. In view of the wide spacing of the profile locations, sixty-five miles, it would be unlikely to have located a sound velocity profile at the place where the contour in Figure III-18 for Leg 5 has its maximum dip. Accordingly, we surmise that some of these dips in the contours might extend very deep in the ocean.

(f) Variations in the Minimum Sound Velocity

The variation in the minimum sound velocity that occurs at a depth of about 1200 meters, in Figure III-17, is seen to amount to about four or five meters per second. The magnitude of this variation can be described in terms of upward and downward movements of the main thermocline and the effect of the increase of sound velocity with pressure. A contour chart of the minimum sound velocity was plotted from the cruise data. This chart* is included as Figure III-19 and shows that there is a north-south spatial variation of the minimum sound velocity. This kind of information is useful in accurately positioning deep, neutrally buoyant floats for oceanic measurements using acoustic signals, as well as in improving the accuracy of locating the origin of explosive or impulsive signals for this region of the Atlantic Ocean.

(g) Temporal Variations

From earlier work in 1964 and 1965, we were led to the hypothesis that the internal Rossby-wave period we could find in this area of the ocean would be approximately three months. We hoped that this cruise of ATLANTIS II would be completed before large changes in the sound velocity structure could occur. As to shorter period waves, one might expect deep-ocean internal tide effects in the observations, since each leg of the cruise took about two days to complete. A study of deep-ocean tides in the hourly bathythermograph (BT) observations (more closely spaced than the velocity profiles) was made by

----
*The chart was contoured by Dr. T. Rossby.

examining the semi-diurnal fluctuations. It appears that
such fluctuations are not large enough to hinder interpre-
tation of depth contours in charts of constant temperature.
Accordingly, we assume the cross-section contour charts of
sound velocity for each leg of the survey are substantially
correct.

In order to measure what temporal changes there were,
a number of repeated sound velocity profiles were made near
the center of the survey area. The repeated profiles are
listed in Table III-2. Graphs of these sets of profiles are
presented as Figure III-20 (a-h).

Most often, the temporal variations of sound velocity
profiles show that the longer the separation in time between
the start of each profile, the larger the deviations between
the two profiles appear to be. One pair of profiles in
Figure III-20 was only a few hours apart while another pair
was about fourteen days apart. Similar behavior was described
in earlier work from ATLANTIS II Cruise #11 (Payne and Beckerle,
1966). In Figure III-20(e) the two profiles, SVP #446 and SVP
#474, which were taken fifteen days apart, exhibit a considerable
variation at great depth, although the sound velocity values
are coincident in the depth region near 2200 meters. We believe
this variation at great depth is real. Our confidence is
supported by the sound velocity measurements on the way down
as well as on the way up for each profile. That is, a compari-
son of the up and down measurements of SVP #446 agree, as do
those of SVP #478.

To further check temporal variations, a line of sound
velocity profiles diagonally crossing the survey area, indicated
by the dashed line in Figure I-1,was studied and is presented
in Figure III-21. As can be seen from the SVP numbering, the
southeastern portion of the ship's track is ordered in the
reverse in time from the northwestern portion. The profiles
in Figure III-21 are separated in time much more than those
along any one leg. Contours of each meter per second have been
drawn on the diagram in order to help establish the relationship
between the profiles. There is obviously a wide variation between

TABLE III-2

REPEATED SOUND VELOCITY PROFILES

SVP	DATE	TIME	TIME INTERVAL	III-20
400	28 June	0915	3 hrs.	(a)
401	28 June	1200		
415	2 July	1830	2 hrs.	(b)
416	2 July	2020		
441	12 July	0700	14 days	(c)
469	28 July	0020		
442	12 July	1534	14 days	(d)
470	28 July	0905		
446	14 July	0400	15 days	(e)
474	29 July	1915		
465	26 July	1700	6 hrs.	(f)
466	26 July	2250		
480	1 August	1255		(g)
481	1 August	1450		
482	1 August	1626		
483	1 August	1825		
484	2 August	0450	3 hrs.	(h)
485	2 August	0805		

successive profiles, particularly above the 400-meter depth.
There is an extraordinary change between SVP #442 and SVP
#447 exhibited by SVP #471. This profile does not have a
constant sound velocity layer around 400 meters and there
is a substantial change in sound velocity at 260 meters as
noted on the chart. One wonders whether or not SVP #471
is a reliable profile. Here again, the measurements on
the way down are in agreement with the measurements made
on the ascent. Moreover, in SVP #470, shown as a dashed
curve, the velocimeter essentially repeats SVP #442 after
a delay of fourteen days, and the same instrument measured
the anomalous SVP #471 only a few hours later!

It seems that the abrupt change in the sound
velocity at 260 meters in SVP #471 would be physically
reasonable, if there was an extremely large downward vertical
displacement of warm water due to anticyclonic rotation. The
200-meter depth sound velocity contour chart (Fig. III-7)
suggests anticyclonic rotation about the position. One might
expect the persistence of an intense eddy in the ocean to be
much longer than the cruise duration because of the great
inertia of the motion. If the eddy at SVP #471 were changing
position during this period, the similarity between SVP #442
and SVP #470, on its western boundary, would be unlikely.
There will be presented in Section IV additional independent
evidence from BT data concerning the existence of the intense
anticyclonic circulation revealed by SVP #471.

Another effort to separate the spatial and temporal
variations for this region of the survey is shown in the
horizontal contour chart for the 200-meter depth, Figure
III-22. The solid contours are taken from sound velocity
profile stations designated "early". The dashed curves show
what the contour pattern looks like when we also include the
sound velocity profiles which overlap the same region taken
later during the cruise. This procedure is possible because
of the interlacing of the tracks and the repetition of some
of the sound velocity profiles. Figure III-22 is interesting
in that the two sets of contours are reasonably related and
merely indicate the improved resolution in the contour pattern
possible with the use of the additional data. They do not show
any conflict in the two sets of data which we would expect if
there were rapid changes in the pattern with time.

LIST OF FIGURES

SECTION III   —   Sound Velocity Measurements

Figure

List of Figures
Section III - Sound Velocity Measurements
(continued)

<u>Figure</u>

SOUND VELOCITY (METERS/SEC)

W.H.O.I. S.V.P. 383
CRUISE A2,22
LAT. 301300 LONG. 662100
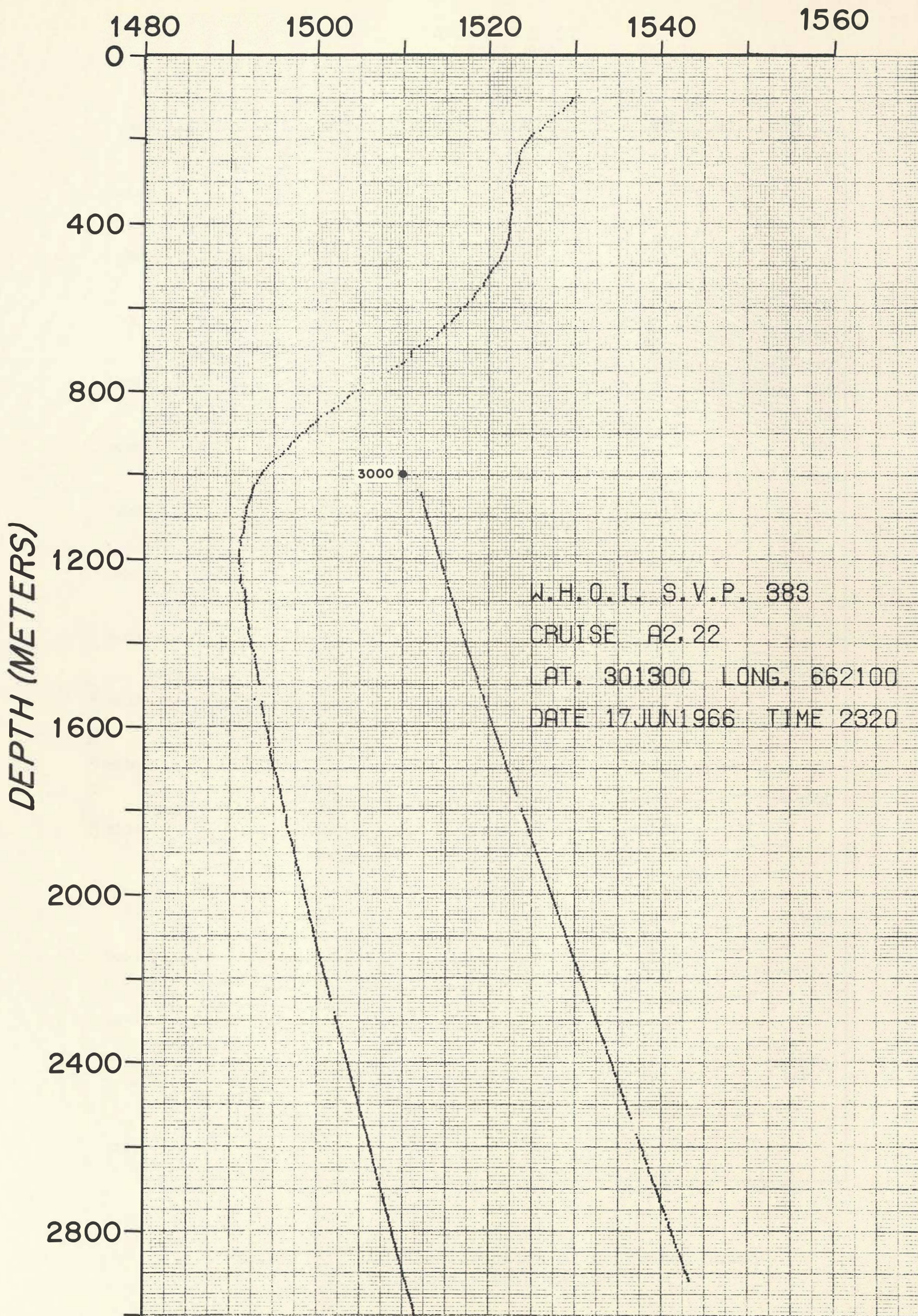DATE 17JUN1966 TIME 2320

Fig. III-1   Sound Velocity Profile #383.

ATLANTIS II - 22
SUMMER 1966

SOUND VELOCITY PROFILE NUMBER

Fig. III-2   Vertical Section of Contoured Sound
Velocity - Bermuda Leg.

RESULTS OF 8 YEARS OF SOUND VELOCITY
MEASUREMENTS NEAR BERMUDA (PANULIRUS)

POSSIBLE VERTICAL WATER
DISPLACEMENT TO EXPLAIN
STATISTICAL OBSERVATIONS
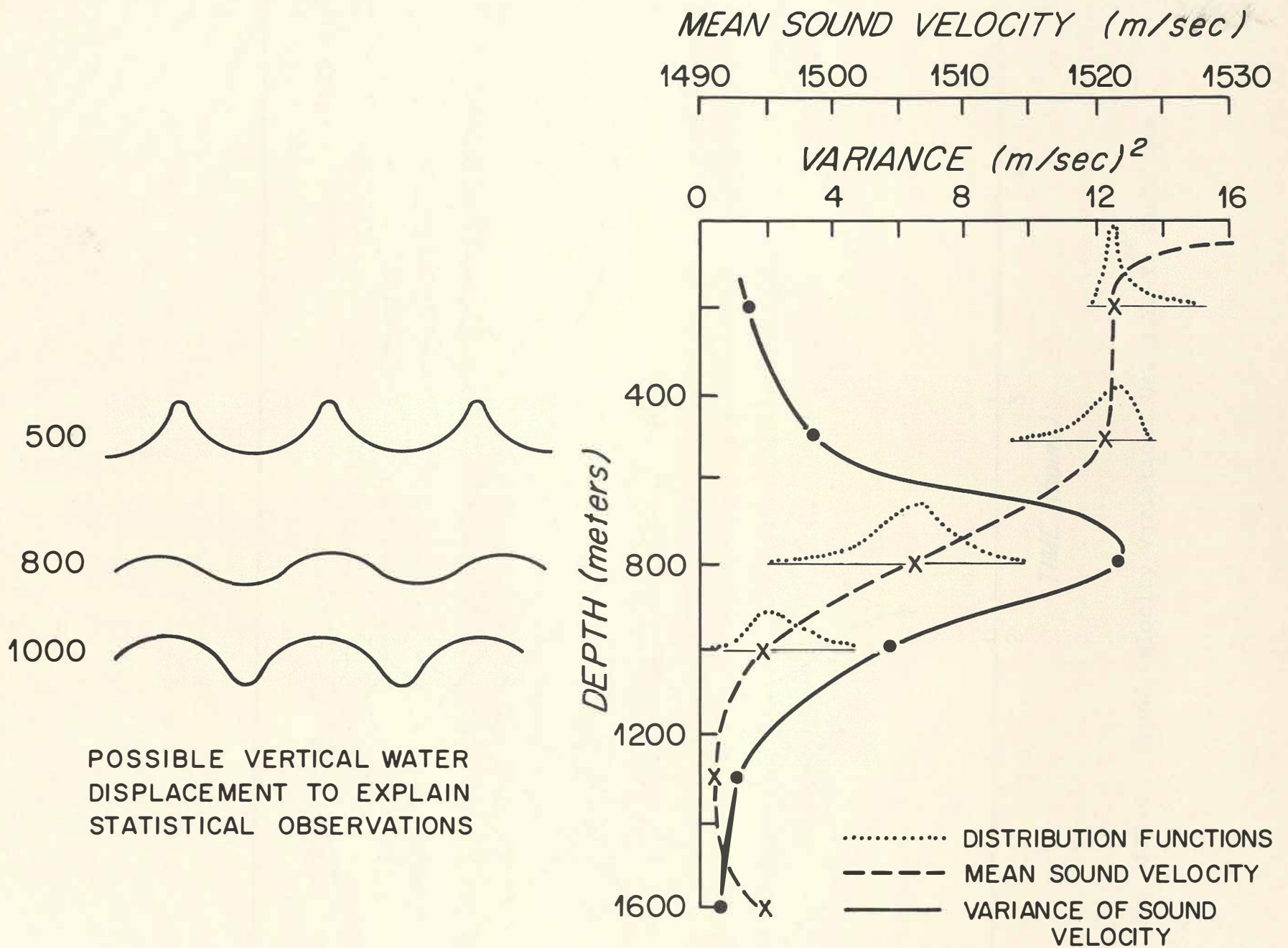
Fig. III-3   Mean and Variance of Sound Speed - Eight
Years of Observations from PANULIRUS.
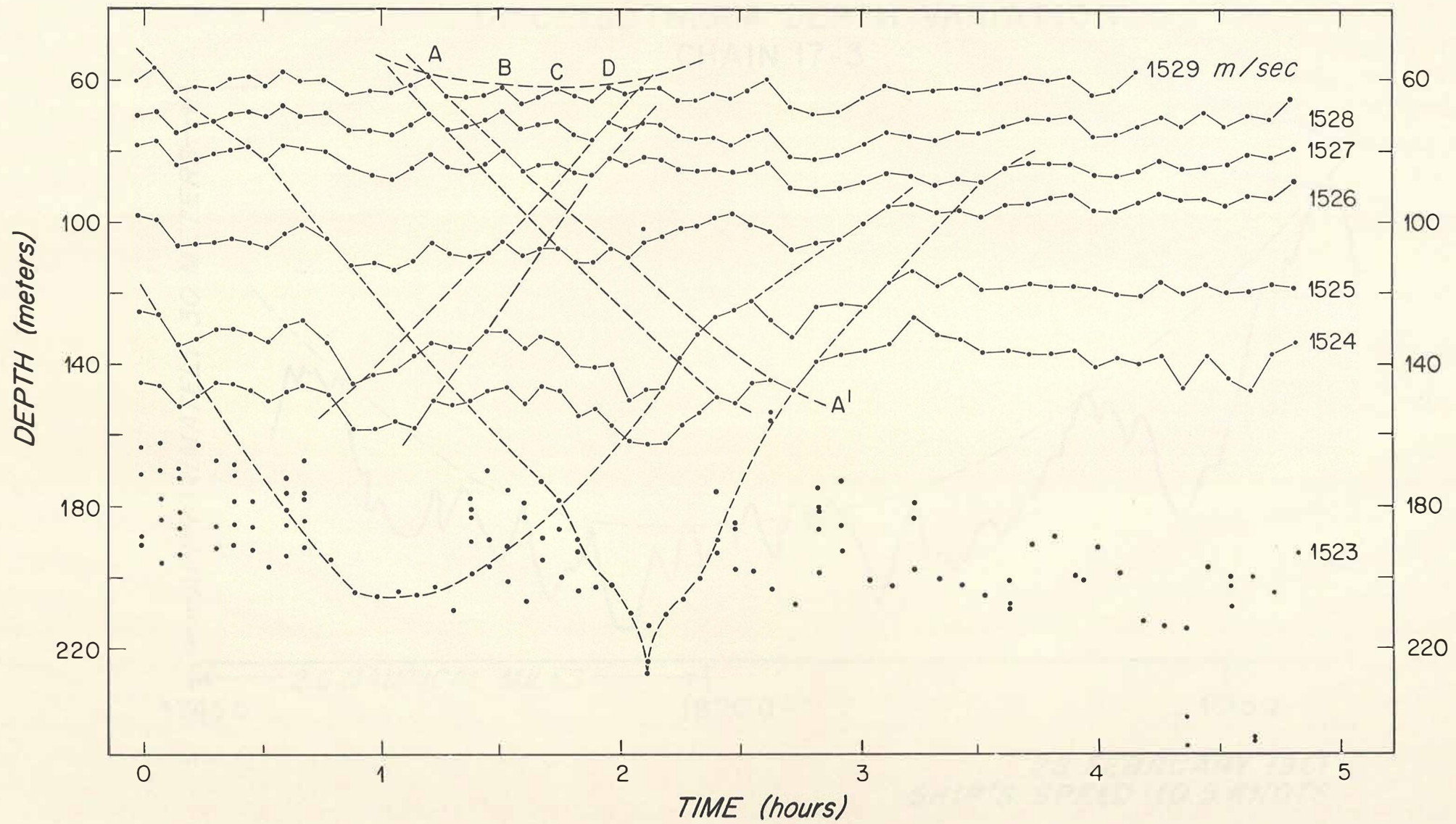
Fig. III-4   Sound Velocity Variations Using Yo-Yo Technique.

14°C ISOTHERM DEPTH VARIATION
CHAIN 17-3
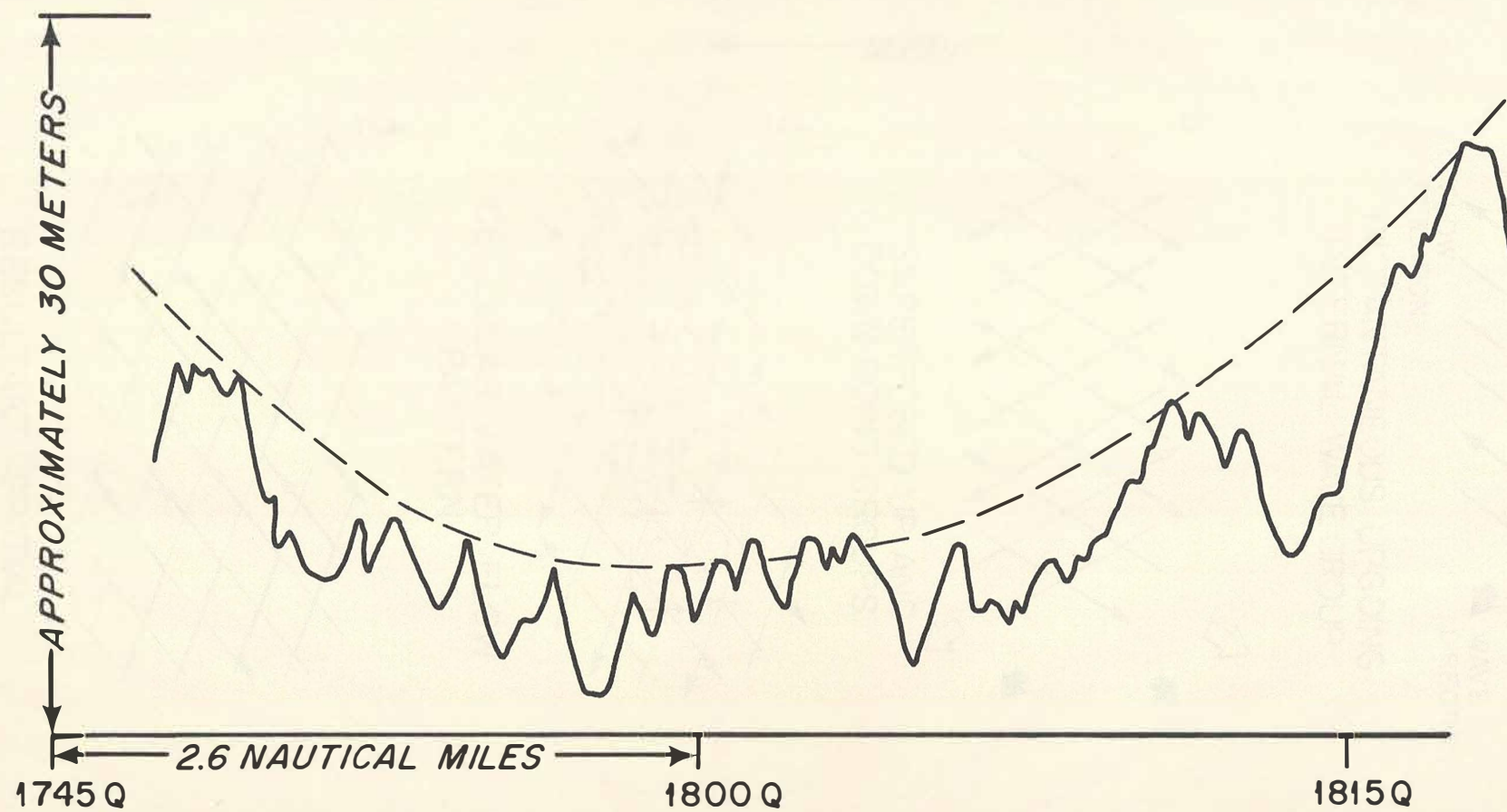
28 FEBRUARY 1961
SHIP'S SPEED : 10.5 KNOTS

Fig. III-5   14°C Isotherm Depth Variation Obtained from
Thermistor Chain Tow #3 on R/V CHAIN Cruise 17.

DISTANCE →

a GROUP DIRECTION

FLOW
DIRECTION

WAVE
DIRECTION

INSTANTANEOUS UPGOING
INTERNAL WAVE GROUP

DEPTH

b

SUPERPOSED UP AND
DOWN GOING GROUPS

c

CELLULAR WATER FLOW
PATTERN

d

RESULTANT SPATIAL
FLOW PATTERN
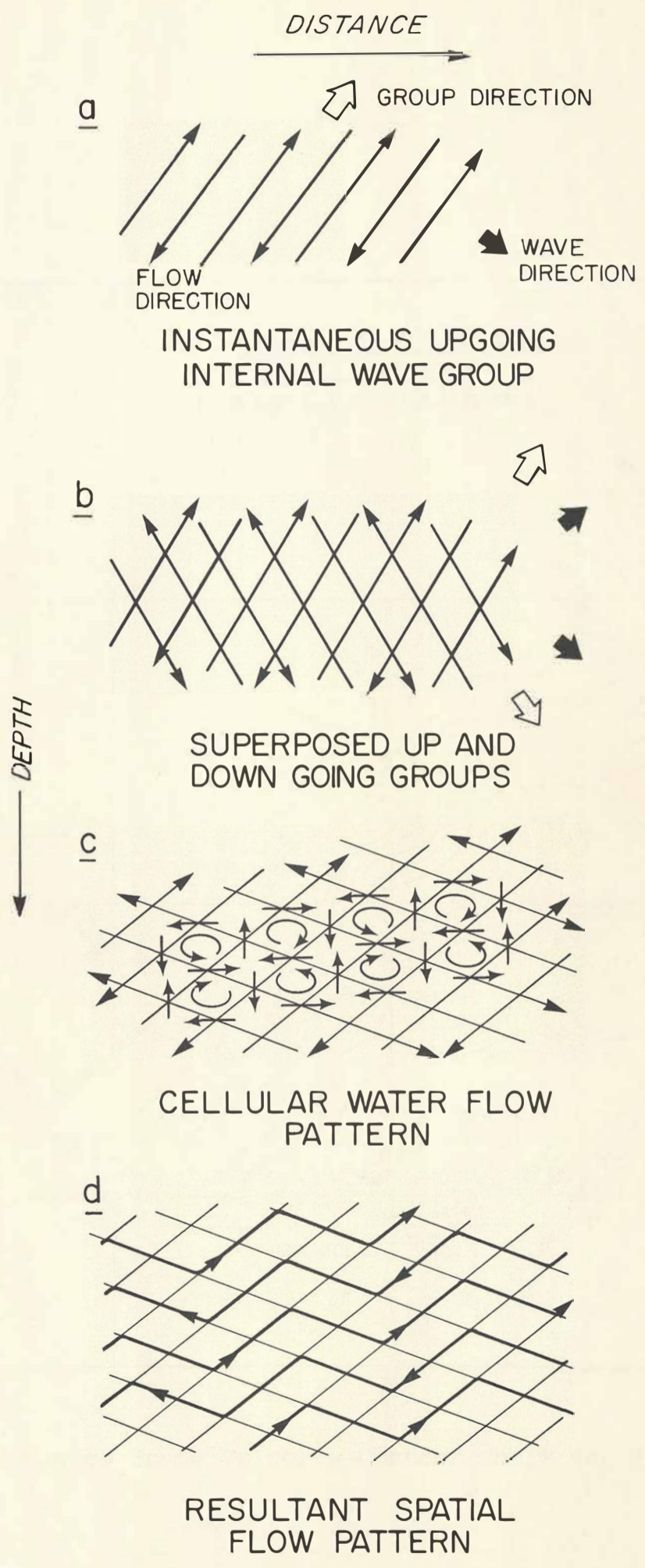
Fig. III-6   Idealized Internal Wave Interference.
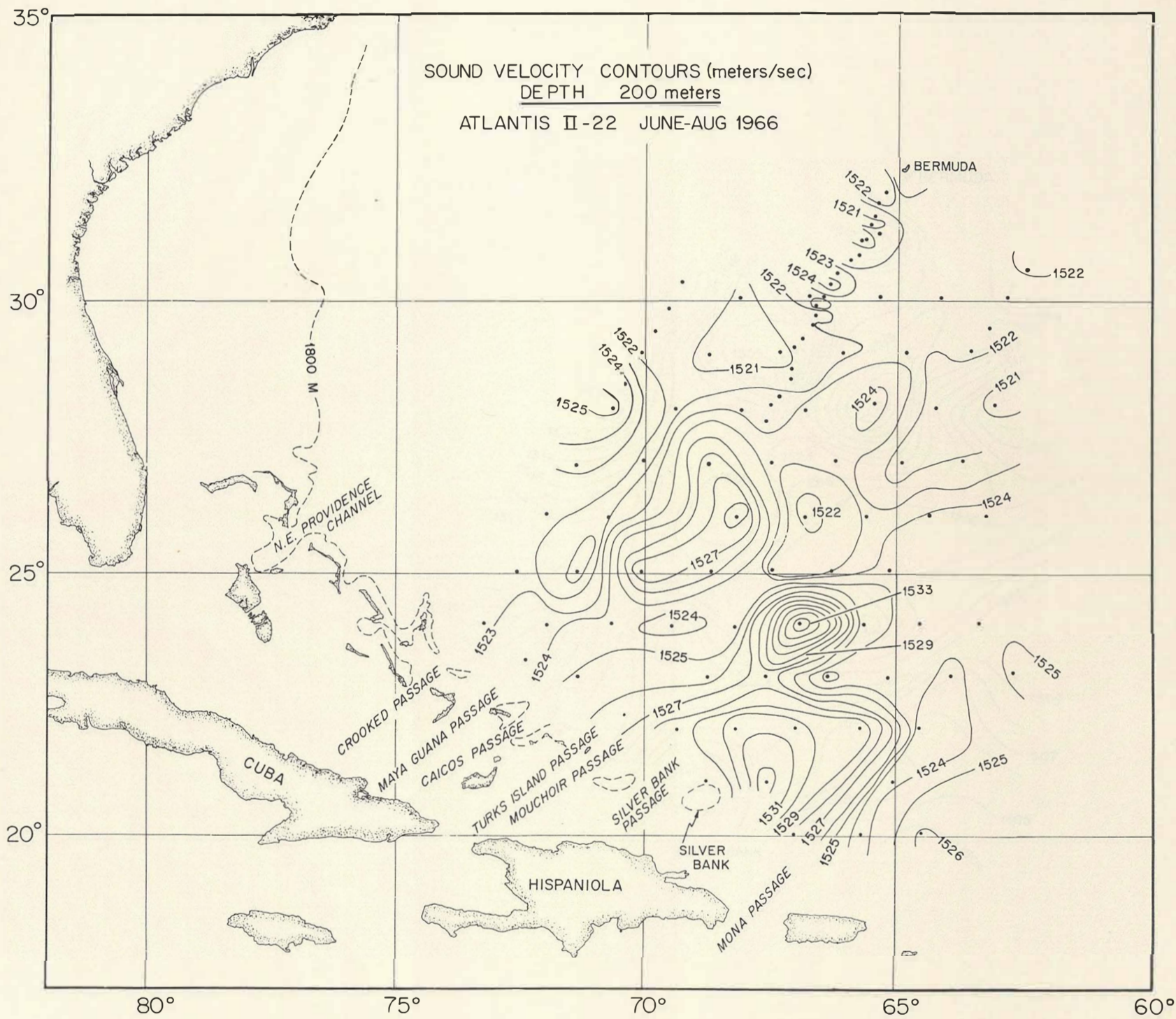
Fig. III-7   Broad-Area Sound Velocity Contour Chart for 200 Meters' Depth.
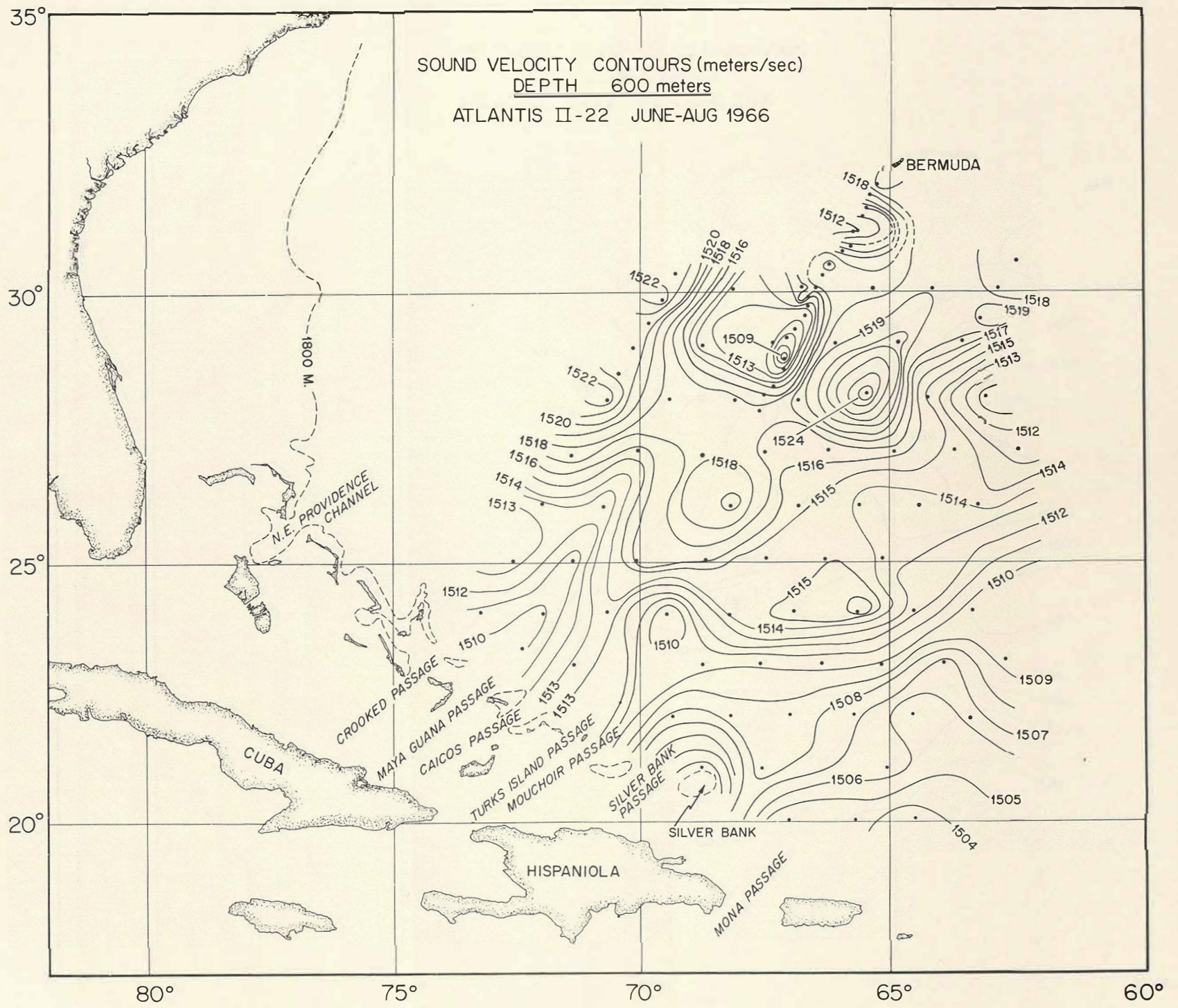
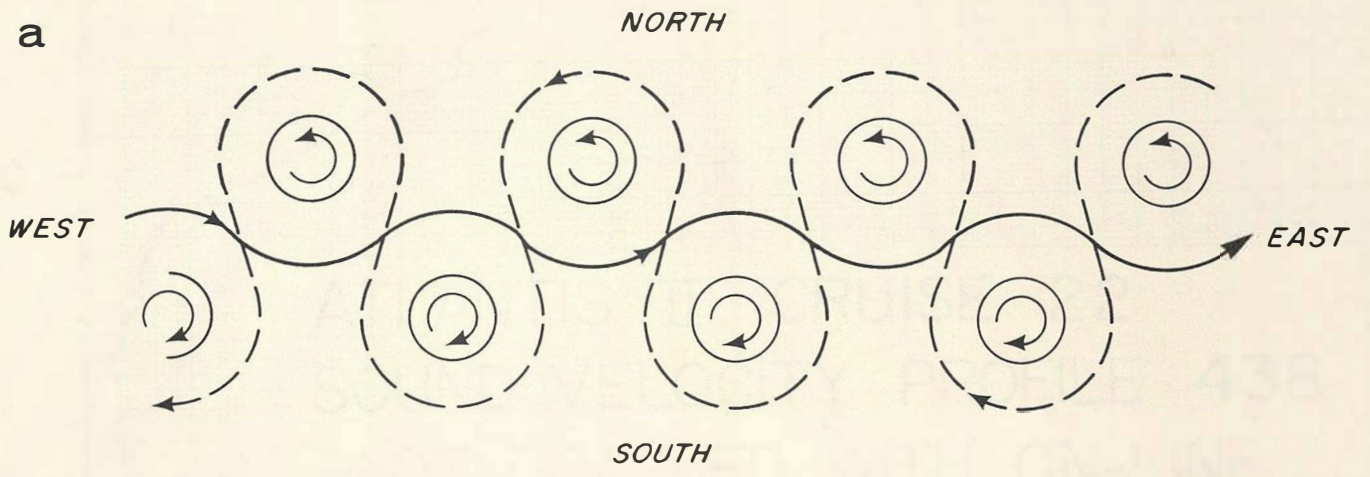Fig. III-8 Broad-Area Sound Velocity Contour Chart for 600 Meters' Depth.
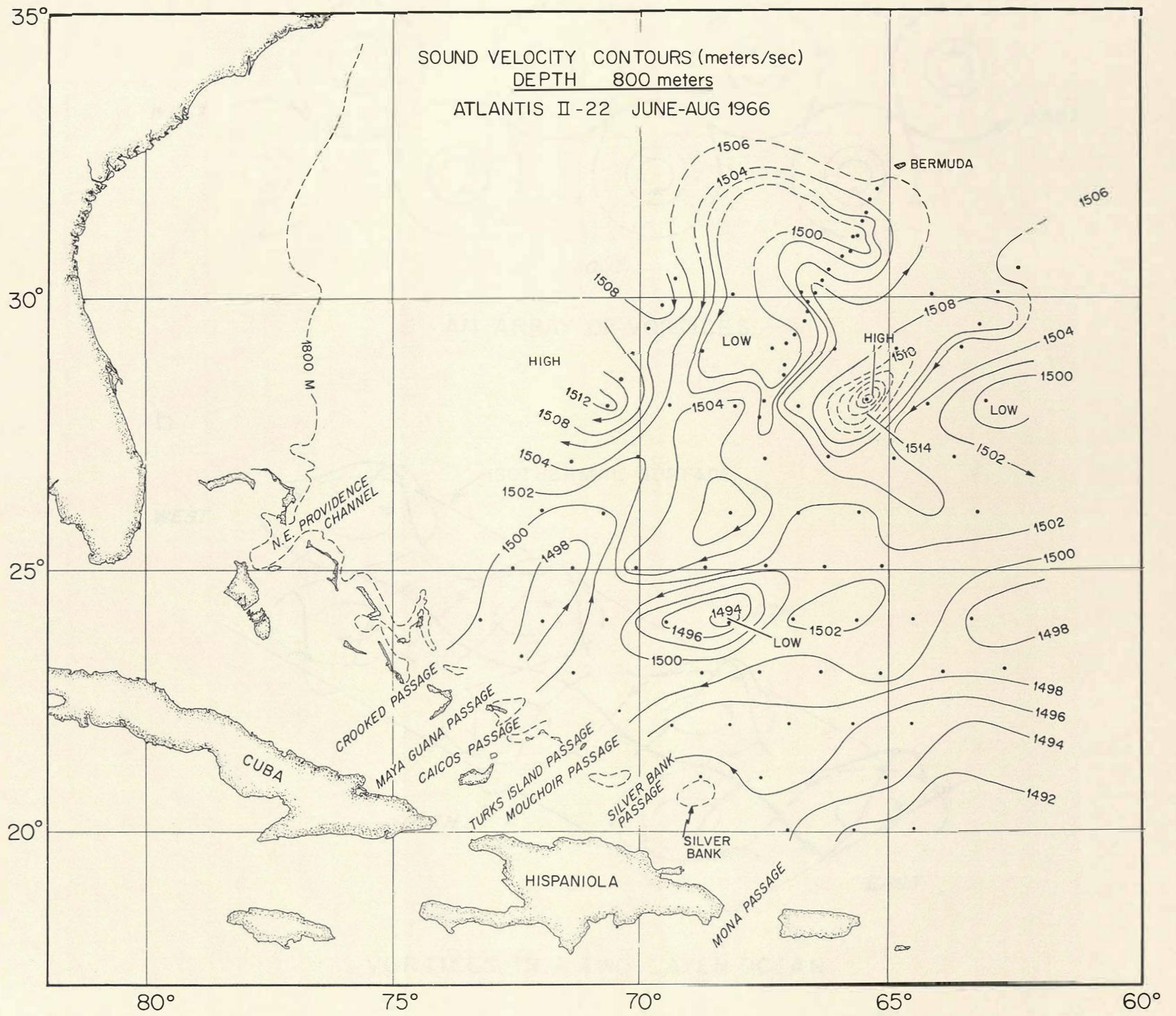
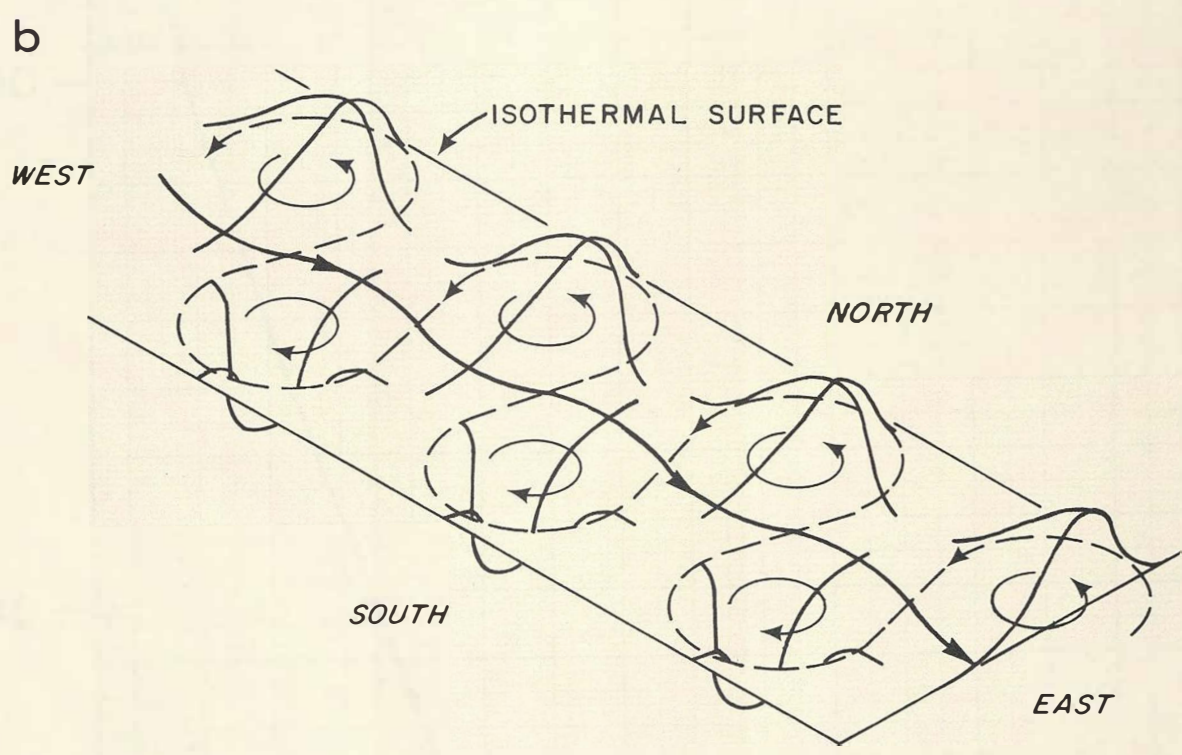Fig. III-9   Broad-Area Sound Velocity Contour Chart for 800 Meters' Depth.

a

NORTH

WEST   EAST

SOUTH

AN ARRAY OF VORTICES

b

ISOTHERMAL SURFACE

WEST

NORTH

SOUTH

EAST

VORTICES IN A TWO-LAYER OCEAN

Fig. III-10   Idealization of Water Flow Directions for an Alternating Array of Vortices.

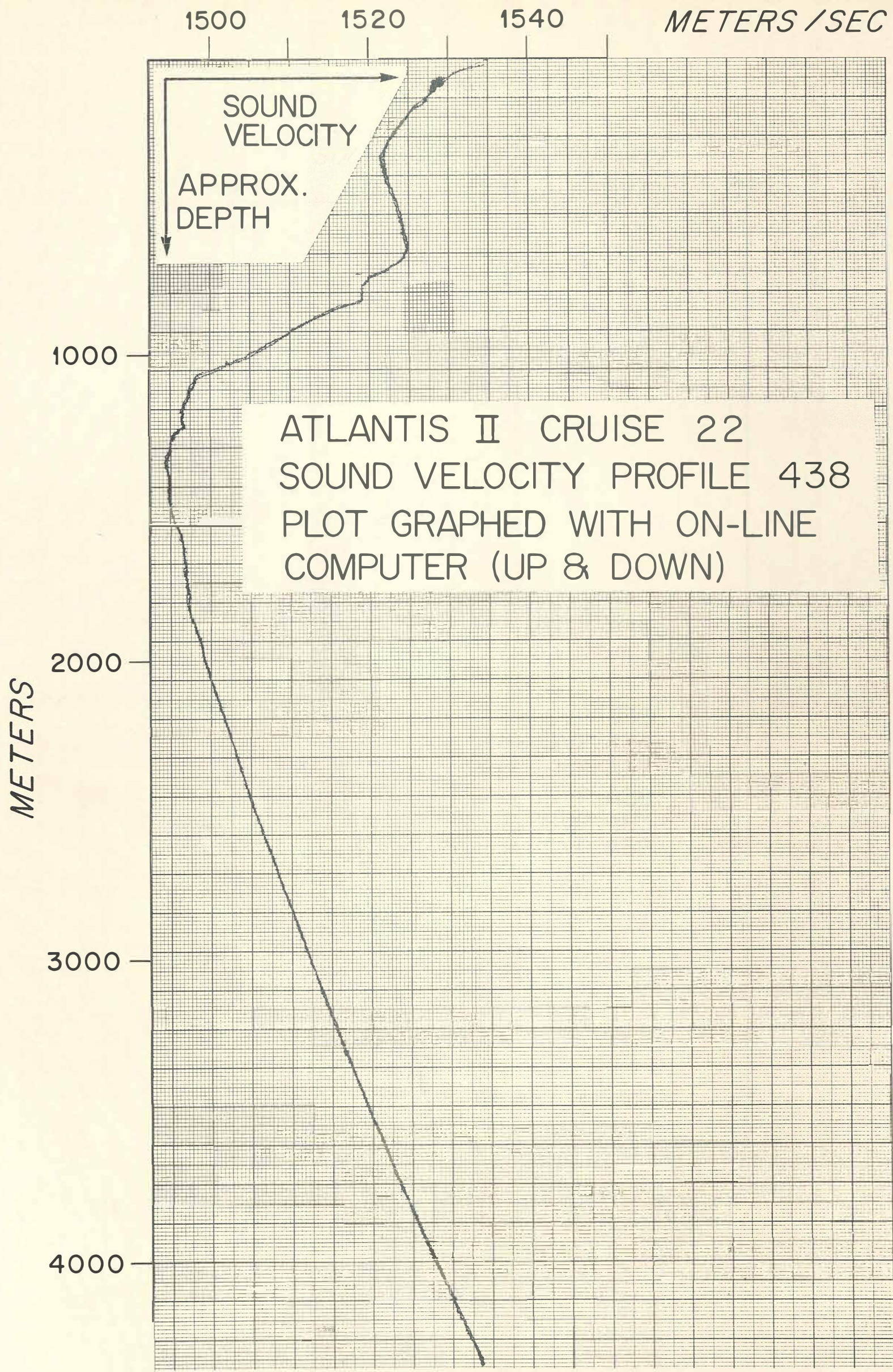**SOUND VELOCITY**

APPROX. DEPTH

ATLANTIS II CRUISE 22
SOUND VELOCITY PROFILE 438
PLOT GRAPHED WITH ON-LINE
COMPUTER (UP & DOWN)

Fig. III-11   On-Line Plot of Descent and Ascent of Instrument
for Anomalous Sound Velocity Profile #438.
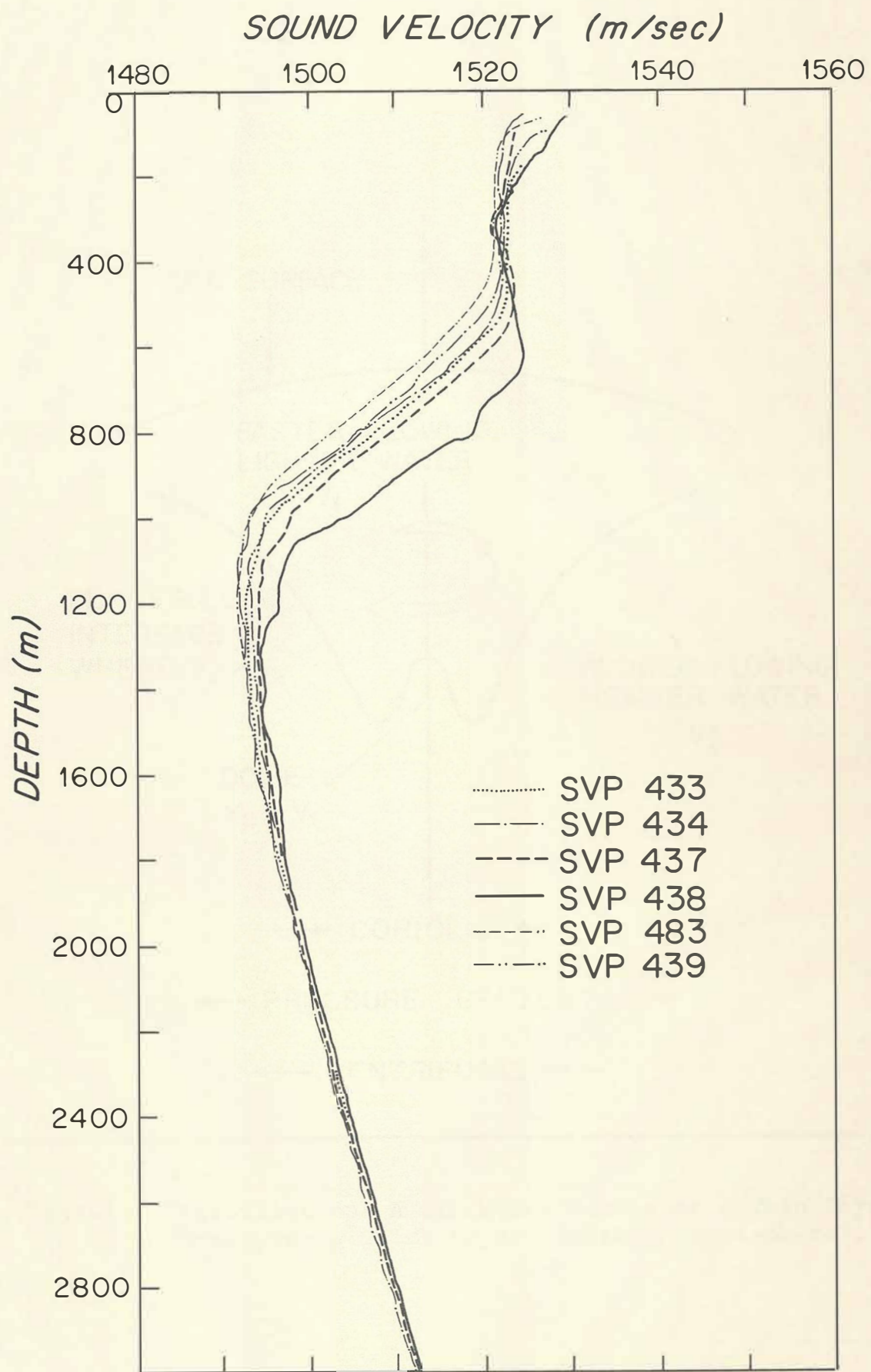
Fig. III-12   Comparison of Sound Velocity Profile #438 and
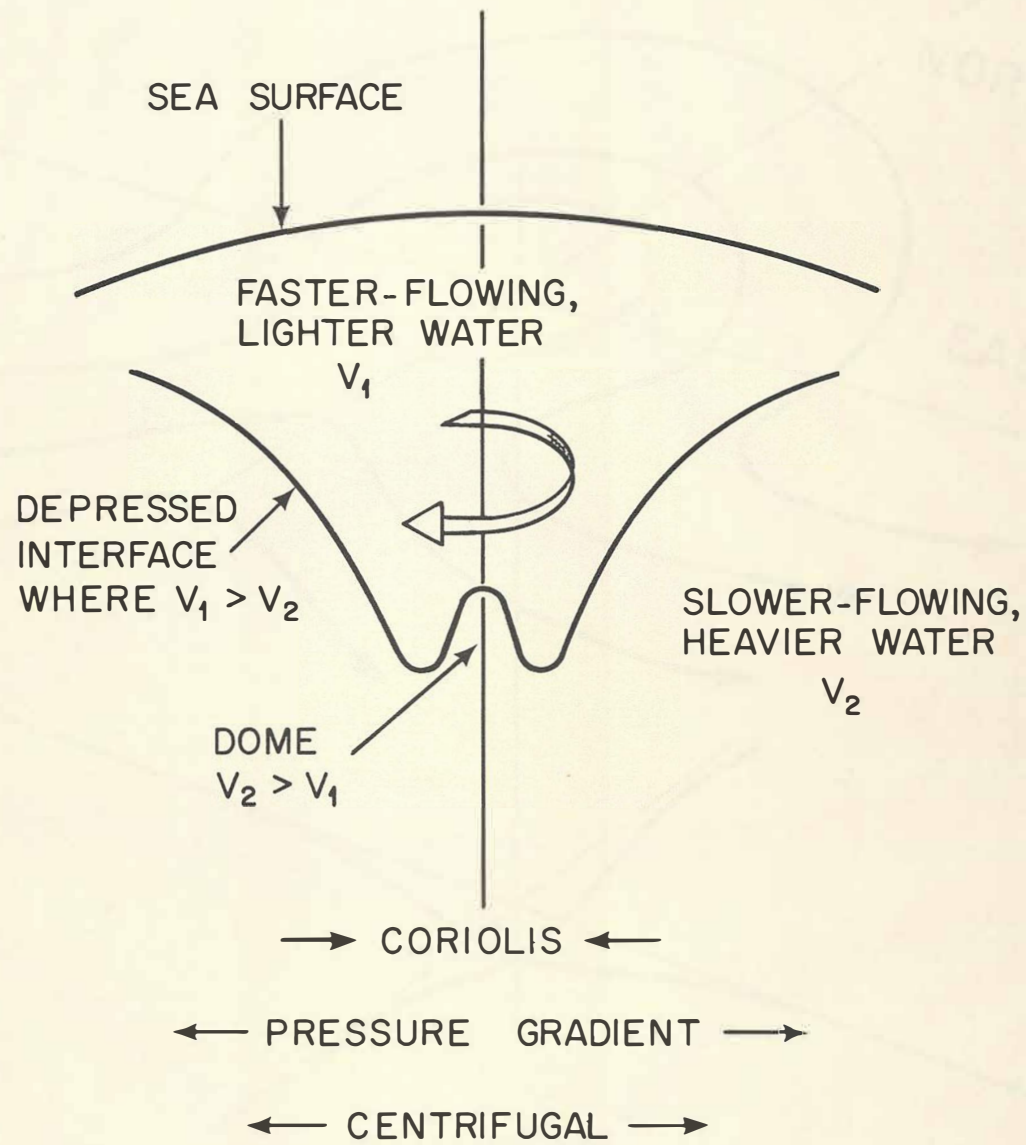Neighboring Profiles (Refer to Fig. I-1 for
Locations).

SEA SURFACE

FASTER-FLOWING,
LIGHTER WATER
V_1

DEPRESSED
INTERFACE
WHERE $V_1 > V_2$

SLOWER-FLOWING,
HEAVIER WATER
V_2

DOME
$V_2 > V_1$

→ CORIOLIS ←

← PRESSURE GRADIENT →

← CENTRIFUGAL →

Fig. III-13   Idealization: A Clockwise Vortex in a Thin Layer
Overlying a Thick Layer (Northern Hemisphere).
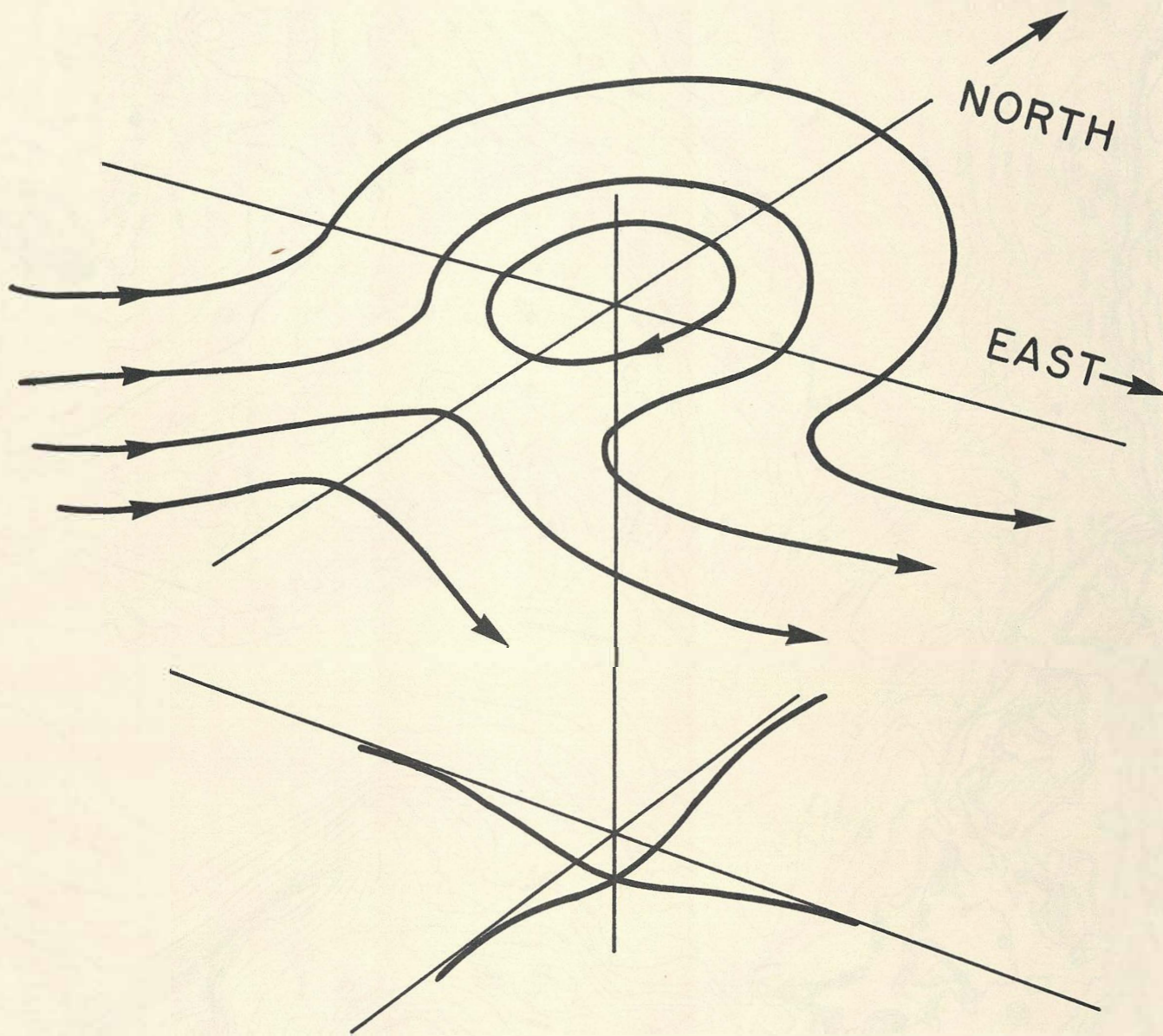
Fig. III-14   Idealized Flow Pattern over a Depression in the
               Bottom with Flow from the Southwest (Northern
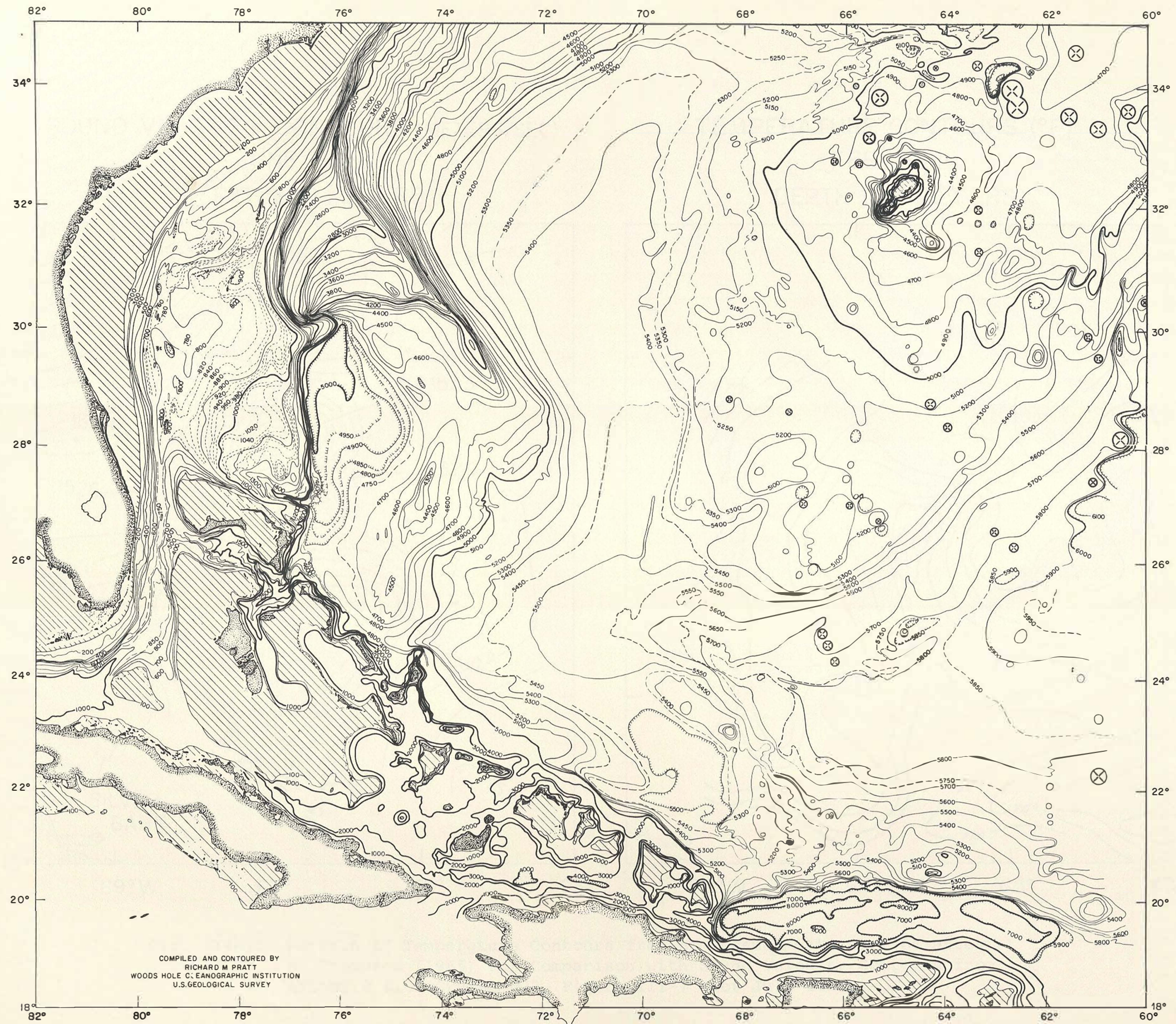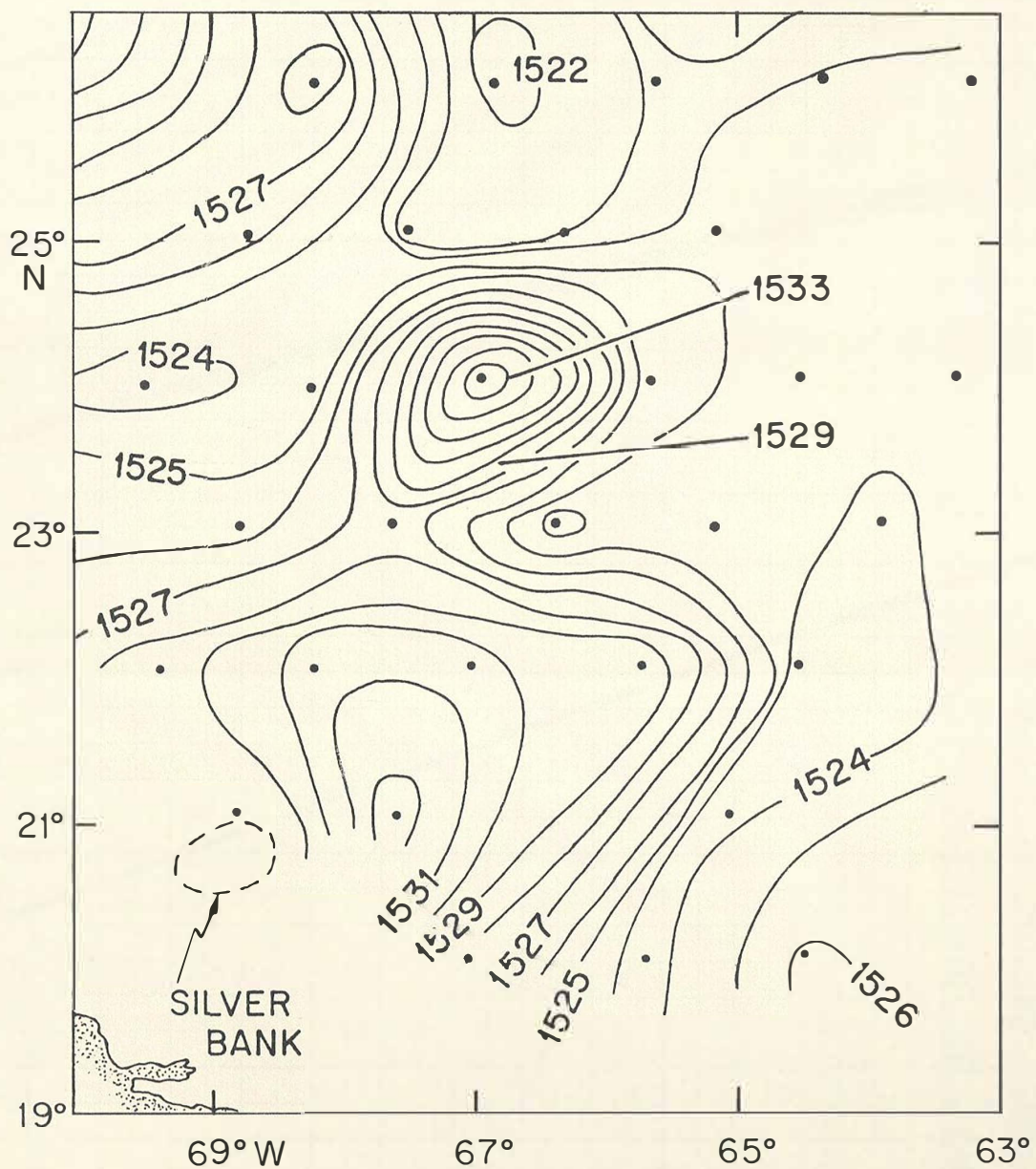   Hemisphere).

Fig. III-15 Deep-Sea Bathymetry of the Northwestern Atlantic Ocean after R. M. Pratt (1968).

SOUND VELOCITY CONTOURS (METERS/SEC)
JUNE 1966
DEPTH 200 METERS

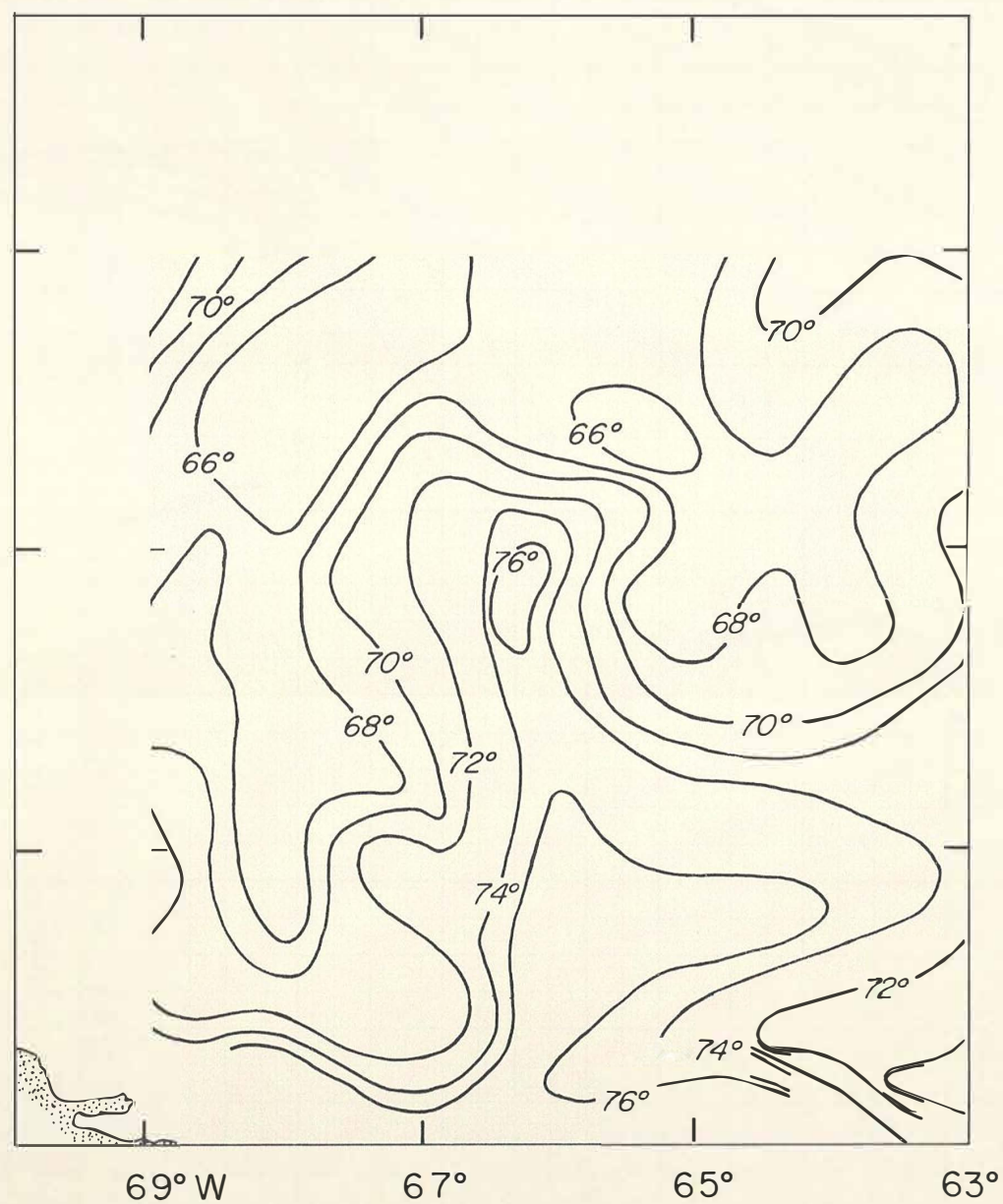TEMPERATURE CONTOURS (°F)
FEB 1964
DEPTH 150 METERS

Fig. III-16   Portion of Temperature Contours from BT Measurements in 1964 after
B. Thompson (1965) for Comparison with Sound Velocity Contours from
ATLANTIS II - Cruise #22, Figure III-7 for July 1966.

Fig. III-17 Collected Sound Velocity Profiles for Leg 1.

SOUND VELOCITY (METERS/SEC)

NORTH-SOUTH LEG 2
CRUISE A2.22
FROM 30JUNE TO 3JULY 1966
S.V.P. 410TO415,417,418

Fig. III-17   Collected Sound Velocity Profiles for Leg 2.

Fig. III-17   Collected Sound Velocity Profiles for Leg 3.
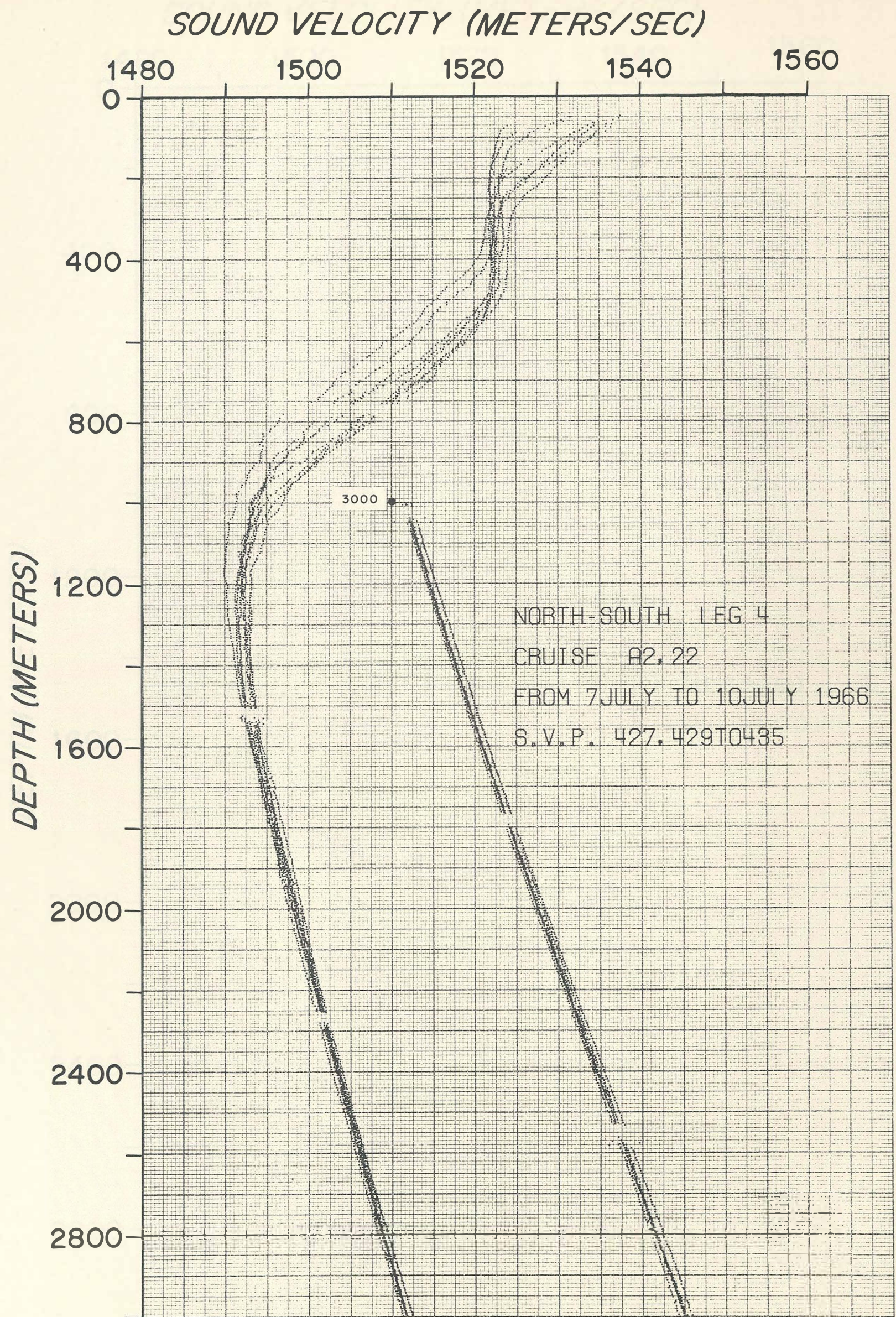
Fig. III-17   Collected Sound Velocity Profiles for Leg 4.

SOUND VELOCITY (METERS/SEC)
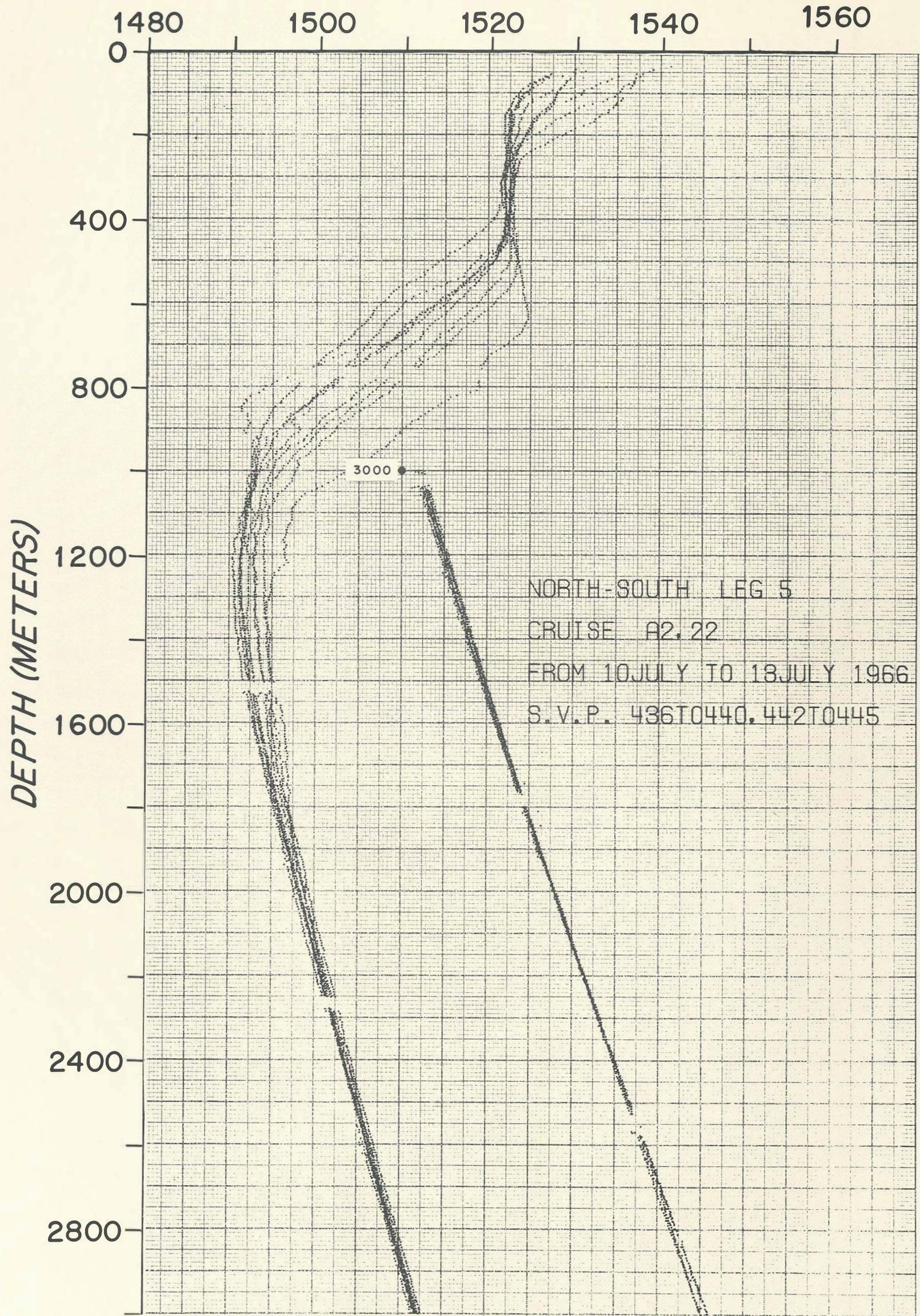
DEPTH (METERS)

3000

NORTH-SOUTH LEG 5
CRUISE A2.22
FROM 10 JULY TO 13 JULY 1966
S.V.P. 436 TO 440. 442 TO 445

Fig. III-17   Collected Sound Velocity Profiles for Leg 5.
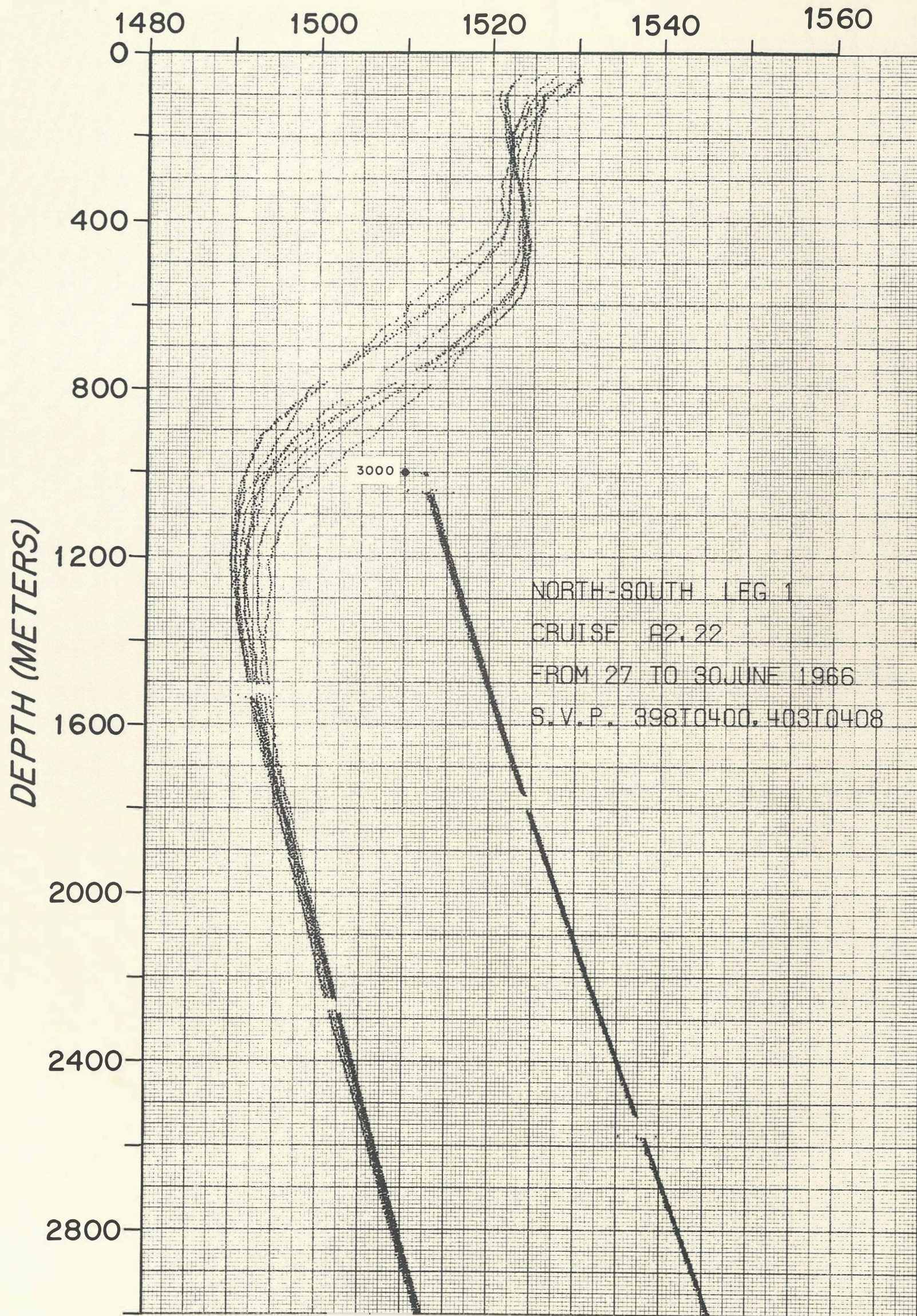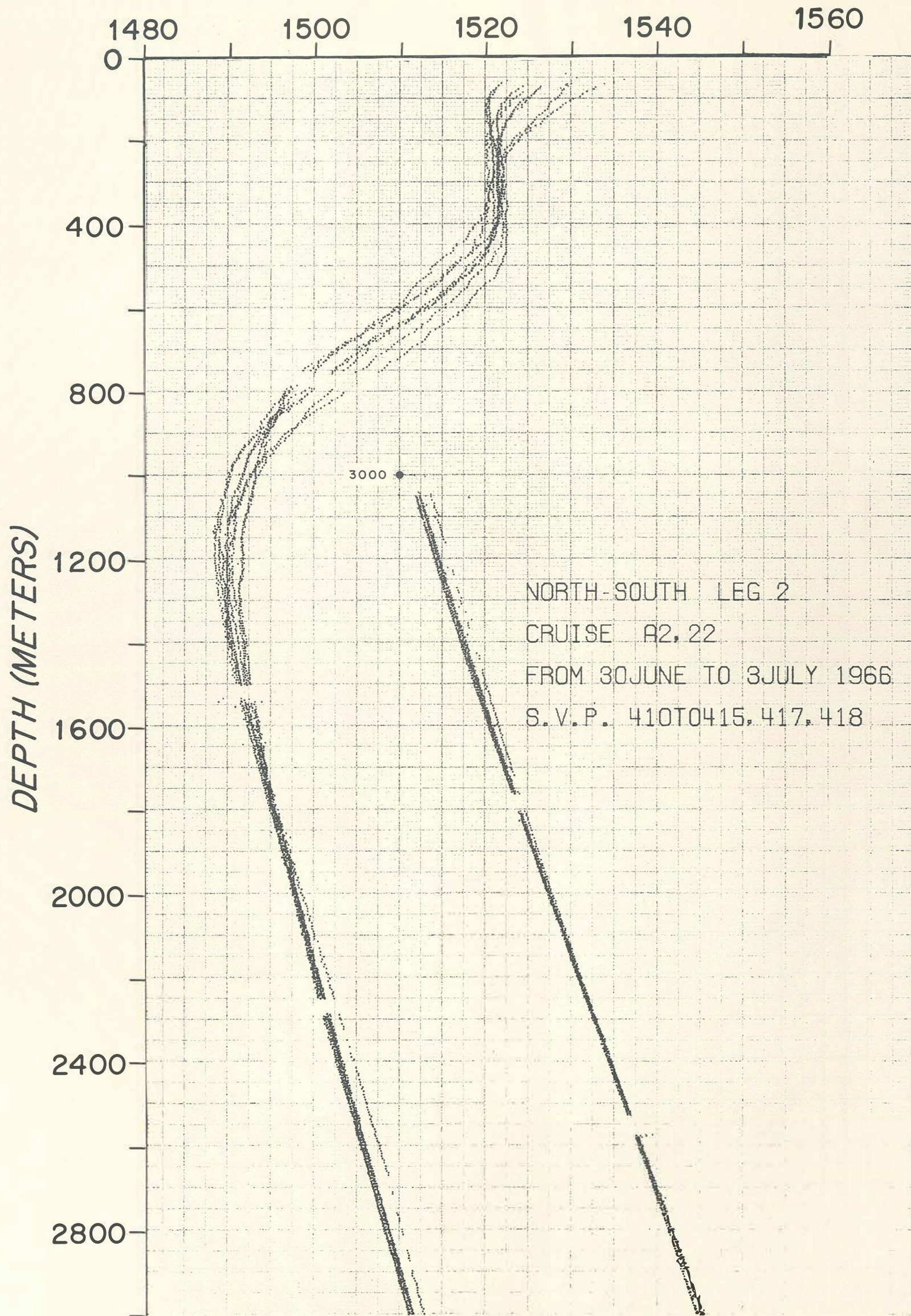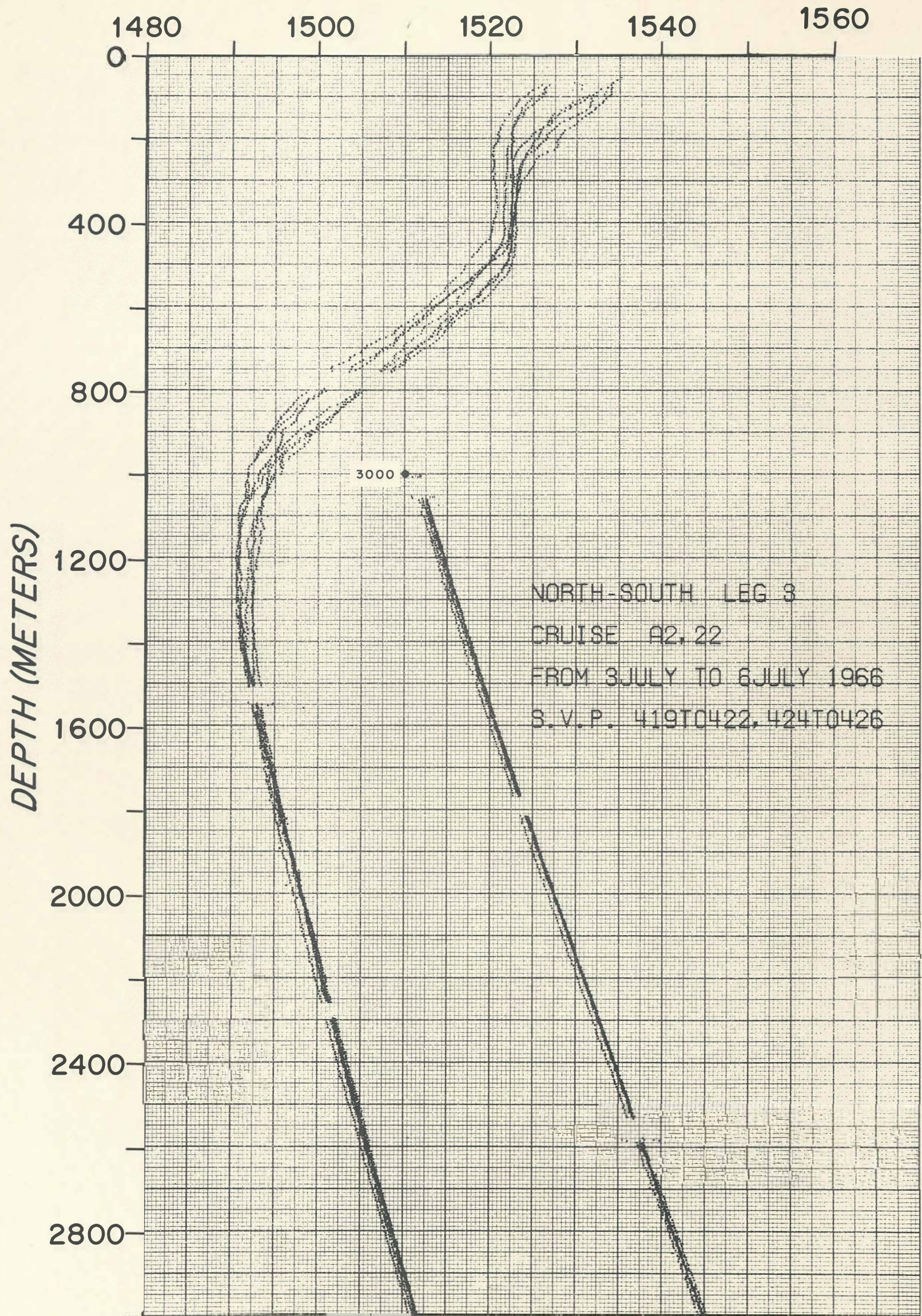
Fig. III-17   Collected Sound Velocity Profiles for Leg 6.

Fig. III-17   Collected Sound Velocity Profiles for Leg 7.

SOUND VELOCITY (METERS/SEC)

DEPTH (METERS)

SVP 456

SVP 458

3000

NORTH-SOUTH LEG 8
CRUISE A2.22
FROM 22 JULY TO 25 JULY 1966
S.V.P. 456 TO 459, 461
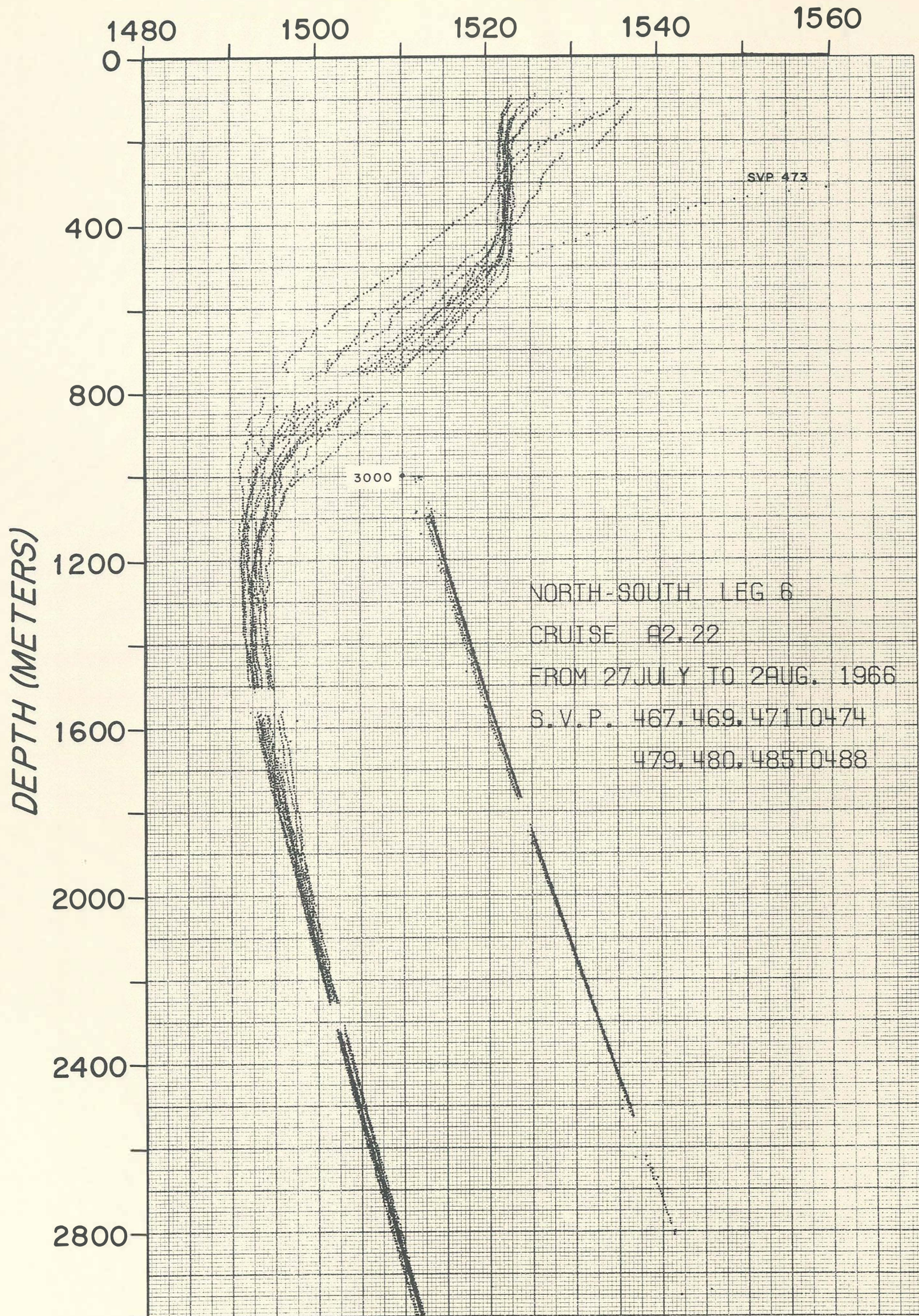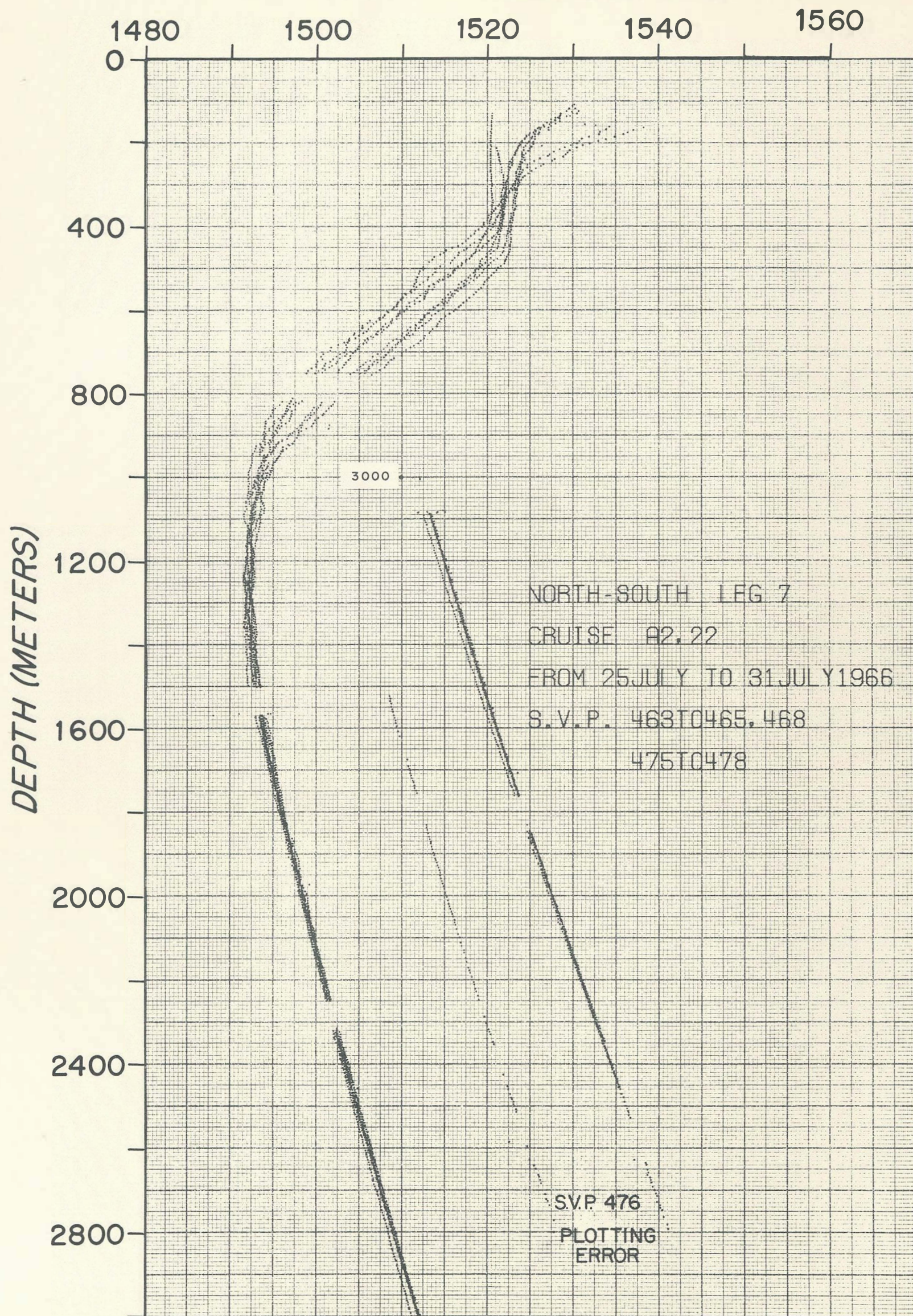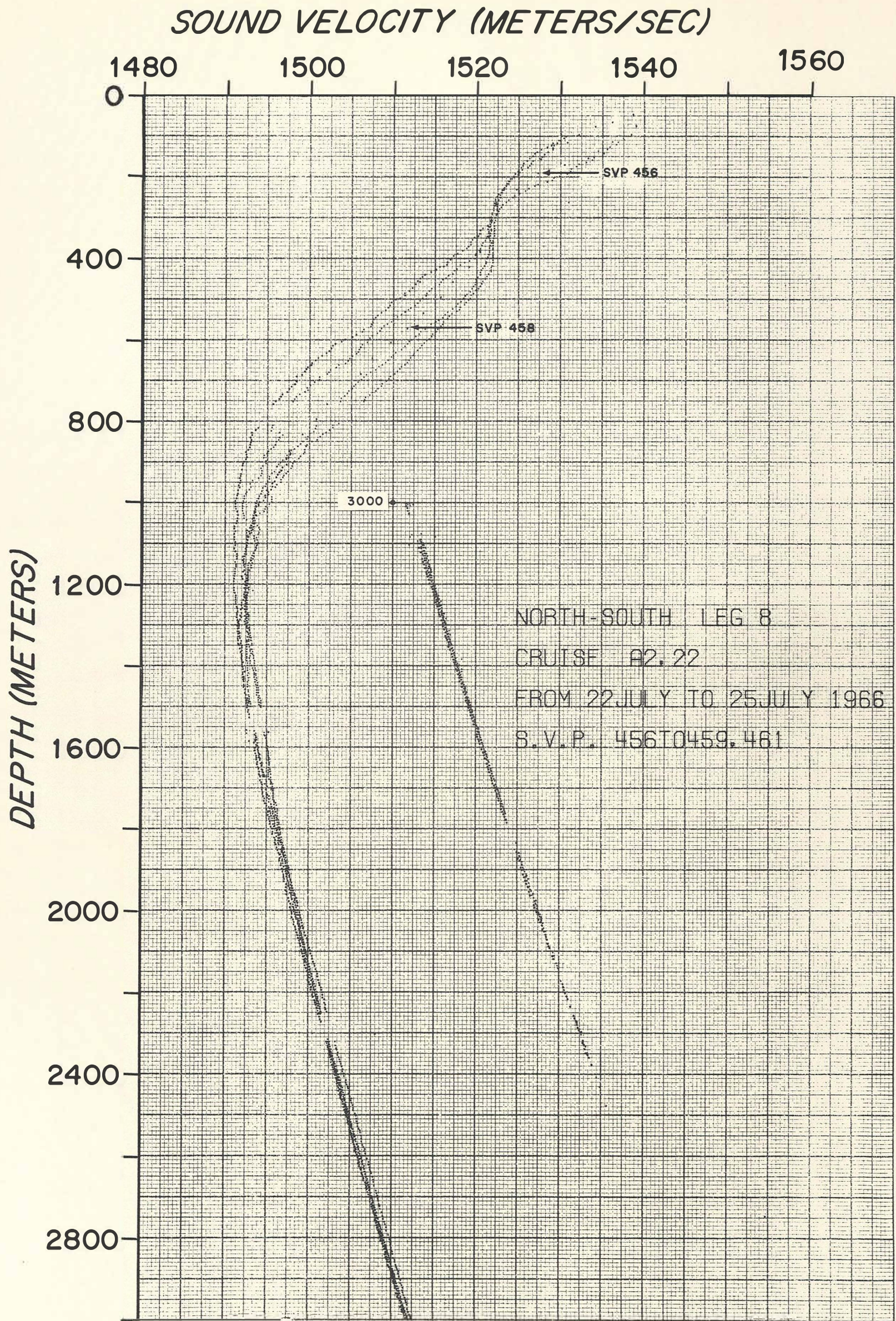
Fig. III-17   Collected Sound Velocity Profiles for Leg 8.

SOUND VELOCITY (METERS/SEC)
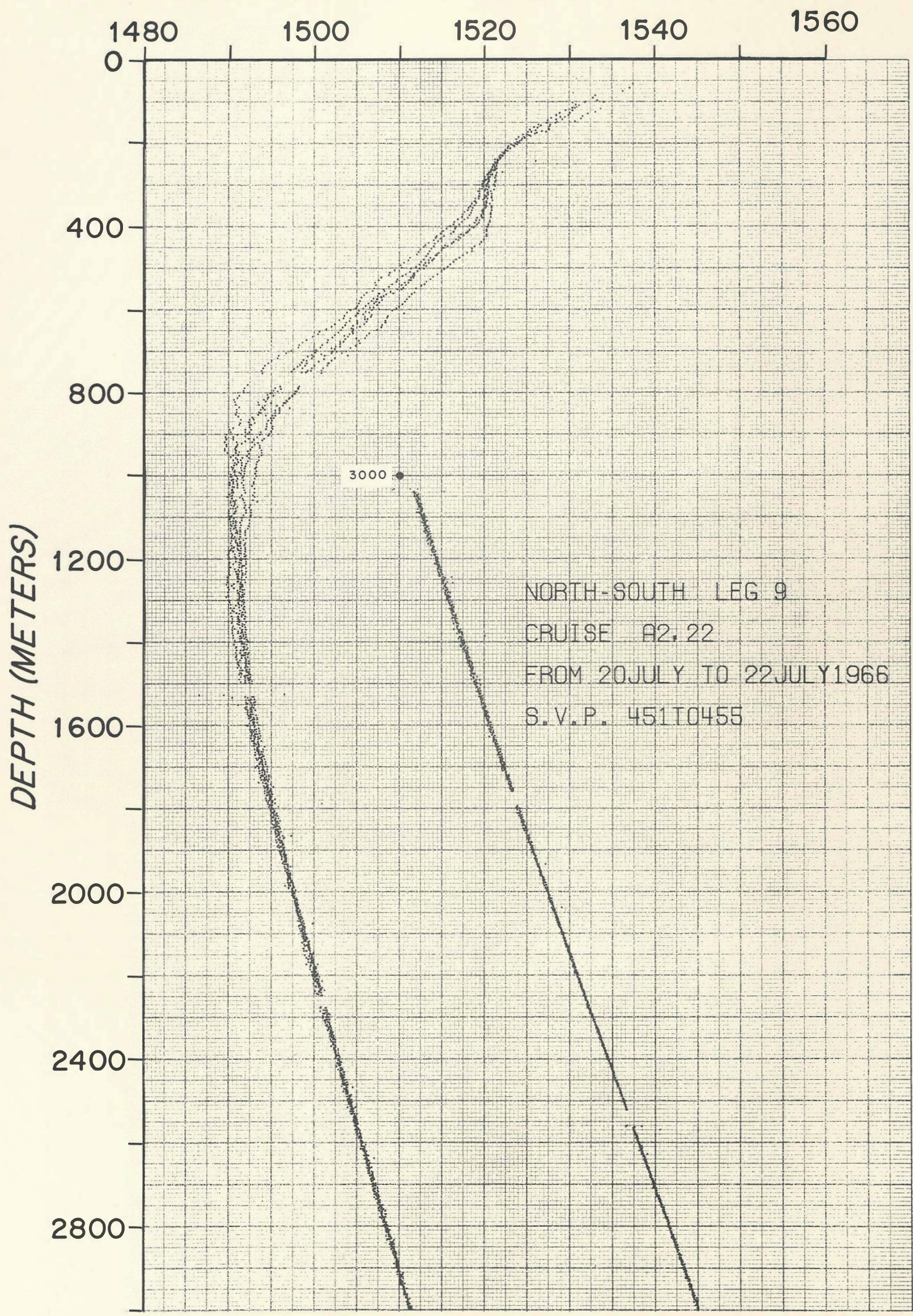
NORTH-SOUTH LEG 9
CRUISE A2.22
FROM 20JULY TO 22JULY1966
S.V.P. 451TO455

3000

Fig. III-17   Collected Sound Velocity Profiles for Leg 9.

SOUND VELOCITY (METERS/SEC)

NORTH-SOUTH LEG 10
CRUISE A2.22
FROM 19JULY TO 20JULY1966
S.V.P. 447.449.450
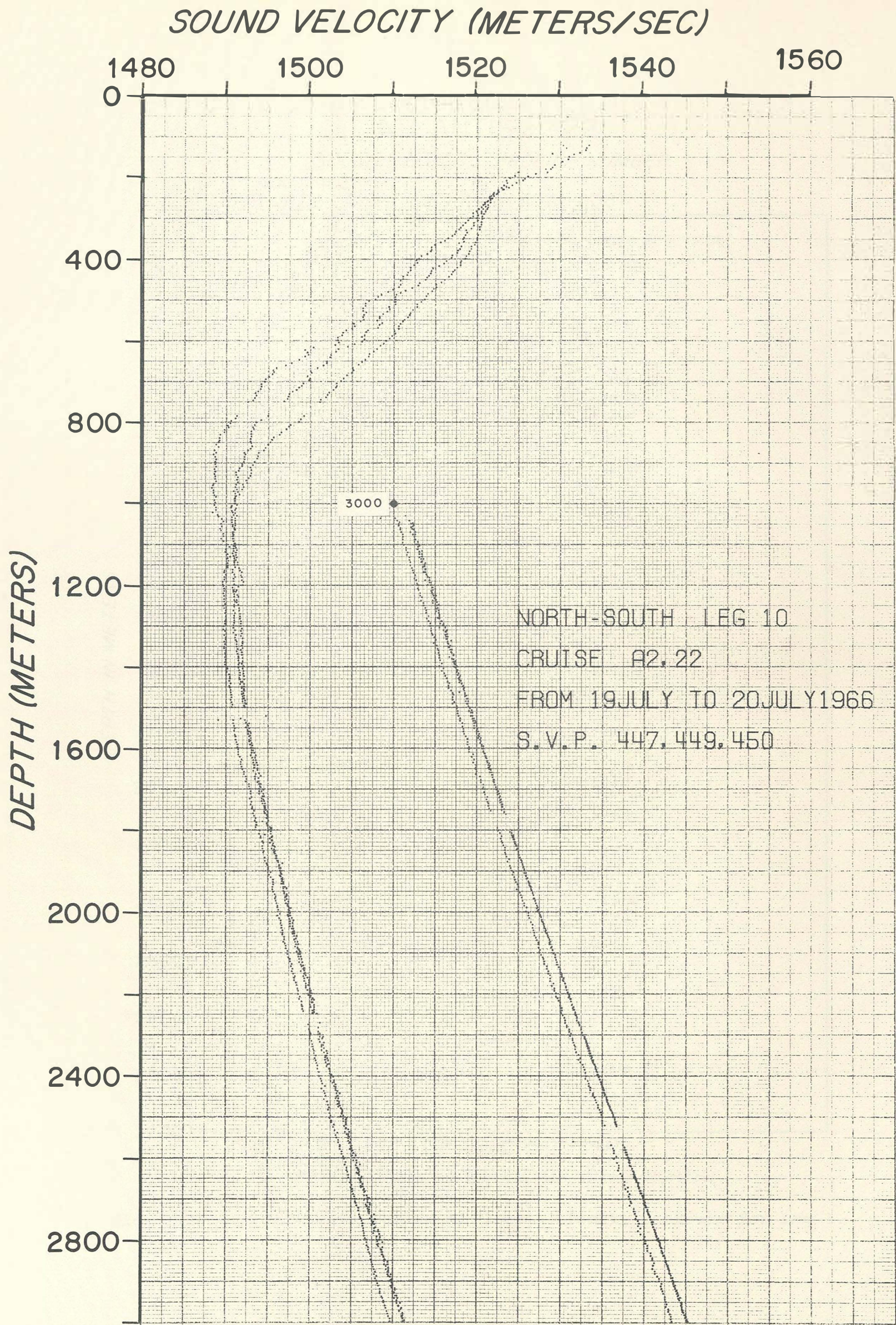
Fig. III-17   Collected Sound Velocity Profiles for Leg 10.

LEG 1
ATLANTIS II-22
SOUND VELOCITY PROFILE NUMBER
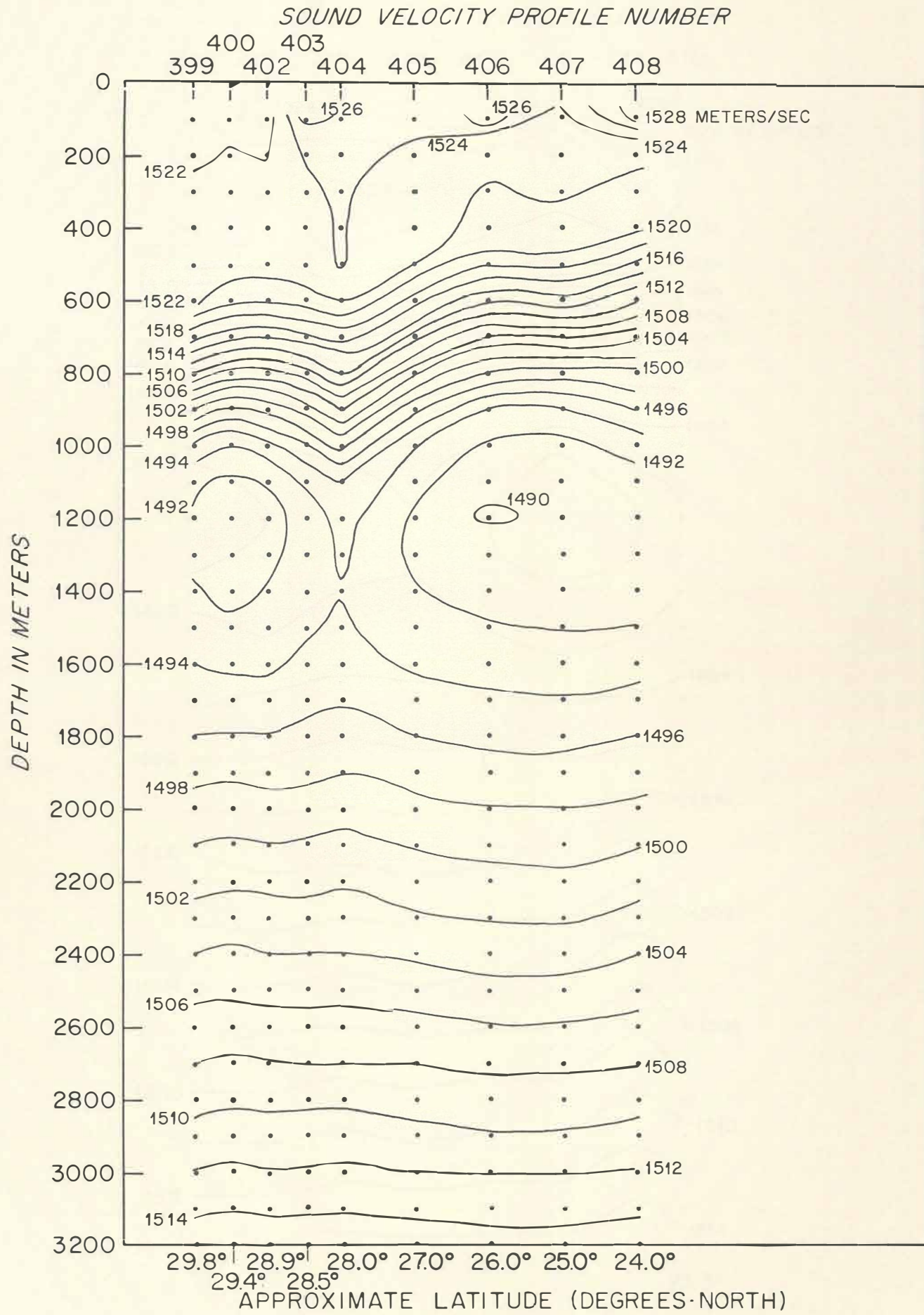
Fig. III-18   Vertical Section of Sound Velocity Contours for Leg 1.
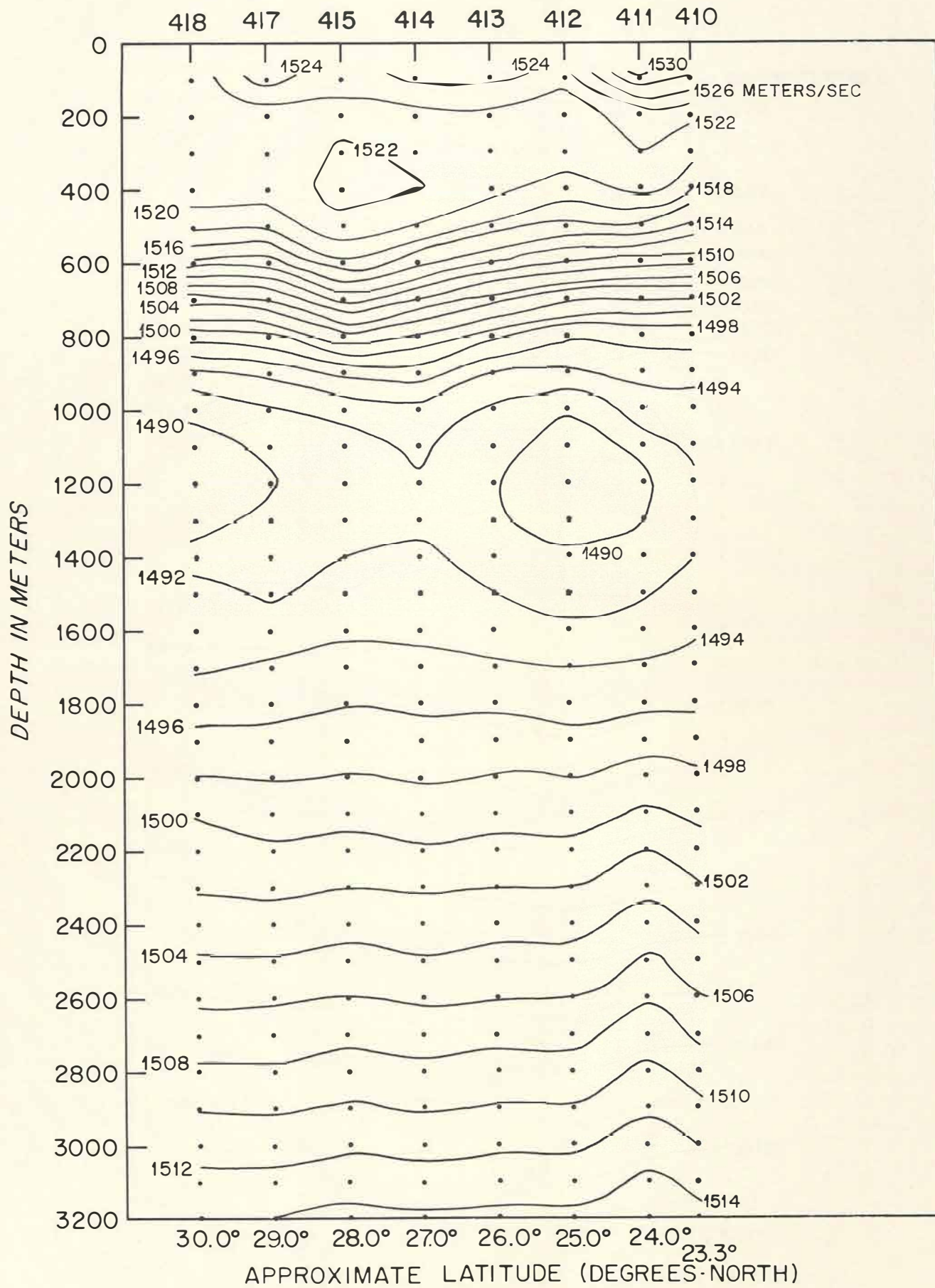
Fig. III-18   Vertical Section of Sound Velocity Contours for Leg 2.

LEG 3
ATLANTIS II-22
SOUND VELOCITY PROFILE NUMBER
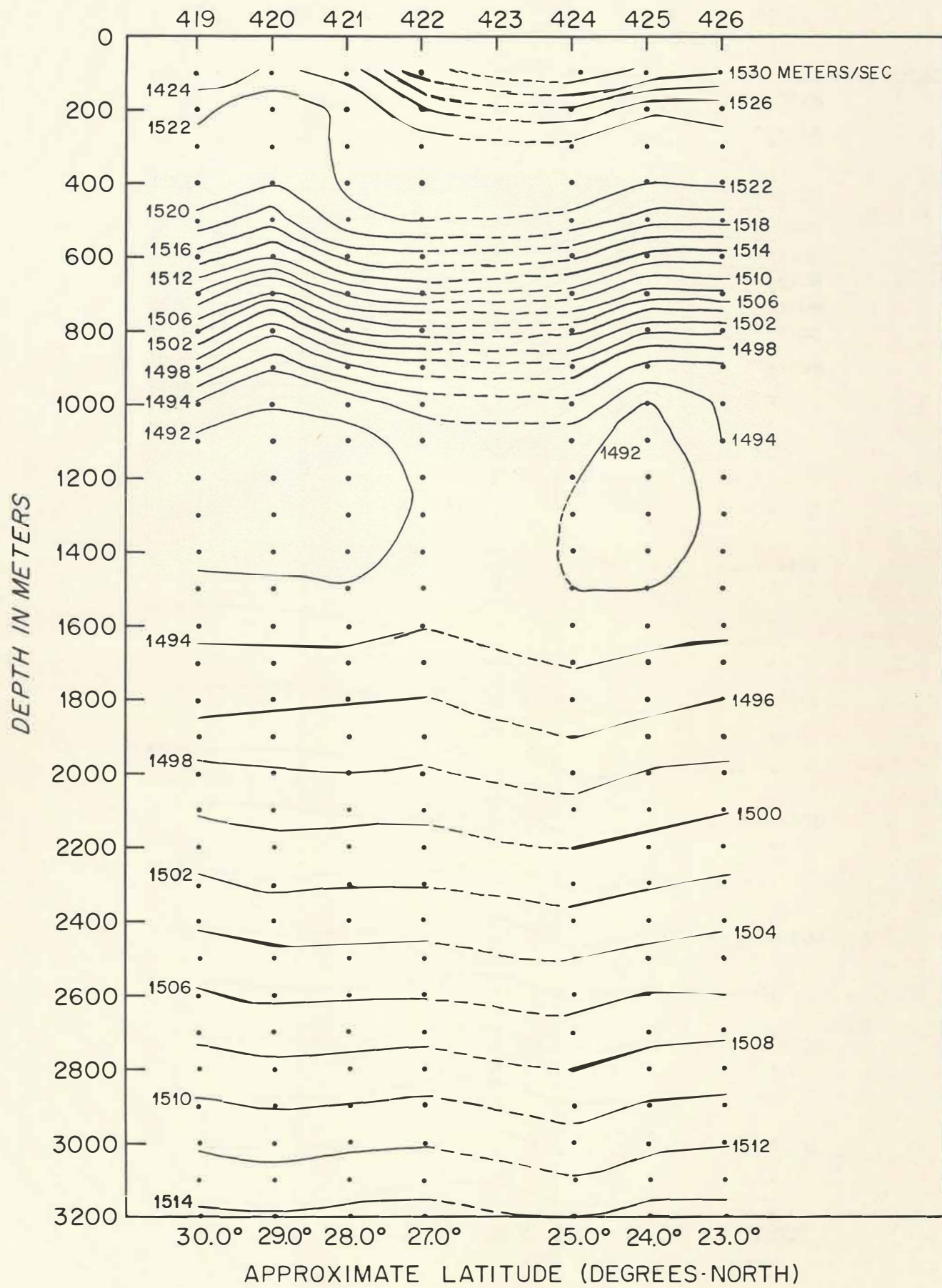
Fig. III-18   Vertical Section of Sound Velocity Contours for Leg 3.
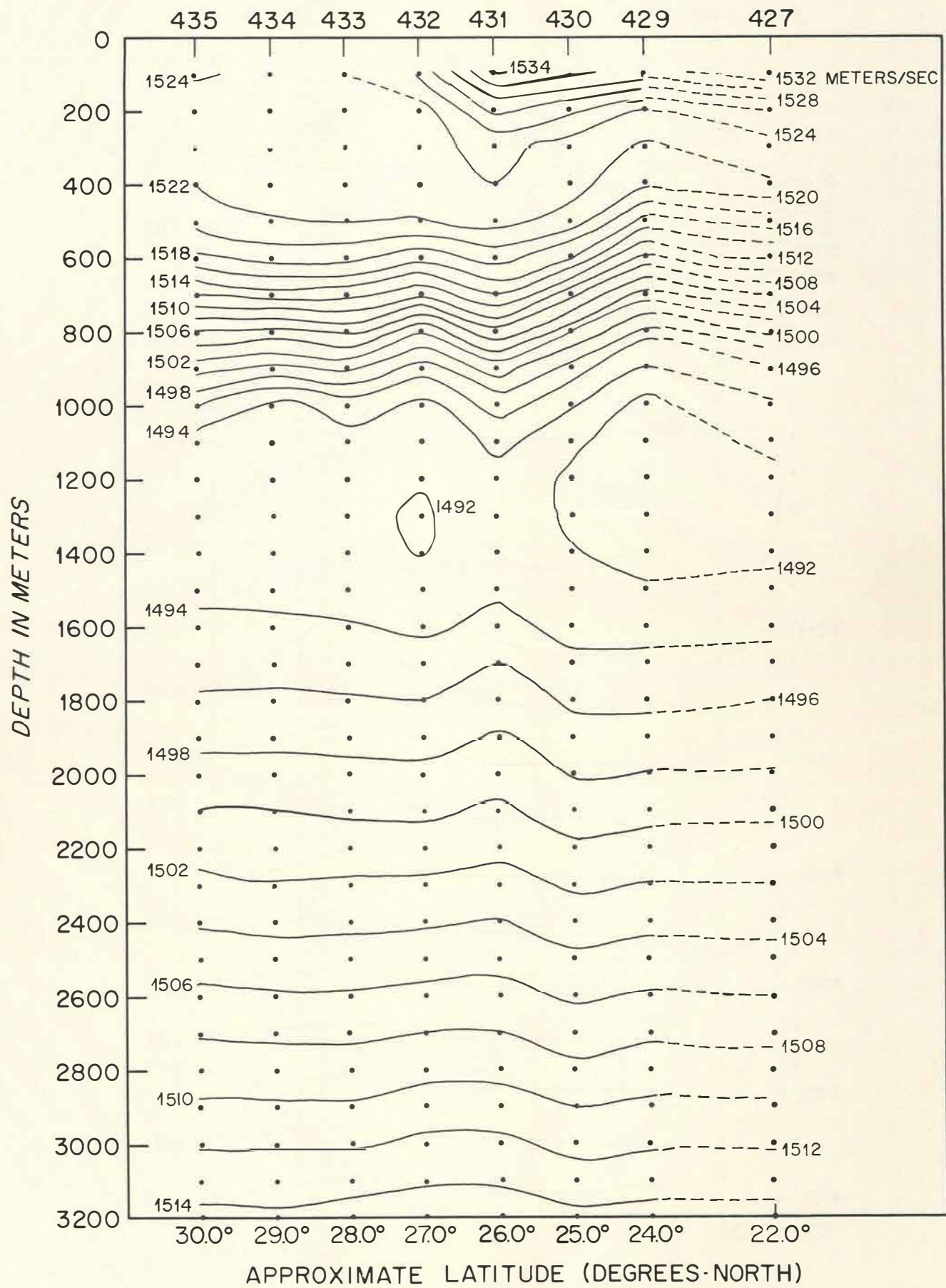
Fig. III-18   Vertical Section of Sound Velocity Contours for Leg 4.

LEG 5
ATLANTIS II-22

SOUND VELOCITY PROFILE NUMBER
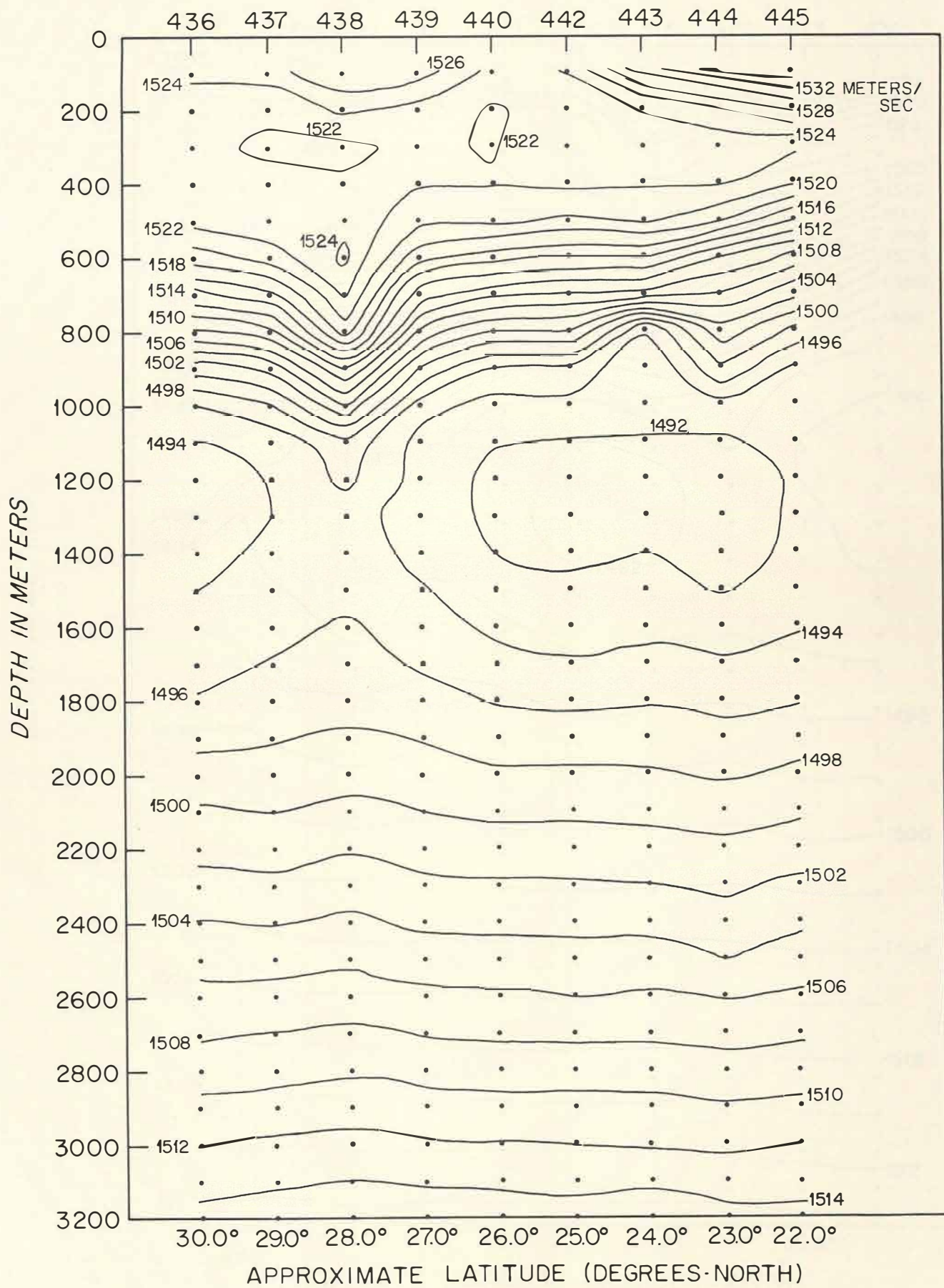
Fig. III-18   Vertical Section of Sound Velocity Contours for Leg 5.
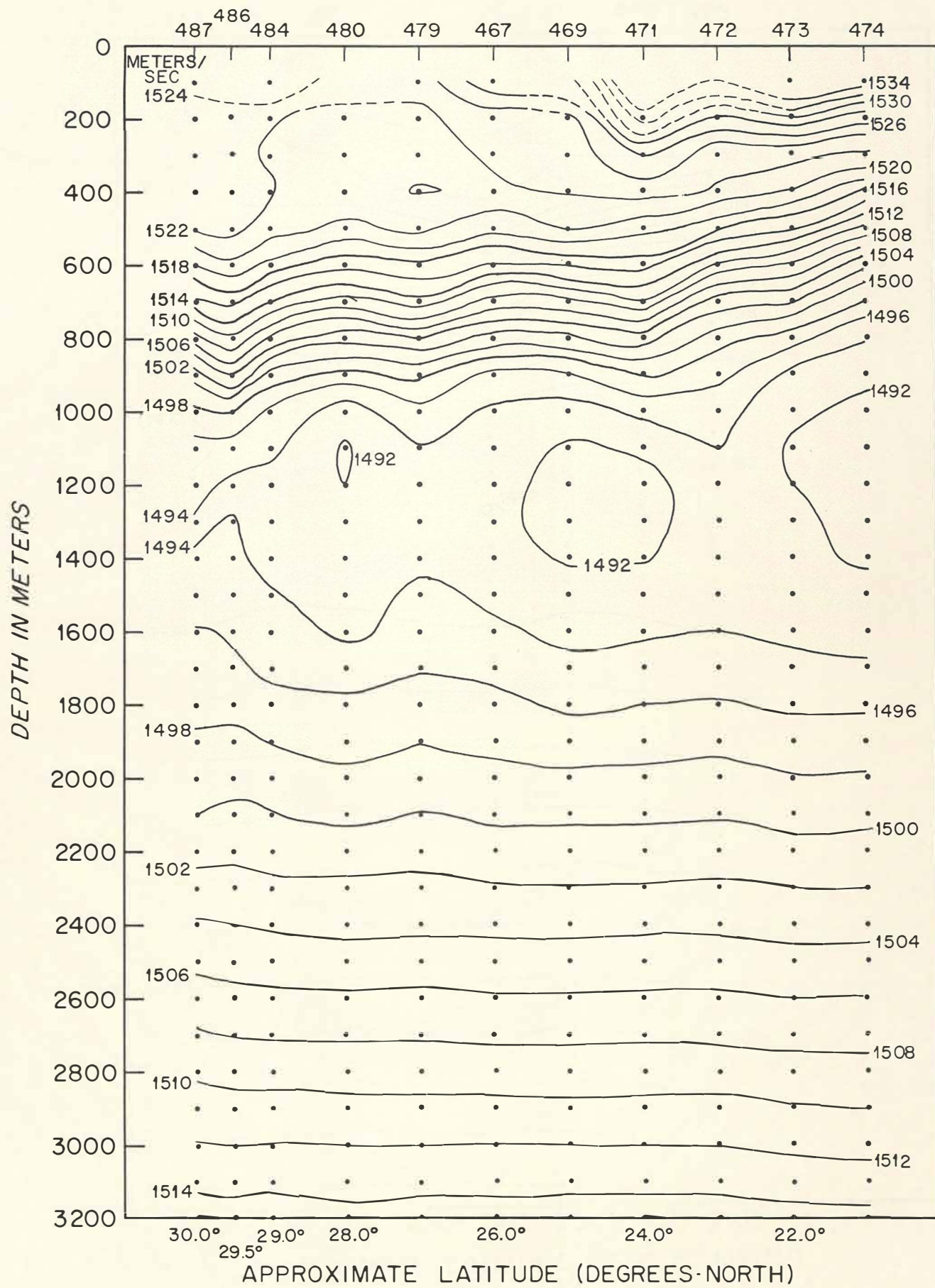
Fig. III-18   Vertical Section of Sound Velocity Contours for Leg 6.

LEG 7
ATLANTIS II-22

SOUND VELOCITY PROFILE NUMBER
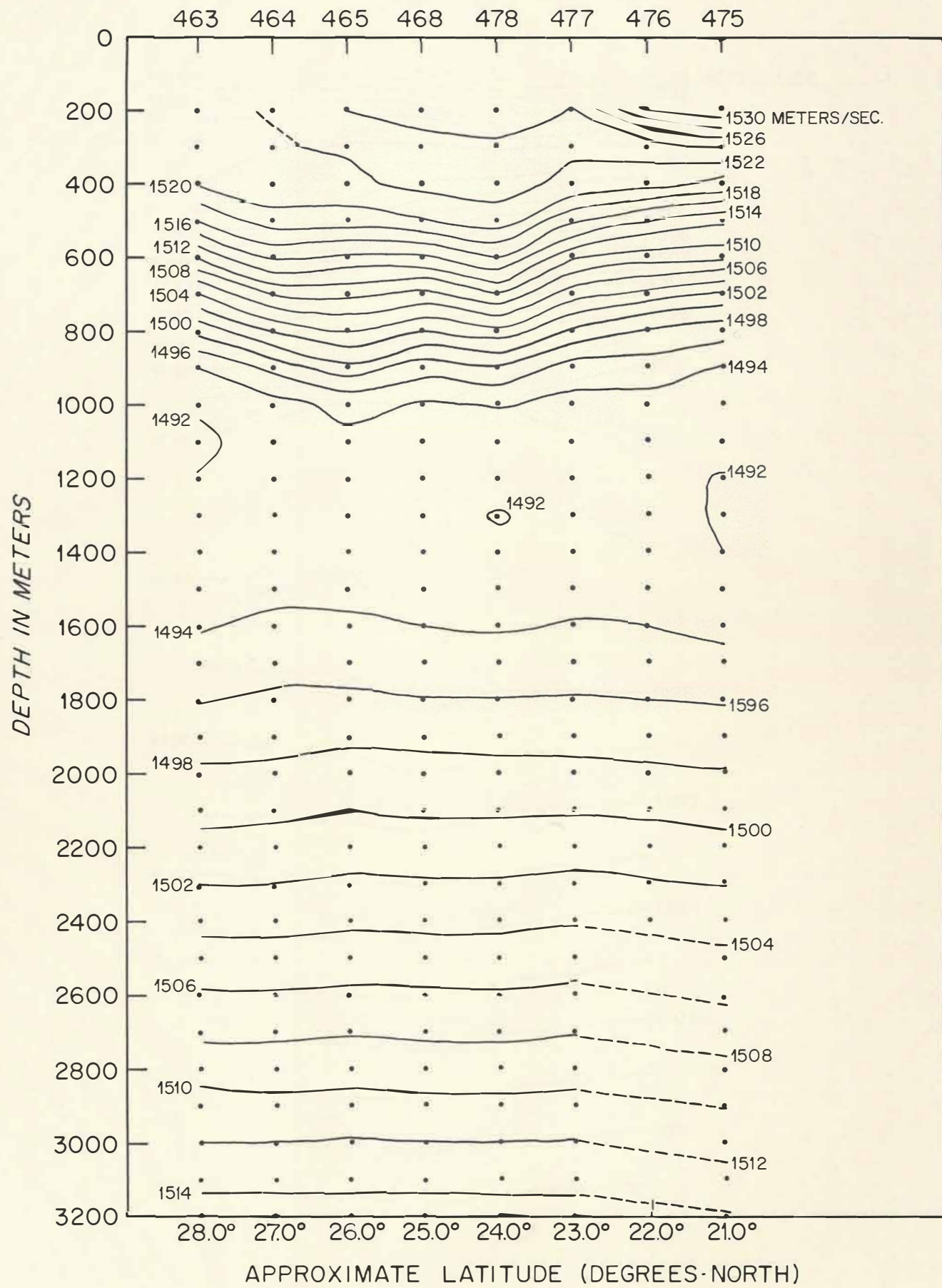
Fig. III-18   Vertical Section of Sound Velocity Contours for Leg 7.

LEG 8
ATLANTIS II-22

SOUND VELOCITY PROFILE NUMBER
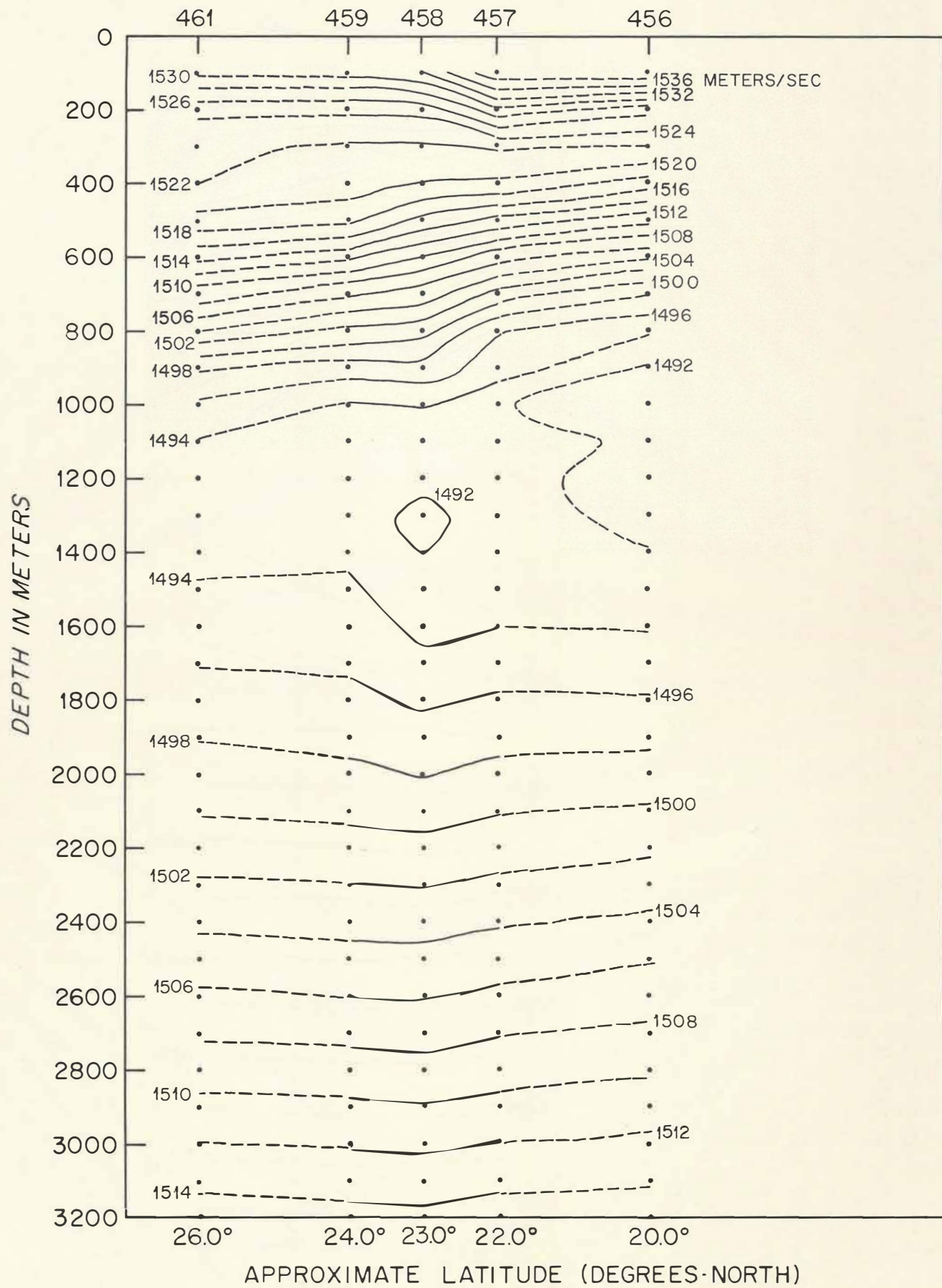
Fig. III-18   Vertical Section of Sound Velocity Contours for Leg 8.

LEG 10
ATLANTIS II-22

SOUND VELOCITY PROFILE NUMBER
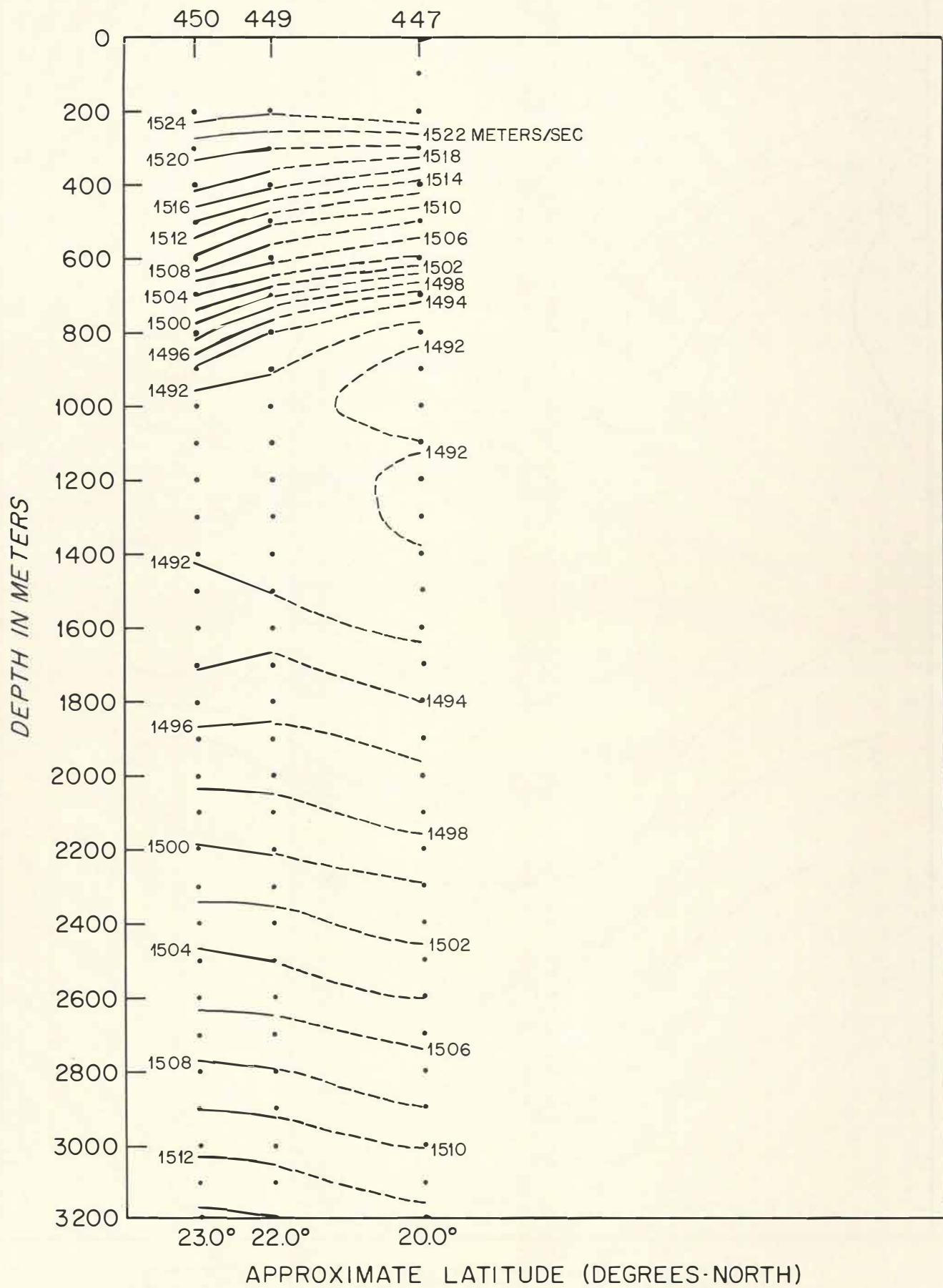
Fig. III-18   Vertical Section of Sound Velocity Contours for Leg 10.
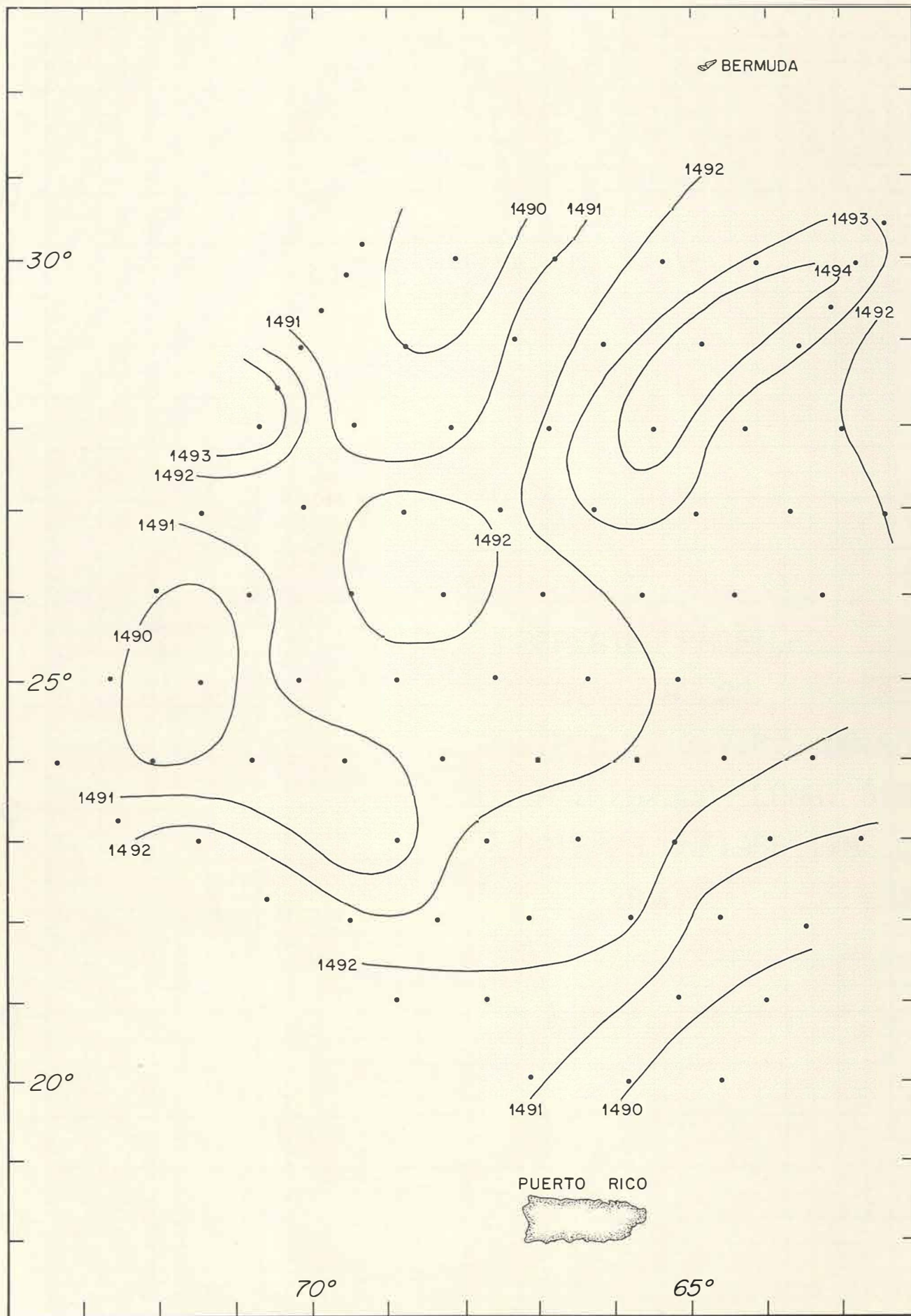
LOCATION OF MINIMUM SOUND VELOCITY
(meters per second)

Fig. III-19   Location of Minimum Sound Velocity for
Summer 1966 in the Sargasso Sea.

SOUND VELOCITY (METERS/SEC)

REPEATED PROFILES
CRUISE A2.22
W.H.O.I. S.V.P. 400.401
LAT. 292300 LONG. 695500
DATE 28 JUNE 1966 TIME 0915
28 JUNE 1200
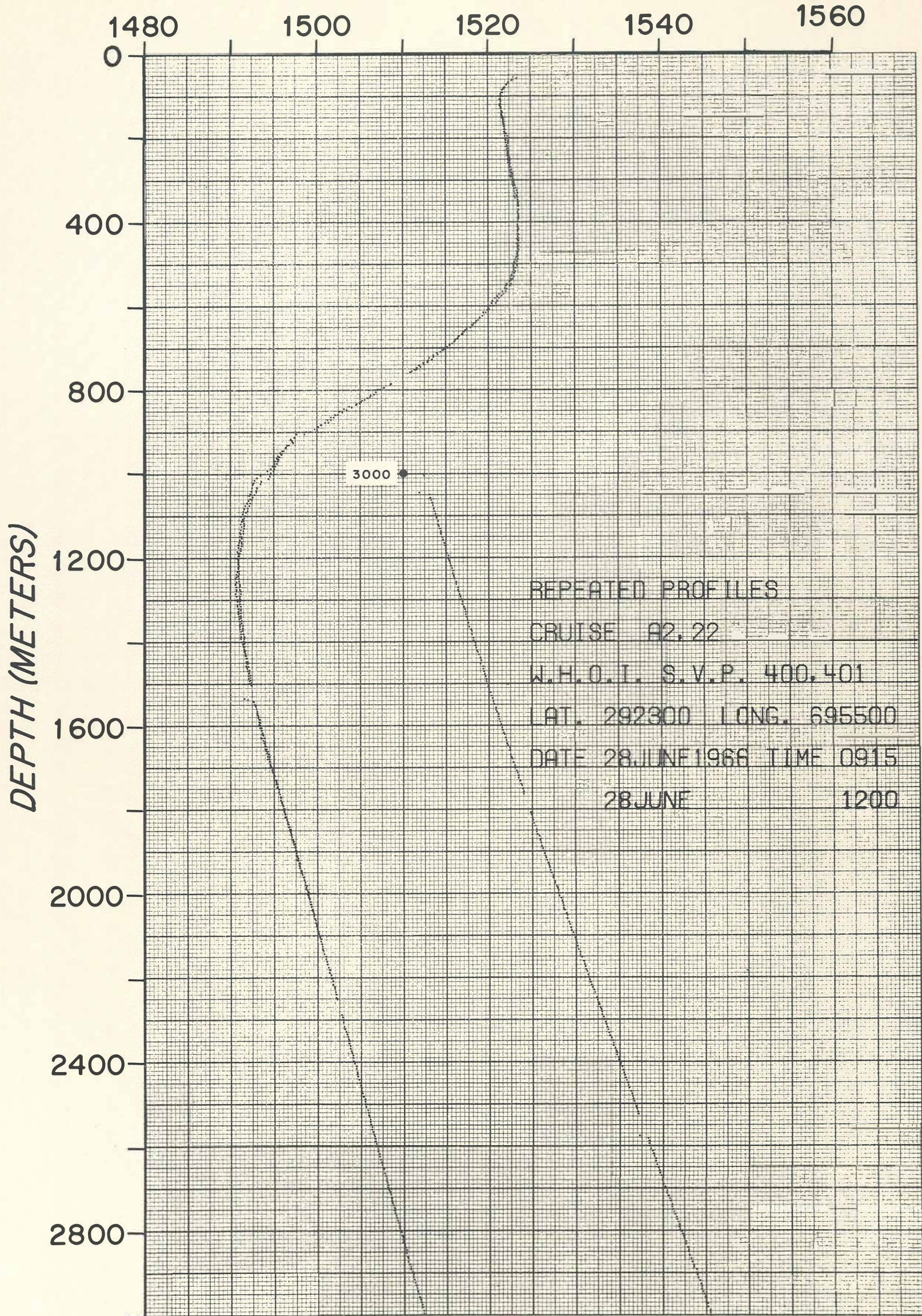
Fig. III-20a Repeated Sound Velocity Profiles #400 and #401.

SOUND VELOCITY (METERS/SEC)

DEPTH (METERS)

REPEATED PROFILES
CRUISE A2, 22
W.H.O.I. S.V.P. 415, 416
LAT. 280000 LONG. 692600
DATE 2JULY1966 TIME 1830
        2JULY   2020

3000
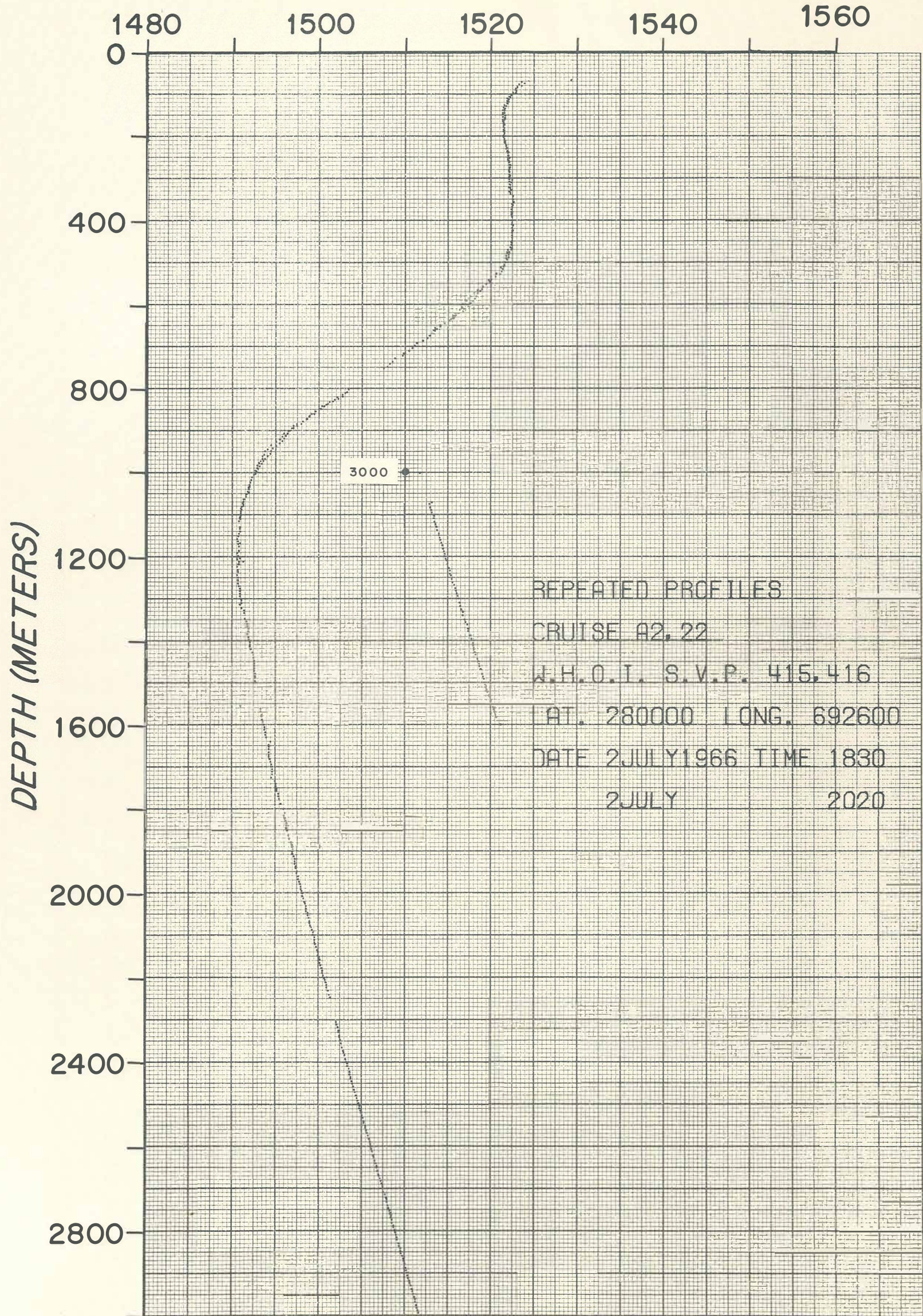
Fig. III-20b   Repeated Sound Velocity Profiles #415 and #416.

SOUND VELOCITY (METERS/SEC)

DEPTH (METERS)

REPEATED PROFILES
CRUISE A2.22
W.H.O.I. S.V.P. 441,469
LAT. 250000 LONG. 662000
DATE 12JULY1966 TIME 0700
        28JULY   0020
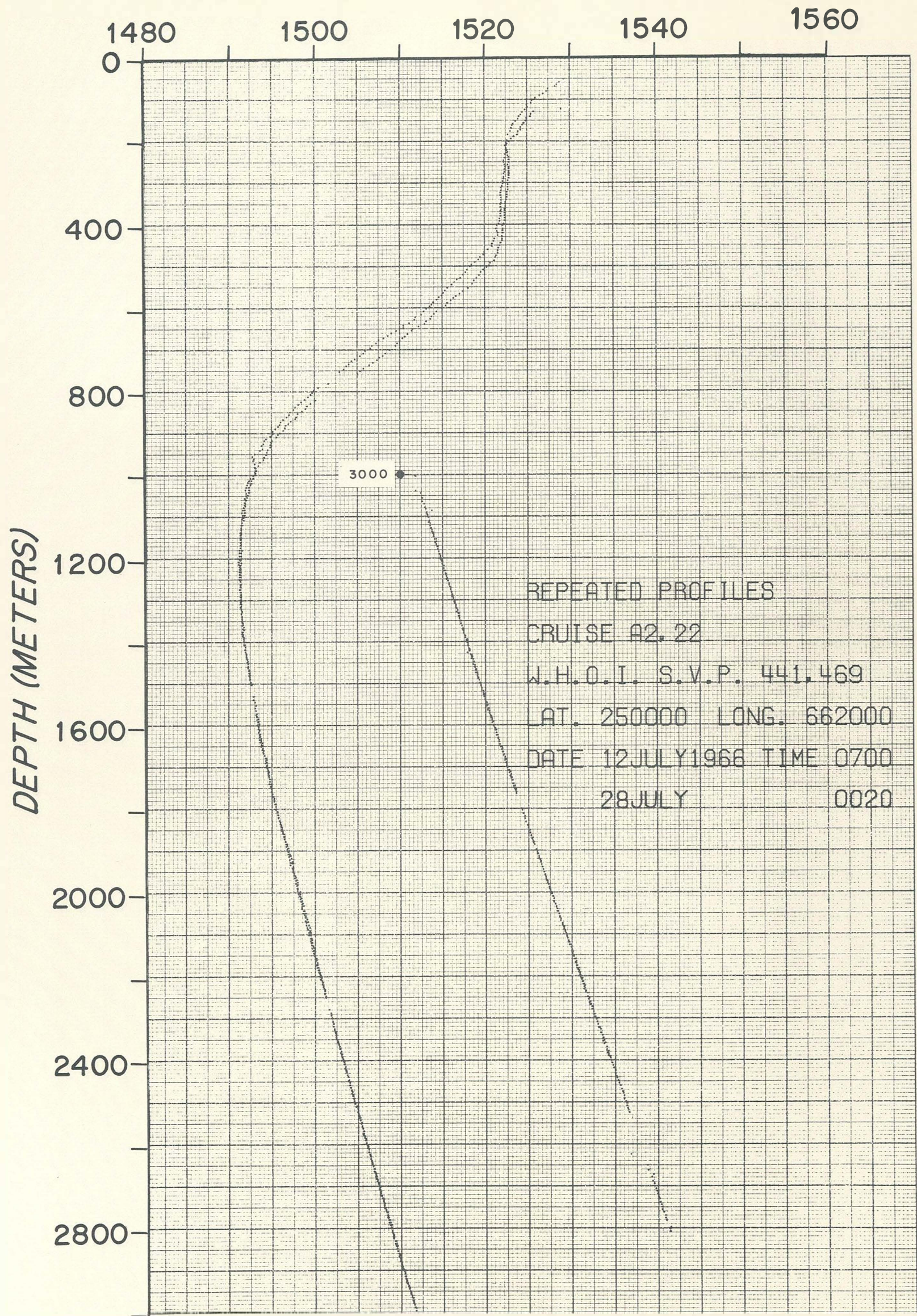
Fig. III-20c   Repeated Sound Velocity Profiles #441 and #469.

SOUND VELOCITY (METERS/SEC)

REPEATED PROFILES
CRUISE A2.22
W.H.O.I. S.V.P. 442,470
LAT. 250100 LONG. 673430
DATE 12JULY1966 TIME 1534
28JULY 0905
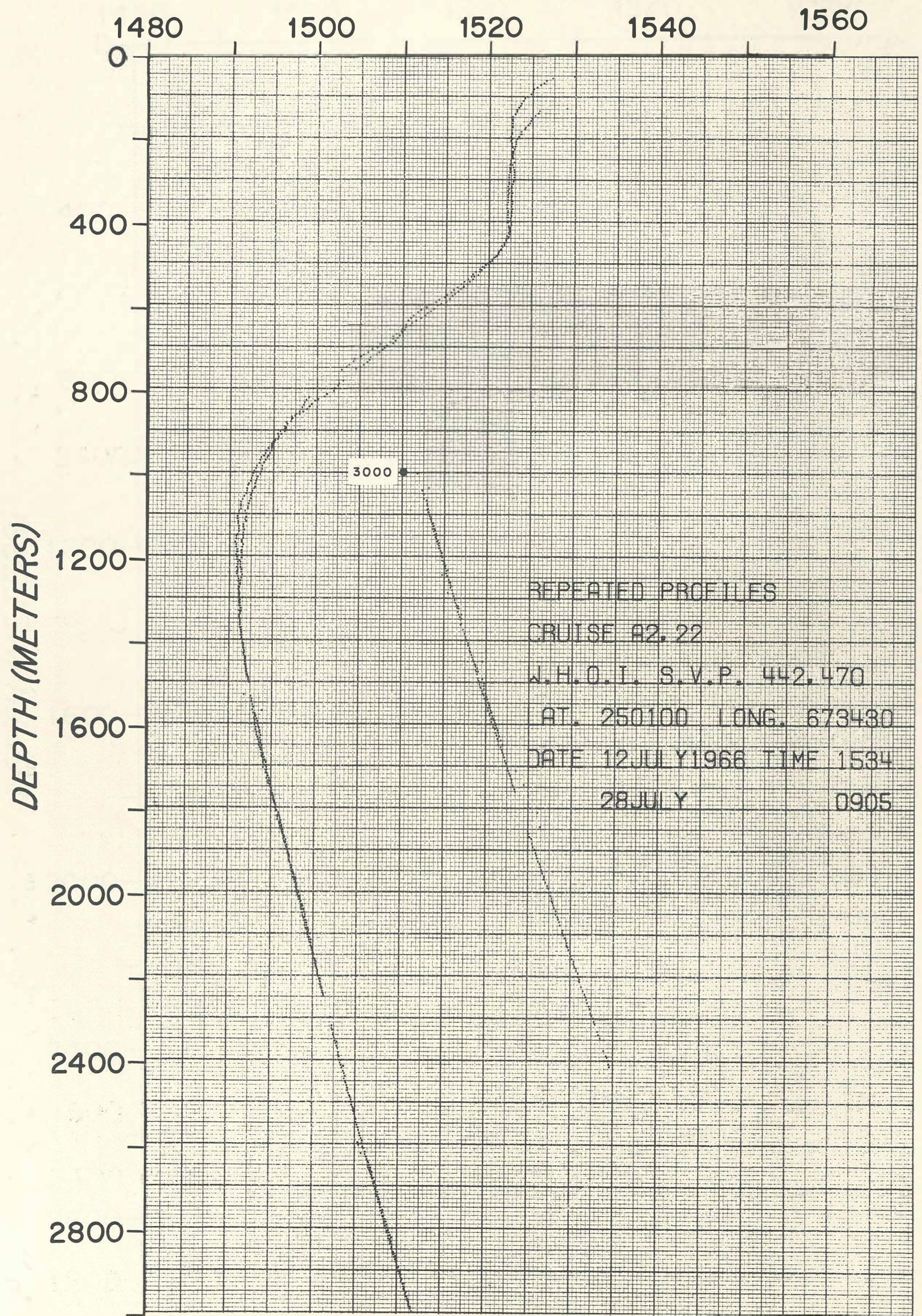
Fig. III-20d   Repeated Sound Velocity Profiles #442 and #470.

SOUND VELOCITY (METERS/SEC)

Text within the figure:

3000

REPEATED PROFILES
CRUISE A2.22
W.H.O.I. S.V.P. 446.474
LAT. 210000 LONG. 685400
DATE 14JULY1966 TIME 0400
      29JULY   1915

DEPTH (METERS)
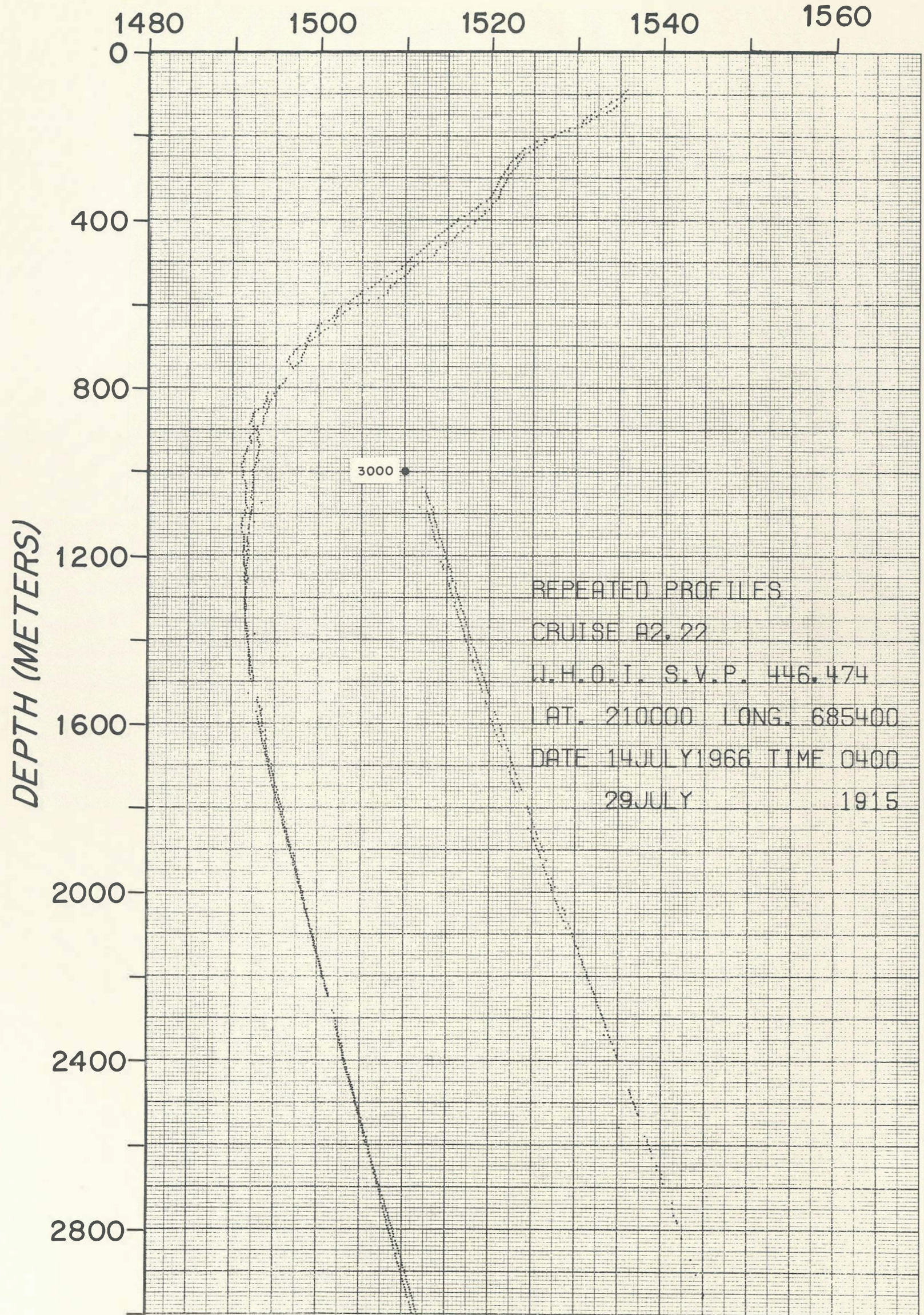
Fig. III-20e   Repeated Sound Velocity Profiles #446 and #474.

SOUND VELOCITY (METERS/SEC)

REPEATED PROFILES
CRUISE A2.22
W.H.O.I. S.V.P. 465,466
LAT. 260000 LONG. 642400
DATE 26 JULY 1966 TIME 1700
      26 JULY   2250

3000
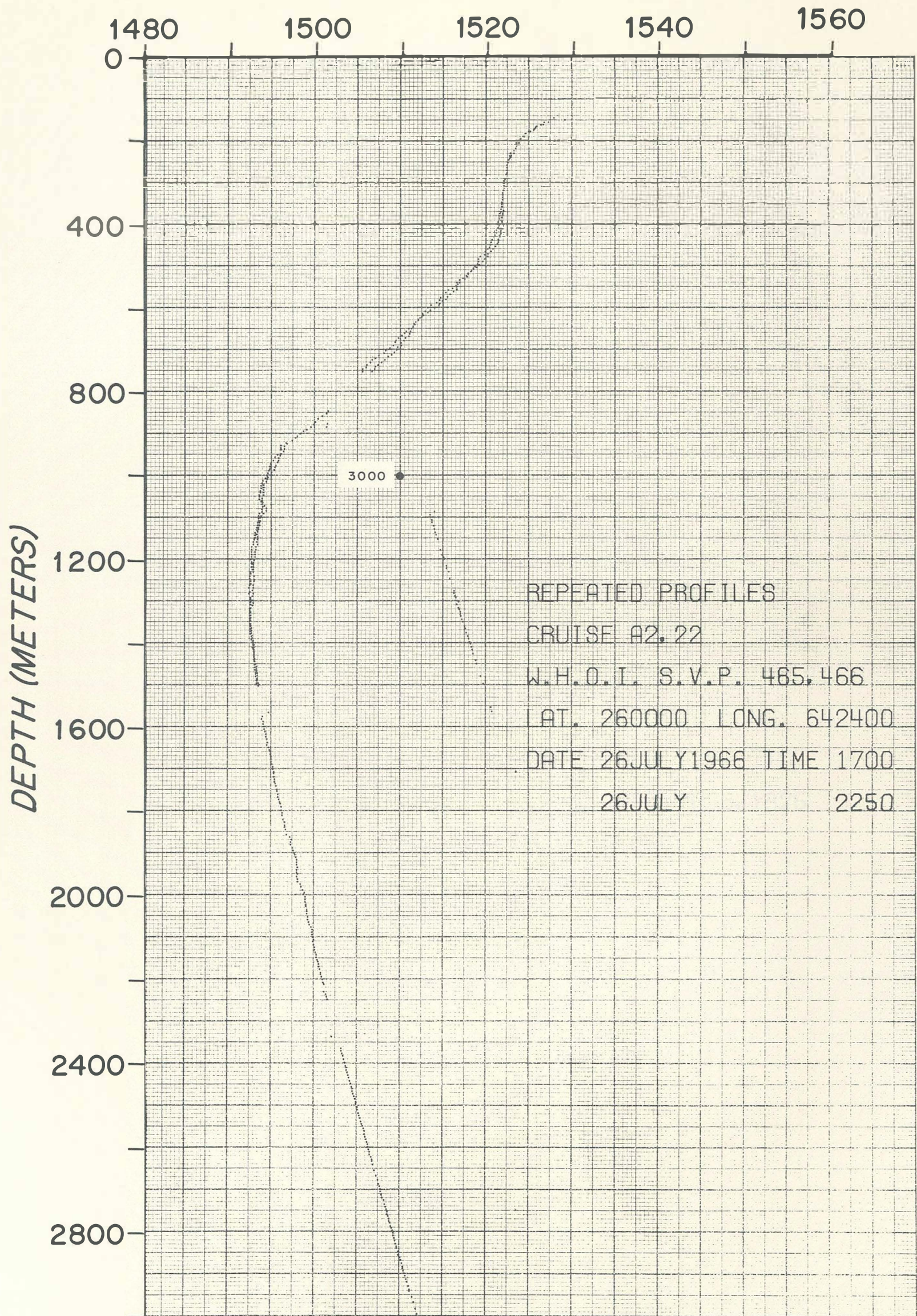
Fig. III-20f   Repeated Sound Velocity Profiles #465 and #466.

SOUND VELOCITY (METERS/SEC)

REPEATED PROFILES
CRUISE A2.22
W.H.O.I. S.V.P. 480TO483
LAT. 280000 LONG. 641600
DATE 1AUG.1966 TIME 1255,
1455,1626,1825
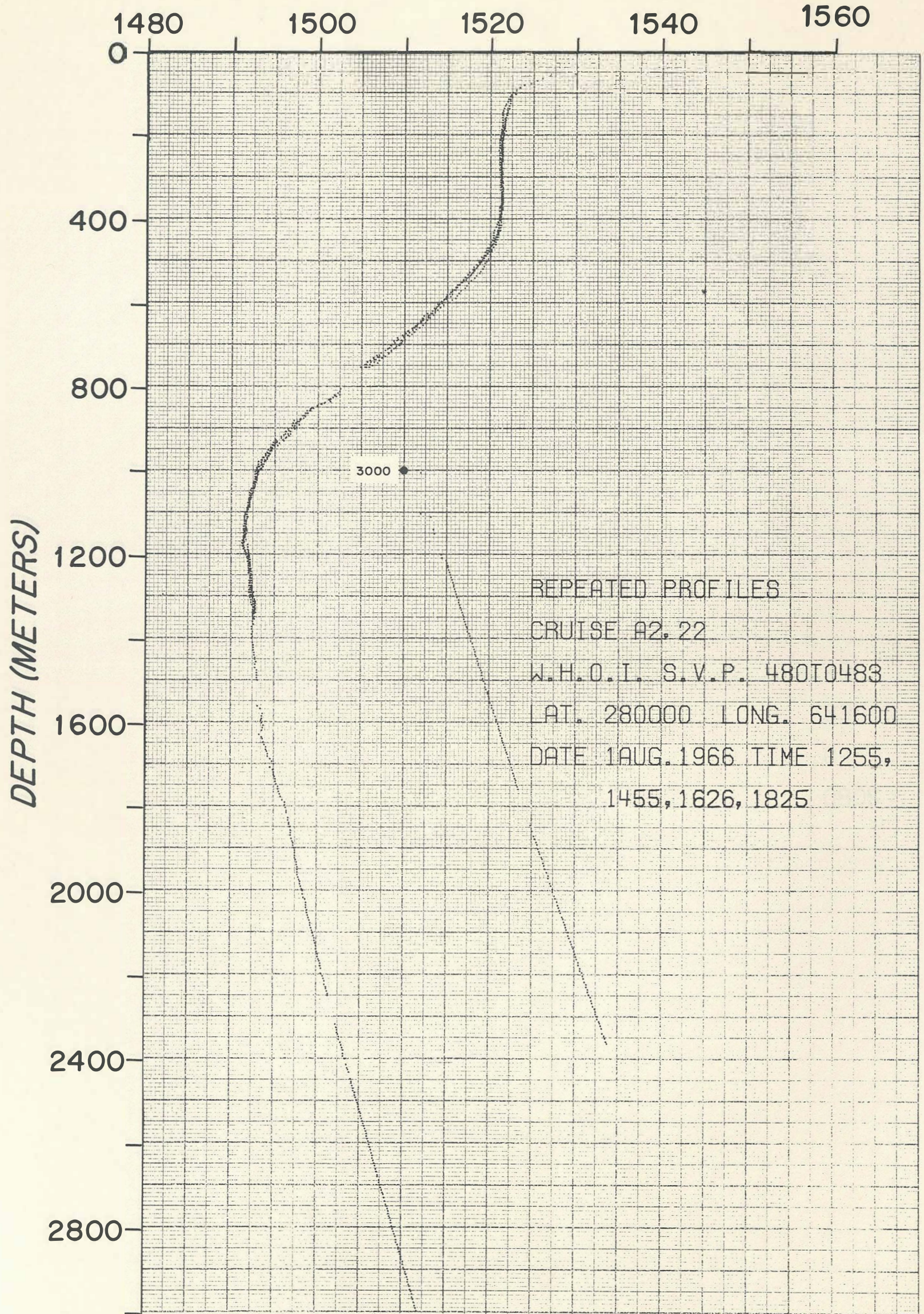
Fig. III-20g Repeated Sound Velocity Profiles #480 to #483.

SOUND VELOCITY (METERS/SEC)

DEPTH (METERS)

3000

REPEATED PROFILES
CRUISE A2.22
W.H.O.I. S.V.P. 484.485
LAT. 290000 LONG. 633500
DATE 2AUG.1966 TIME 0450
2AUG. 0805
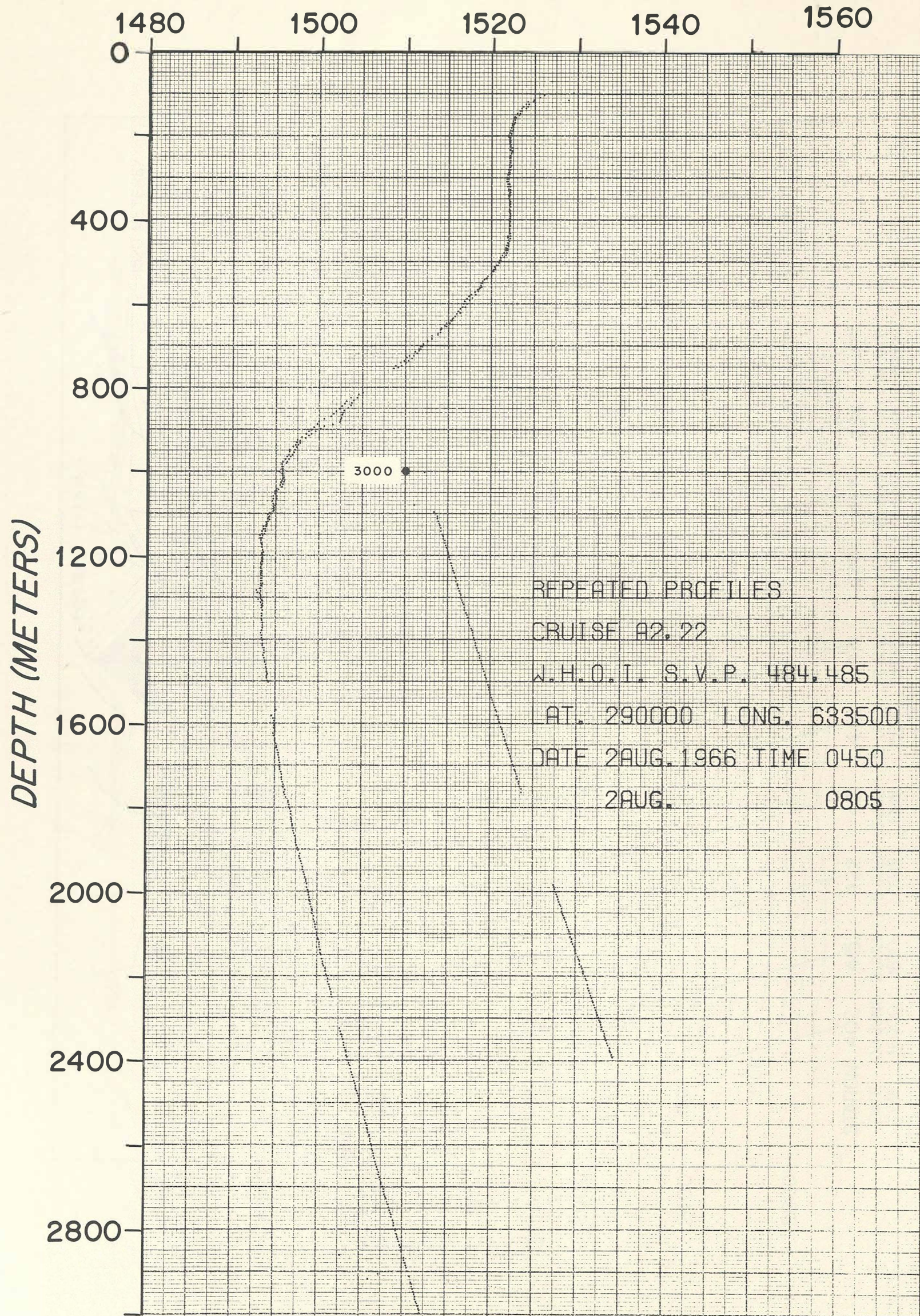
Fig. III-20h   Repeated Sound Velocity Profiles #484 and #485.
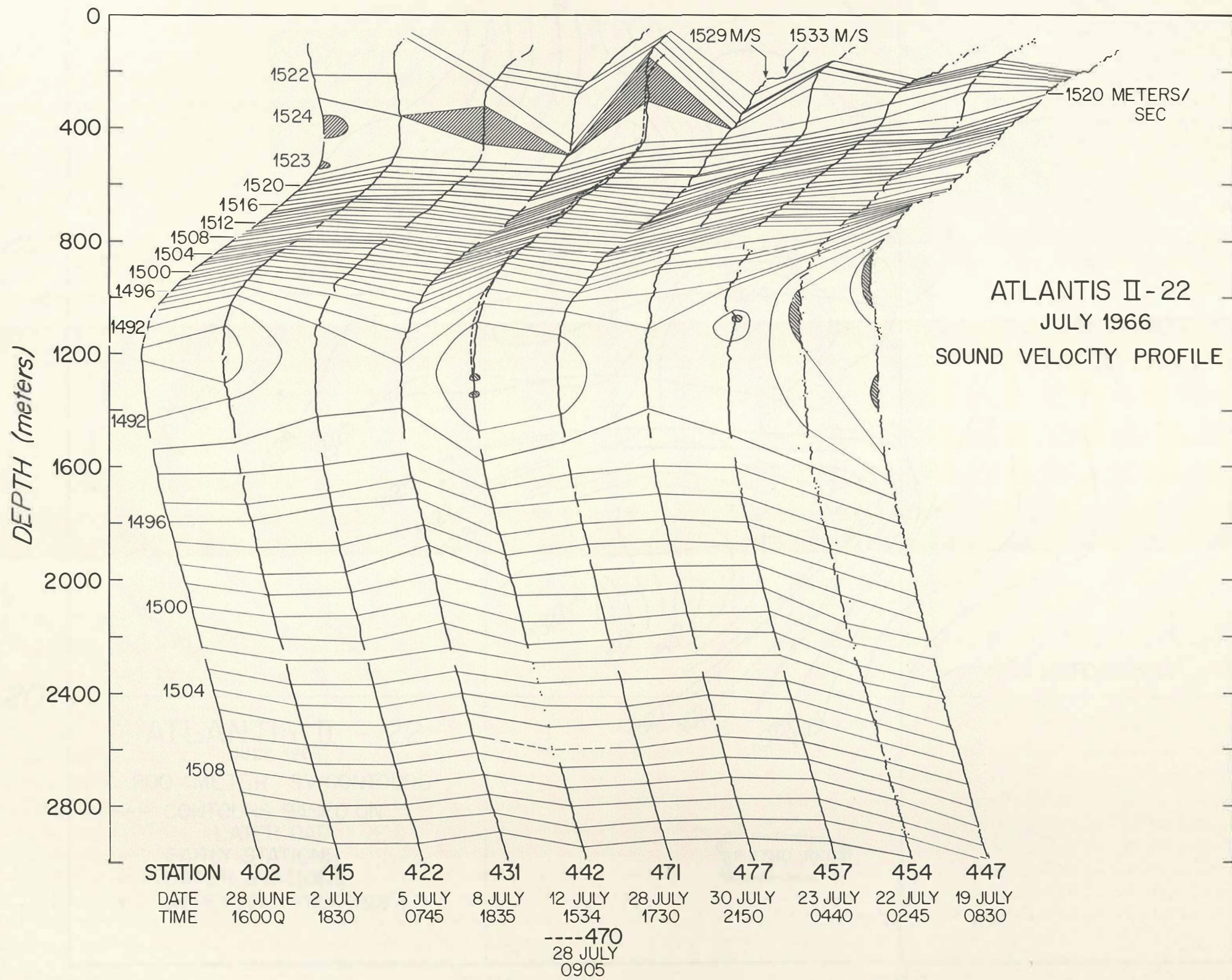
Fig. III-21 Diagonal Line of Sound Velocity Profiles across the Survey Area (see Fig. I-1).
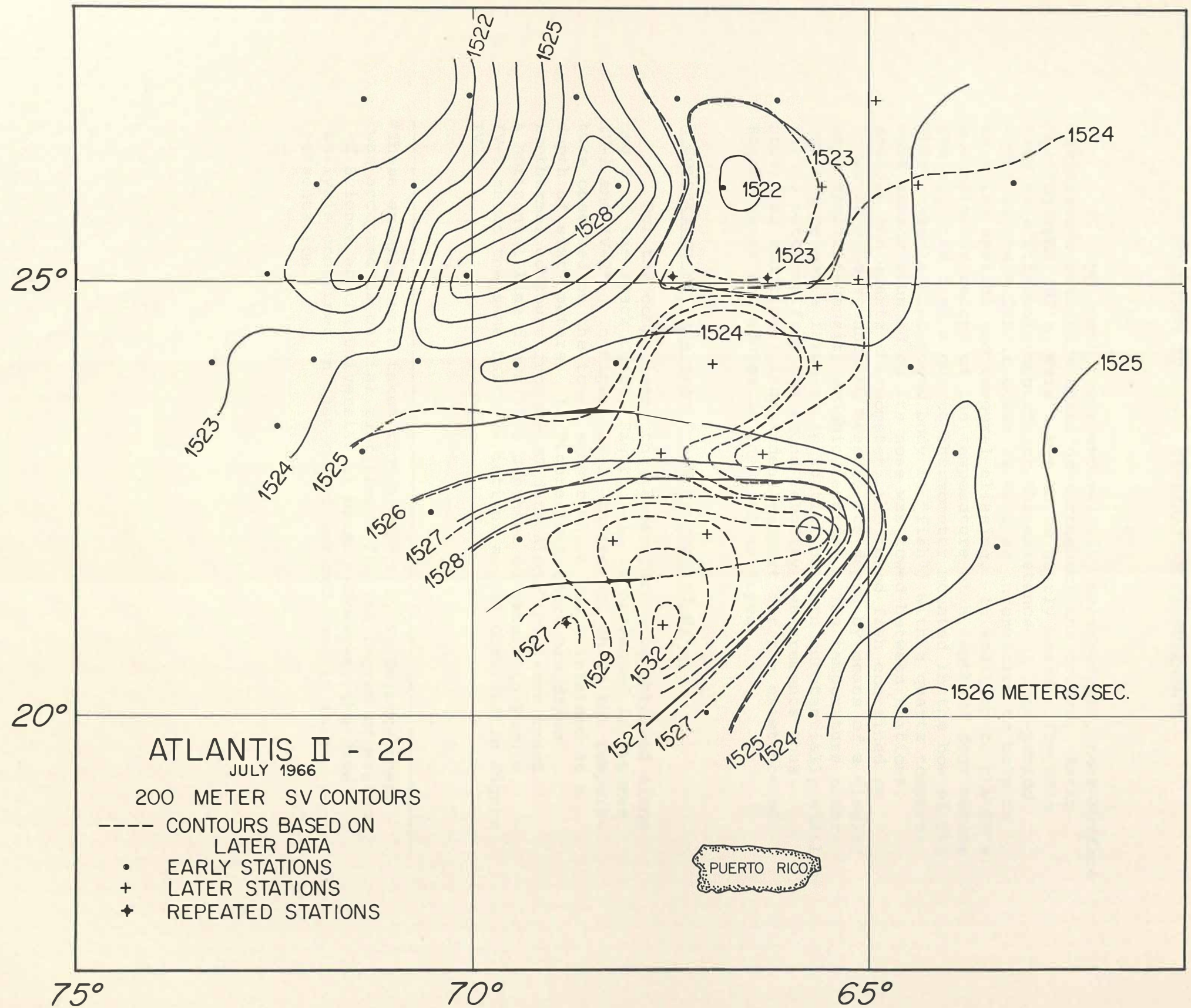
Fig. III-22   Sound Velocity Contours at 200 Meters for Comparison of Earlier and Later Observations.

SECTION IV   –   TEMPERATURE MEASUREMENTS

     To supplement the sound velocity measurements, near-surface
temperature data were obtained throughout the cruise. Bathy-
thermographs (BT's) were taken on an hourly basis. The BT's
provide additional support for the existence of long-period
waves in the Atlantic Ocean as well as information to help us
minimize spatial and temporal aliasing. In addition to the BT's,
a continuous record of the temperature at a depth of four meters
was obtained from a quartz thermometer mounted in the bow of the
ship. Also a 2000-pound body (a "fish") with a quartz tempera-
ture sensor mounted on its nose was towed between stations.
Besides the quartz thermometer, the towed fish contained an
inverted echo sounder to measure its depth by means of a display
on a variable-density graphic recorder. The temperature obser-
vations reveal a large-scale spatial pattern substantially similar
to the patterns from the sound velocity measurements thus
providing additional independent support for the existence of
Rossby waves and eddies in the area surveyed.

A Comparison of Data from Towed Sensor and BT's

     For the comparison, the temperature data obtained along
Leg 3 of the Track Chart, Figure I-1, is presented in Figures
IV-1 and IV-2*. In Figure IV-1, the record shows the tempera-
ture observed on the towed sensor which was maintained at a
depth of sixty meters. In Figure IV-2 there are drawn
isothermal contours from the BT data along this same track.
A horizontal line drawn at a depth of 60 meters in Figure
IV-2 shows the same basic variations as one observed in Figure
IV-1.

----

*These examples were taken from a report by V. Delnore that
 was accepted as partial fulfillment for the Degree of Master
 of Science at the University of Miami. However, the data
 analysis contained in that report was not used in this
 presentation.

In addition, it is clear from the towed temperature sensor data, which consisted of closely spaced measurements, that large-amplitude fluctuations of high frequency along the track are not present and therefore aliasing in the widely spaced data is not serious. Moreover, an examination of very much longer (fourteen-day) periodicities in the temperature data shows that, although these have larger amplitudes, they are small compared to the amplitude of very long wavelength spatial variations that are interpreted as evidence for the existence of Rossby waves and eddies.

A Variable-Depth Towed-Sensor Experiment

The line of sound velocity profiles termed the Bermuda Leg (Track Chart, Fig. I-2) was used to construct the sound velocity contours shown in Figure III-2. These contours show pronounced fluctuations in the thermocline region. To examine this section again using the quartz thermometer on the towed fish as an independent check on these variations, the Bermuda Leg series of SVP's was interrupted. The tow began at the position of SVP #388 and went in a southwesterly direction. The towed sensor was raised and lowered every ten minutes between depths of 200 and 400 meters by changing the speed of the ship. The average ship speed was about eight knots with the speed ranging between four and twelve knots. A total distance of about 100 nautical miles was covered.

Sample records of the depth indication from the variable-density recorder and of the temperature and ship speed from the eight-channel Sanborn recorder are shown in Figure IV-3. During this work standard bathythermographs (BT's) were also taken from the surface to a depth of 200 meters. Thus between the BT data and the towed fish data, temperature measurements extend from the surface to 400 meters.

This technique was not operating satisfactorily until the ship had travelled back along the track to about SVP #378, and the experiment was continued until about SVP #374 (see Figures I-2 and IV-4). An adjustment and averaging of up and

down measurements were necessary to take account of the thermal lag of the quartz thermometer probe. The contour interval of two-tenths of a degree C is used in the zone of low stability water below 200 meters. Above 200 meters where the water is very stable the bathythermograph data was used with a contour interval of one degree C.

In Figure IV-4 there is a pronounced rise in the temperature contours in the region where the temperature gradient is weak, which emphasizes the sensitivity of this technique. The amplitude of the disturbance decreases toward the upper part of the layer because of the greater stability of the upper water layer. The rise in the temperature contours is in the same region as that observed in the contours obtained from the sound velocity profiles in Figure III-2.

This measuring technique, a variable-depth towed body controlled by the ship's speed, appears to have some advantages in simplicity and reliability over other methods of ocean measurement. The method appears to be adaptable to computer processing at sea and it should allow ocean measurements covering much greater depth intervals with a continuous vertical sampling, where resolution is needed. A temperature sensor or sound velo-cimeter having a rapid response time would be more suitable than the slow-responding quartz probe. A horizontal sampling interval of about one-half mile ought to be adequate for most of the large-fluctuation horizontal scales that occur in the ocean.

The Bathythermograph Measurements

In addition to the quartz thermometer measurements taken at 4 and 60 meters, the bow sensor and the towed sensor, bathy-thermograph measurements were taken every hour throughout Cruise #22 of ATLANTIS II, except, of course, while at an SVP station. The BT measurements were much more closely spaced than the sound velocity profile measurements and therefore the temperature measurements contain considerably more information about the first 250 meters of the ocean. The location of the BT stations are shown throughout the track chart, Figure I-1, by small dots, to give some feeling of the control of the data (the large dots indicate sound velocity profile stations).

Since the survey covered twelve degrees in latitude an
effort was made to remove the north-south trend in the depth
measurements obtained from the BT data. It was found that
the average values for the depth obtained for each degree
of latitude could be fitted with a linear north-south trend of
approximately six meters per degree of latitude with the deeper
depths occurring in the southern regions of the survey area.
If the temperature measurements relate to ocean circulation,
it was felt that the interpretation of the observations would
be more significant after the north-south trend in the data
was removed. Therefore, we constructed an interpretive
chart of the depth variations for a 20°C isothermal surface
obtained from these BT measurements after the north-south
trend was removed. Once this had been done, lines of equal
depth were drawn revealing the pattern in Figure IV-5. The
lines of equal depth are at 20-meter intervals. Although
some smoothing was performed, for the most part an attempt was
made to honour each measurement.

The density of observations along the individual tracks
of the ship and the gap of approximately sixty miles between
these tracks made the selection of the lines of equal depth
occasionally arbitrary in the interior region of the survey.
For this reason, the 120-meter line for the 20°C temperature
is dashed in the north-central portion of Figure IV-5. Its
chosen location, which is not critical, is in keeping with our
view of the circulation pattern.

The arrows in Figure IV-5 do not indicate measured
currents, rather they were inserted between the lines of
constant depth to indicate the direction of the expected flow.
We expect that a clockwise flow should exist around a region
where there is a depression in the depth of the 20°C isothermal
surface, and, conversely, a counterclockwise flow should occur
around a rise in the temperature surface. (A theoretical dis-
cussion of circulations in the ocean is presented in Section V.)

Partial verification of the arrows in this circulation
pattern can be obtained by comparing the heading of the ship
and its true course between every pair of Loran fixes, indicated

approximately by the BT locations on the track chart, Figure
I-1. The average value of the ship's set throughout the
cruise was 1.8 degrees to starboard and this agrees with
the gyrocompass error obtained from the ship's navigation
logs. The component of the ocean flow normal to the ship's
track is taken to be estimated by the deviation of each set
from the average. All of these deviation-directions were
plotted along the tracks on the 20°C isothermal surface and
compared with the expected flow directions indicated along
the lines of equal depth. The magnitude of some of the devi-
ations was as large as nine degrees, although most were in
the interval between one and four degrees. There were many
areas where the comparison was ambiguous and this is not
surprising since water flow at the surface could easily be
different from flow at the depths between 100 and 300 meters
and since there are uncertainties in the method of estimating
the set. We have omitted this chart with all these compari-
sons because it is too complex. Instead, we mention three areas
of substantial agreement, areas where the circulation suggested
in Figure IV-5 was intense enough at the surface to influence
the ship. These areas are: (1) the large central eddy where
a large number of sets indicated clockwise circulation;
(2) the area at 24°N 67°W where there was a definite clockwise
circulation; and (3) the area around 23°N 67°W where counter-
clockwise circulation was prominent at the 100-meter depth.

Some Analogies and Speculations

        There are several major features in the circulation
pattern of Figure IV-5 that are quite striking. First we wish
to describe these features and then to try to interpret them
in terms of vortex theory and the bathymetry.

        The most striking feature is the large clockwise circul-
ation located in the center of this pattern at 26°N 69°W, where
the greatest depth of the isothermal surface occurs. Just to
the east of this large eddy there is a large but weaker counter-
clockwise back eddy that seems to be associated with the first.

The third major feature is that the boundary between these two central eddies appears to be shedding eddies, since there seems to be an eddy street along a line running southwesterly from the southern side of this central circulation. Notice how the two rows of eddies have the appearance of alternating arrays of clockwise and counterclockwise eddies that seem to be in a fairly stable configuration with each other. The ratio of the separation of the rows to the space between the eddies is about 0.25 which compares favorably with the value of 0.281 for a quasi-stable von Kármán vortex street. Of special interest is the evidence of a relatively intense clockwise eddy at 24°N 67°W which is located at the same place as the clockwise eddy on the 200-meter contour chart of sound velocity (Figure III-7).

A fourth major feature occurs in the northern portion of the pattern where the path for the direction of flow from west to east at 100 meters' depth contains meander features like those that have been found in the near-surface thermal front zone (Voorhis and Hersey, 1964; Katz, 1969; and Voorhis, 1969). We observe in this region of the pattern an apparent separation of flow indicated just to the northeast of the central eddy by the 100-meter and 140-meter depth lines. At 28°N 66°W there is a clockwise eddy indicated by the 100-meter flow line. There is also evidence for the existence of this eddy in the sound velocity contour charts for the depths of 800 meters and 200 meters shown in the previous section. A fifth and final feature concerns the flow pattern suggested near the boundary with the Bahama Bank where there are numerous passages. The pattern suggests that the flow may be into and out of these passages.

The pattern of the lines of constant depth in Figure IV-5 resembles the flow pattern around a rotating cylinder in a stream of water if we tentatively choose the cylinder boundary to approximate the largest closed path (160-or 180-meter curves) around the central eddy (Prandtl and Tietjens, 1931, reprinted in Goldstein, 1938). The analogy has many weaknesses and it is not meant to imply that the dynamics are the same. Nevertheless, the similarity does lead us to suspect that the large central eddy may undergo an acceleration to the northeast, which is to

the right of the apparent upstream direction. Thus, the location
of this eddy should be expected to move about in response to
seasonal changes in the Gulf Stream flow and inflowing streams
from the Bahama Bank passages, as well as to changes in its
circulation and the apparent shedding of eddies from its
boundary region.

The period of apparent eddy shedding is expected to be
close to the calculated period of 110 days for Rossby waves of
near-zero group velocity and of wavelength 445 km (250 miles),
appropriate to this ocean region. Moreover, the westward phase
velocity for such waves is about 4.5 km/day (1/10 knot), and
we might well expect circulatory currents in the large central
eddy to exceed this speed. Consequently, the interpretation
that the pattern in Figure IV-5 represents a portion of a
relatively strong, finite amplitude, baroclinic wave propagating
slowly to the northwest seems likely. Notice, for instance,
that the deepest closed curve within the large, central eddy
is displaced closer to the western side of the larger-diameter
closed paths around the eddy.

The mathematical analysis of finite-amplitude waves is
one of the most difficult in hydrodynamics. This kind of wave
may be viaualized as a propagating cellular system of relatively
intense vortices, in which the circulatory flow velocities in
the central regions of the vortices are greater than the pro-
pagation speed of the wave (Godske et al, 1957). From this
viewpoint, the large central eddy would be expected to make
meandering excursions to the northeast and southwest and we
might expect its intensity to be seasonally dependent. It is
unfortunate that numerous current measurements are not available
to relate the temperature surface in Figure IV-5 to more
specific theoretical calculations.

A second interesting relationship appears when the
contour lines of the 20° isothermal surface, Figure IV-5,
are superposed on the bathymetry contours for this region.
In Figure IV-6 the dashed lines represent the 20° isothermal
contours and the solid lines, the bathymetry contours (from
Pratt, 1968; also seen in Figure III-15). Both contours are
labelled in meters.

Observe that the large, central clockwise eddy designated "A" is located over the large, central basin of the Hatteras Abyssal Plain. The central portion of this eddy, labelled 220 meters, is just southwest of a narrow elongated depression in the bottom trending northeasterly. The intense clockwise eddy "B" is located over the deep 5800-meter contour of the Nares Abyssal Plain at the Vema Gap. Further southeast, the clockwise eddy "C" is located over the deeper water in the saddle-point region of the outer ridge separating the Nares Abyssal Plain and the Puerto Rico Trench. The 160-meter dashed contour of clockwise eddy "D" is located just north of the deeper region of the Z-shaped 5400-meter depth contour at the Bahama Bank. A small clockwise eddy "E" to the south of the main eddy "A" is close to the relatively narrow, tongue shaped, 5700-meter bottom contour. The broad counterclockwise eddy "F" does not appear to be related closely to the bathymetry beneath it. However, we should expect that some of these eddies, which possess relatively great amounts of angular momentum and are only loosely coupled to the shape of the ocean bottom, would be able to undergo occasionally large lateral shifts without greatly changing their shapes.

In a coordinate system that moves with an eddy, the stream line that defines the shape of the eddy tends to be relatively steady. Consequently, the back-eddy "F" may have been associated with the broad, shallow zone on the Bermuda Rise to the north of it as defined by the closed 5200-and 5100-meter contours. By the same reasoning, a slight southwestward shift of eddy "B" would have the 160-meter dotted contour make a sharp counter-clockwise turn about an apparent mound of sediment. Such a shift of the pattern would also place eddy "D" more into the valley of the Z-shaped bottom contour near the Bahama Bank.

The intense clockwise eddy "G" appears to be shifted only very slightly to the east of a depression in the bottom, which is indicated by hashed marks on the inside of closed bathymetry contours*. The scale of the dashed contours at "H"

----

*Some opinions have been expressed regarding the quality of the bathymetry of this chart in this region. While it is clear from more recent data that the area is complicated there do not appear be serious contradictions.

and "I" also shows some similarity to the scale of the bathy-
metry contours. A dotted 120-meter depth curve in the isothermal
surface further north shows a hook-like bend that seems to
have some conformity to the gradual bends of the 4900-meter
bathymetric contour.

Of course, there are a number of dissimilarities that
are evident in making comparisons, for example, the dashed
60-meter curve in the northeast is not easily related to the
bathymetry beneath it. Nevertheless, it is clear from the
various comparisons that the scales of the bathymetric features
are similar to the scales in the isothermal surface pattern.
This suggests that some causal relationship might exist and
that some of the features in the pattern may persist over long
periods of time.

With respect to the influence of the ocean bottom on
circulation patterns, there is a growing theoretical litera-
ture (Rossby, 1939; Warren, 1963; Welander, 1968; and Rhines,
1969a and 1969b). Conservation of potential vorticity would
imply that flow lines tend to be clockwise over depressions in
the bottom and counterclockwise over mounds, in the northern
hemisphere. Rhines points out that very small-percentage changes
in bottom depth can have an effect on the flow patterns when
the period of the long waves is large compared to a day. There
is also the possibility that the shape of the ocean bottom, with
regard to sediment distribution, may be influenced or reinforced
by the manner in which particulate matter settles out of clock-
wise and counterclockwise eddies. For example, it would be
interesting to determine whether the mound in the bathymetry
mentioned earlier and observed just to the northeast of the
Silver Abyssal Plain in Figure IV-6 is a sediment hill indicating
large sediment fallout.

LIST OF FIGURES

SECTION IV   —   Temperature Measurements

Figure

NAUTICAL MILES SOUTHWEST (240°) OF BERMUDA

Fig. IV-1   Towed Temperature Sensor Data at 60 Meters for Leg 3.

NAUTICAL MILES SOUTHWEST (COURSE 240°) OF BERMUDA
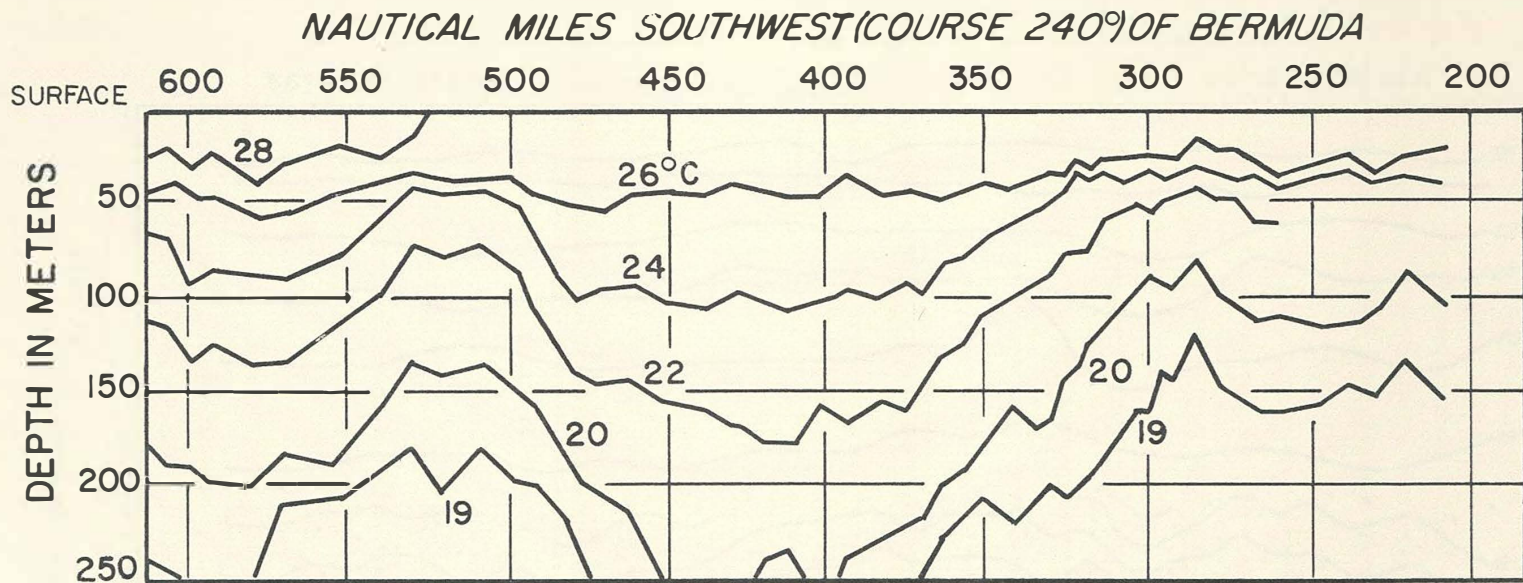
Fig. IV-2   Vertical Section of Isotherms from Bathythermographs for Leg 3.

FISH DEPTH vs. TIME

ATLANTIS II CRUISE 22

FISH TEMPERATURE ⟷ TIME ⟷
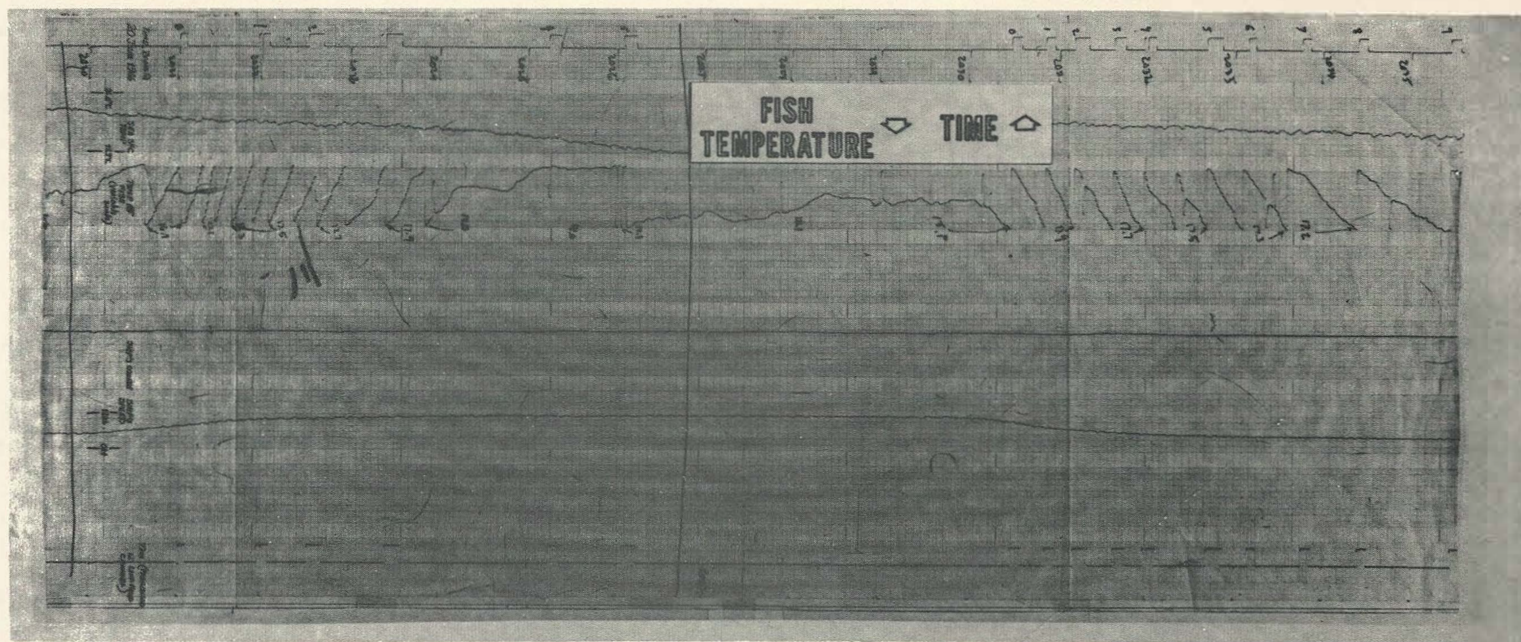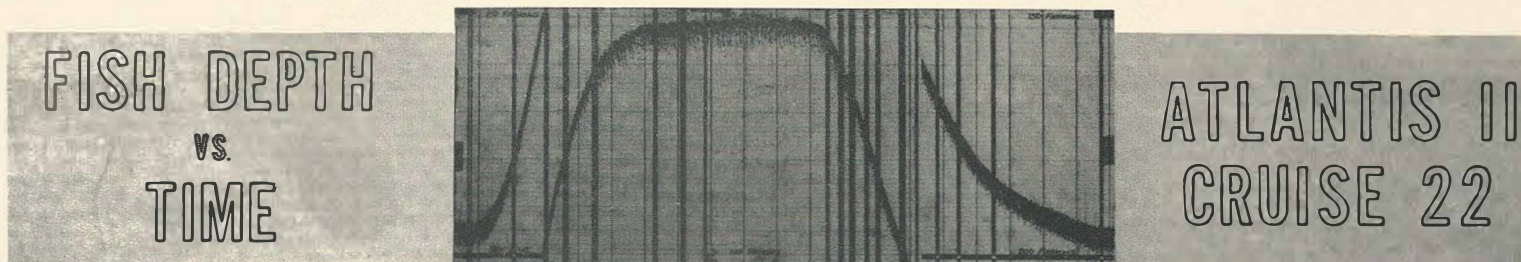
Fig. IV-3   Sample Sanborn Recording of Towed Temperature Sensor
Measurements and Variable Depth of Towed Fish Versus
Time for Bermuda Leg.

60 nm

66°40'W-29°21'N   67°10'W-28°29'N

26°
22°
21°
20°
19°
18.0°
17.8°
17.6°
17.4°
17.2°
17.6°   17.0°

DEPTH IN FATHOMS

BT DATA

TOWED FISH DATA

TIME ; ——— HOURS ——→

TEMPERATURE CONTOURS

ATLANTIS II CRUISE 22
JUNE 20, 1966
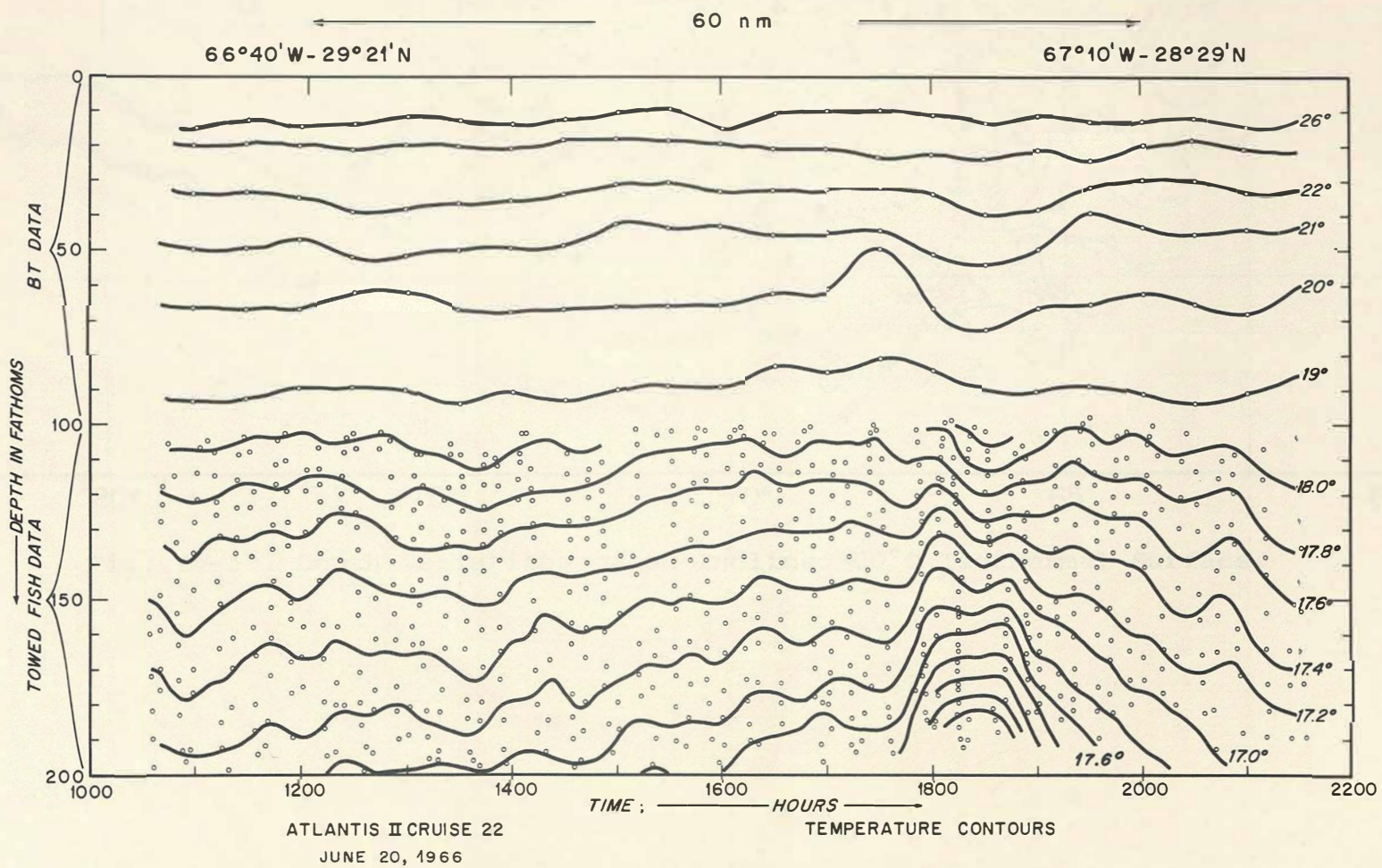
Fig. IV-4   Vertical Isotherm Section Obtained from Towed
Variable Depth Sensor and BT's - Bermuda Leg.
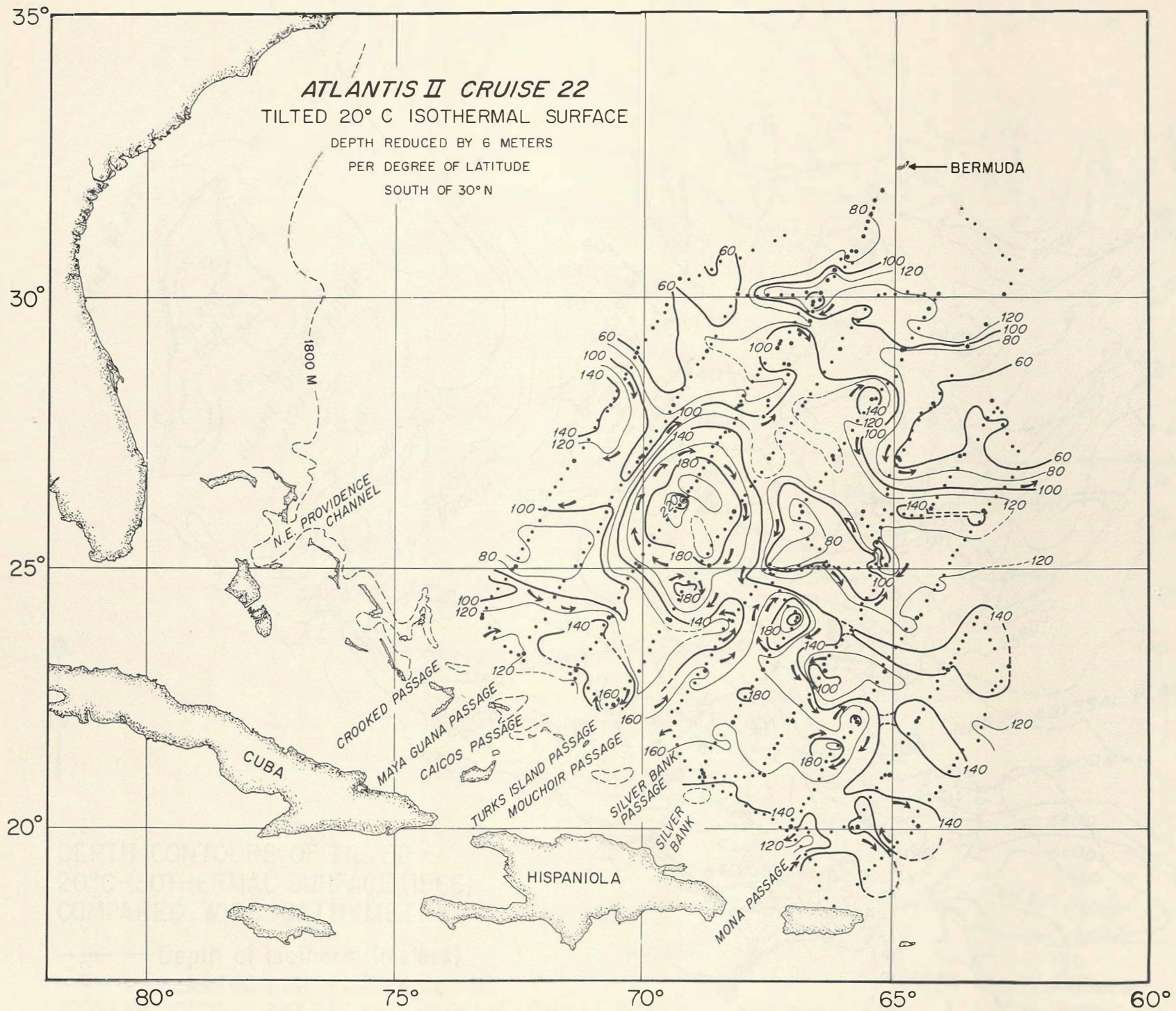
Fig. IV-5   Depth Variations of an Inclined 20°C Isothermal Surface.

DEPTH CONTOURS OF TILTED 20°C ISOTHERMAL SURFACE (1966) COMPARED WITH BATHYMETRY

- – – – – Depth of isotherm (meters)
- ·········· Selected intermediate depths

ISOTHERM DEPTHS REDUCED BY 6 M/DEG. OF LAT. SOUTH OF 30°N
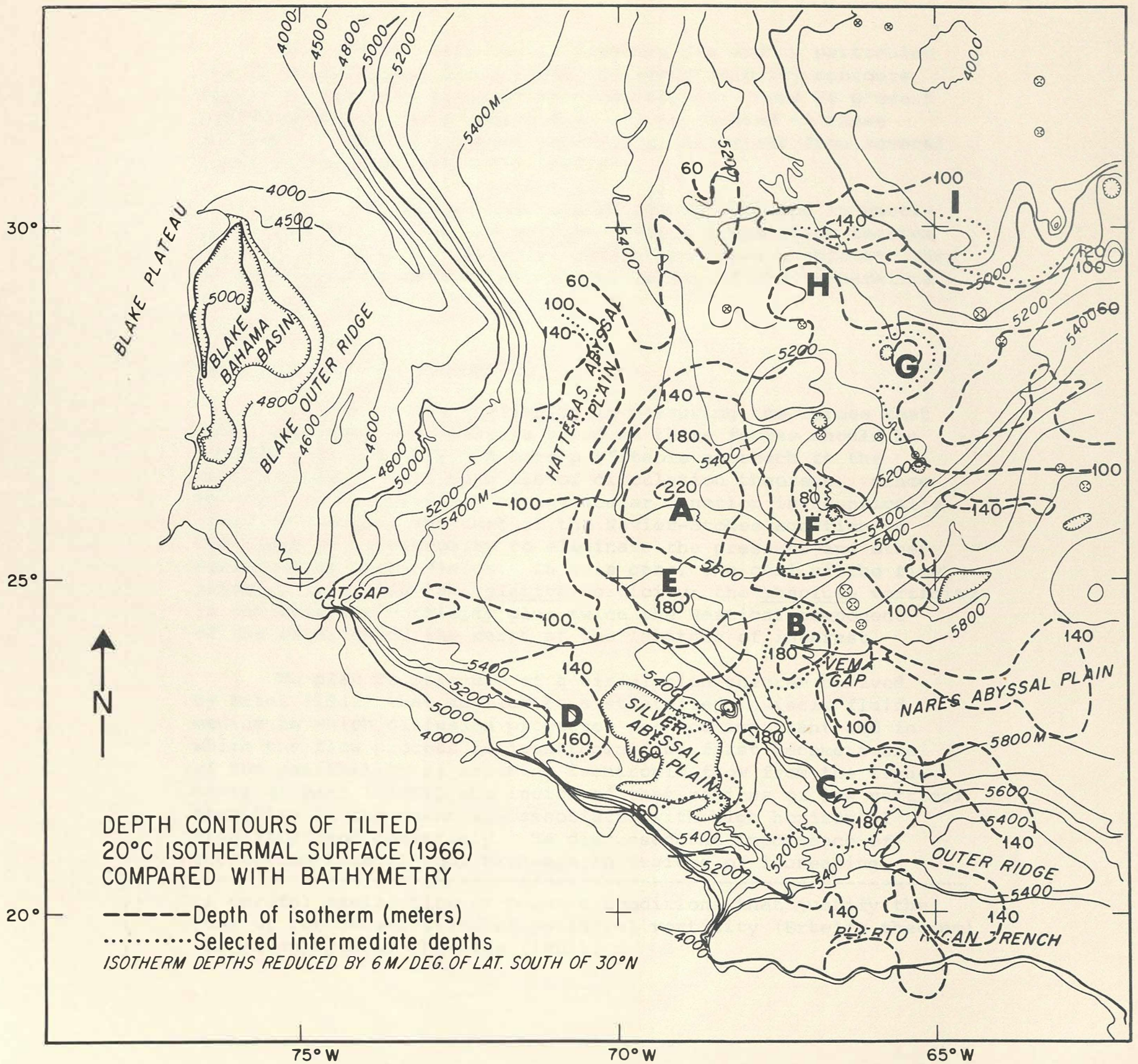
Fig. IV-6   Comparison of 20°C Isothermal Surface and Deep Ocean Bathymetry.

SECTION V   —   A GENERAL CIRCULATION THEOREM

Much of our data on the Sargasso Sea and in particular
the 20°C isothermal surface and the sound velocity contours
appear to indicate large-scale circulations. Here we present
semi-quantitatively a theory that may be related to these
patterns. This theoretical approach is different from several
lines of research mentioned earlier.

After discussing the general assumptions and in parti-
cular isentropic flow, we outline Ertel's circulation theorem
(1942), and show how it can be related to these problems*. Then
we apply this theorem in an interpretation of the temperature
variations in the ocean.

Discussion of the Assumption

In view of the difficulty in measuring the forces that
drive the ocean, an analysis based on these forces should be
avoided when possible. A more profitable approach to the
analysis might be to make use of circulation theorems. Since
the curl of the gradient of any scalar function is identically
zero, we can take the curl of the Navier-Stokes equation in
the limit of no viscosity to eliminate the pressure and other
conservative force fields. In this case, the curl of the flow
velocity is called the relative vorticity; the absolute vorticity
is the relative vorticity plus twice the vertical component
of the rotation of the earth at the latitude of interest.

We plan to make use of a circulation theorem derived
by Ertel (1942) that applies to a stratified inviscid fluid
medium in which diffusion processes are not important and in
which the flow process is isentropic. We first became aware
of the possibility of assuming isentropic flow from the argu-
ments of Parr (1936), who indicated that regions of low vertical
stability in the ocean are associated with high horizontal
stability, and conversely. He discussed the importance of
increasing lateral eddy exchange in regions of increasing
----
*A careful explanation of oceanic conditions that justify the
 use of the conservation of potential vorticity (Ertel's theorem)
 is given by N.A. Phillips (1963).

vertical stability. Montgomery (1938) also encouraged the application of isentropic analysis to ocean circulation, and more recently, Tabata (1967) compared an isentropic analysis and a geostrophic analysis of the northeast Pacific Ocean. These, coupled with the recognition that the Sargasso Sea appears as a highly layered structure much of the time, strongly suggest that flow may well be nearly isentropic in zones of high vertical stability. The main forces, such as wind, that drive the ocean are at the surface; and only a short distance into the ocean turbulent exchanges are negligible or at least very much reduced. Therefore, we imagine flow to be mostly along layers, although these layers may change depth and thickness. Recently, Lynn and Reid (1968) interpreted deep abyssal water flows as density surfaces without turbulent mixing.

Although we assume the fluid is without viscous diffusive processes that are turbulent and heat exchanging, this does not mean that turbulent processes are unimportant in the ocean, nor that very complicated interwoven eddy-like flow exchanges cannot take place in the fluid, but only that the latter motions are still laminar flows. Welander (1955) has shown pictures of how complicated thin-layered laminar flow can be. In our case, the flow is taken to be layerwise isentropic, i.e., the layers may interweave among each other. The only reasonable approach from an experimental point of view in complicated cases is a statistical approach, since it is difficult to distinguish these very complex laminar flows from true turbulence.

Also we will neglect the effects of salinity in the theory that follows, although a complete theoretical treatment should include it. We think this is reasonable for the Sargasso Sea because of the well-established temperature-salinity relationship. If we can neglect the turbulent diffusion of salinity between layers, an isentropic surface becomes a surface of constant temperature. We merely assume that the fluid particle carries its salinity with it as well as its temperature. How good an approximation this is will depend on the agreement we find with observations.

Suppose that the change of salinity with depth that occurs in the ocean results from horizontal transport in a layer that rises to another depth, rather than by vertical diffusion across layers. According to this hypothesis salinity inversions and temperature inversions can still be expected to occur in the measurements without heat transfer or salt transfer directly across layers, if we assume the two layers of slightly different temperature first wrap around each other by virtue of their particular laminar flow and perhaps by virtue of the influence of a seamount that enhances counterclockwise circulation. In this way colder-temperature water from below can be carried up above warmer-temperature water. Following this laminar flow process, the diffusion process may take place very slowly on a molecular level between the intimately interwoven layers. The slow heat transfer and salt exchange can take place across such layers by diffusion according to this mechanism, with much of the flow up to this point being described as non-turbulent or laminar. The above hypothetical mechanism for temperature/ salinity inversions would not be detected by the oceanographic measurements currently in use.

We consider non-turbulent diffusion between the interwoven layers of the ocean because it is unlikely that a major heat source exists in the interior of the ocean that could bring about turbulent vertical mixing. Even if such a heat source were available, we suspect that eventually the ocean circulation would adjust itself to balance this heat flux by developing a layered transport while minimizing turbulent heat transfer across layers. We also expect that there may be vertical turbulent mixing brought about by the interaction of large, breaking, internal waves (see Section III, Yo-Yo experiment) but we want to avoid bringing such a process into the treatment. We consider the hypothesis that vertical water movements take place as a consequence of large-scale layer-wise horizontal eddy exchange processes that vary with depth and location.

Ertel's Circulation Theorem

There is a general circulation theorem first derived by Ertel in 1942 for an inviscid, stratified, compressible, fluid in non-turbulent flow. The theorem, which follows from

then the continuity equation becomes

$$\frac{D}{Dt} T = 0 \qquad\qquad \text{Eq. V-3.}$$

which states that the fluid particle moves along an isothermal surface.

Then in Eq. V-2 if we set the arbitrary scalar field ψ equal to the temperature and use the condition $\frac{D}{Dt}\rho = 0$, the equation reduces to

$$\frac{D}{Dt}\left(\nabla T \cdot \Omega\right) = 0 . \qquad\qquad \text{Eq. V-4.}$$

From Eq. V-4, we see that the fluid particle also moves on a surface of constant potential vorticity which is equal to the scalar product of the temperature gradient by the absolute vorticity. In general these two surfaces intersect each other for a given fluid particle along some kind of curve, which is called the trajectory of the fluid particle, which may vary in time as well as position and depth. This trajectory of a fluid particle at a given instant runs at a tangent to the streamline that passes through its position. A streamline is the curve in space at a given instant of time that is everywhere parallel to the flow velocity in the field. Hence the trajectory is the envelope of the system of streamlines for successive instants of time. Only when the streamlines are steady will streamlines and trajectories coincide.

When the horizontal scales for the variation of temperature in the ocean are very much larger than the vertical scales, then the gradient of temperature is mostly vertical. Therefore, as a particle moves along a path of constant temperature, Eq. V-3, it mostly experiences only changes in the vertical temperature gradient. It is reasonable for our purposes to approximate the absolute vorticity by the Coriolis parameter, f, and the vertical component of the relative vorticity, ζ, so that Eq. V-4 may be written simply

$$\frac{D}{Dt}\left(\frac{dT}{dz}(f+\zeta)\right) = 0 . \qquad\qquad \text{Eq. V-5.}$$

The pair of equations V-3 and V-5 need to be simultaneously satisfied for a fluid particle.

The very simplest non-trivial solution that one can have for a particle as you travel along with it is that

$$\frac{dT}{dz}\left(f+\varsigma\right),$$

the _potential_ vorticity, be proportional to the temperature. The proportionality factor may be a function of the initial time at the position where the fluid particle is considered to begin its travels, or

$$\left(\frac{dT}{dz}\right)\left(f+\varsigma\right) = K(t_0)\,T \qquad\qquad \text{Eq. V-6.}$$

A very special case leads to an especially simple formula. If the local temperature gradient is approximately inversely proportional to the depth of the isothermal surface, i.e.,

$$\frac{dT}{dz} \propto \frac{T}{z_0-z},$$

then Eq. V-6 becomes

$$\frac{f+\varsigma}{z_0-z} = K(t_0). \qquad\qquad \text{Eq. V-7.}$$

Eq. V-7 states that the absolute vorticity divided by the depth, i.e. **the** absolute _potential vorticity_, equals a constant which is a function of the initial time, or in the steady case equals a constant dependent only on the initial position. This special form of Ertel's Theorem can help to interpret the oceanographic phenomena described in earlier sections.

Discussion of Ertel's Theorem

Now that we have obtained a linearized form of Ertel's Theorem, Eq. V-7, we first need to describe the oceanographic situation to which this theorem applies. Then we present some examples from the data collected on Cruise 22 of ATLANTIS II.

Suppose that we consider a simple idealized vortex
such as the one shown earlier in Figure III-13. If we sketch
two isotherms on a cross-section of the vortex we would obtain
two curves similar to those in Figure V-1(b). The rotation
is clockwise so the circulation is out of the page on the
south side of this diagram and into the page on the north
side. In Figure V-1(a), we have sketched the bathythermographs
that would be measured by an observer making lowerings at
stations marked N and S in order to show a possible thermo-
cline oscillation. As this figure shows, the two isotherms
are increasing in depth toward the south, and they are also
increasing in separation. Thus, the local vertical gradient
is inversely proportional to the isotherm depth in this simple
example as described in Eq. V-7. So this simplified form
of Ertel's Theorem may be applicable in oceanographic situations.

In order to see how the idealized situation of Figure
V-1 compares with oceanographic data, we show in Figure V-2
the isothermal contours for the vertical section along Leg 3
of the track chart (Figure I-1). This north-south section
through the Sargasso Sea shows many isotherms and it is not
difficult to see from this cross-section that there is some
tendency for the spacing between the isotherms to increase
as the depth of the isotherm increases. For example, the
product of the depth of the 21°C isotherm by the local tempera-
ture gradient is about $(4 \pm 1)°C$ (somewhat constant).

The isotherm contours shown in Figure V-2 are a vertical
temperature cross section through the large central eddy shown
in the depth of the 20°C isothermal surface, Figure IV-5.
The arrows drawn in Figure IV-5 are the hypothetical directions
of the flow of water consistent with the vortex motion described
in Figure V-1. As pointed out earlier, there was some
evidence that the eddies apparent in Figure IV-5 have an
influence on the sea surface since ATLANTIS II was set in her
course in a clockwise sense during the trip across the main
central eddy and had similar sets while crossing some of the
other smaller eddies.

The characteristics of the circulation pattern shown
by the 20°C isothermal surface have been discussed earlier.
In any event, the pattern observed in Figure IV-5 gives
a strong impression that the flow of the water occurs on
an isothermal surface. But it is particularly important
to appreciate that this circulation pattern, suggested by
the lines of constant depth, is drawn on a surface that
has a tilt with respect to the horizontal. The labels of
depth in meters are the deviation from this inclined surface.
The inclination is 6 meters per degree of latitude getting
deeper toward the south. If one draws the lines of equal
depth for the 20° isothermal surface without removing the
tilt of the surface then the large-scale pattern of the
apparent flow does not give the appearance that the flow
is in that surface particularly in the case of the large
central eddy. Figure IV-5 gives the general impression that
the circulation occurs in this isothermal surface which is
tilted, and this is the kind of evidence that suggests that
the circulation in the Sargasso Sea, away from boundaries,
is approximately isentropic flow and that a circulation
theorem such as Ertel's theorem appears to have important
application. The individual lines of equal depth on the
isothermal surface appear to be lines of equal absolute
vorticity, with different values applying to lines of
different depth. Of course the real proof of this will
come from another study of this ocean area in which the
surfaces of constant temperature can be measured along with
accurate measurements of the current distribution over the
entire field of study. Then one would be able to make a
numerical comparison between the curves of constant potential
vorticity and the observed flow pattern.

Even though the particle path is quite complicated,
the Ertel Theorem may still apply approximately. It is quite
possible as mentioned earlier to have rather complicated inter-
woven laminar flows, i.e., non-turbulent flows; in which the
fluid particle remains in a constant temperature layer; but
which would give rise to temperature inversions. This can
come about if a horizontal shear flow occurs in an isothermal
layer, possibly as depicted in Figure V-3, which shows a portion
of the isothermal layer developing into the shape of a three-
dimensional curl. It should be clear that the lowering of a

temperature measuring device through the water could yield
a temperature inversion for the particular location, however,
the mixing process is not necessarily turbulent but could be
going on very slowly at molecular diffusion rates.

Finally we should consider the notion of the steadiness
of this isothermal pattern (Figure IV-5). Under certain
linearizations of Ertel's Theorem applied to a horizontal
flow in which there is a strong vertical temperature gradient,
Howard (1968) showed that an approximation to the absolute
potential vorticity remains steady. This does not mean that
the temperature surface remains steady or that the vorticity
remains steady, but rather that a relationship between the
vorticity and the temperature surface remains steady. In
this case, one does not need to stay with a fluid particle,
but the approximate expression for the absolute potential
vorticity is constant over the entire field. However, there
is some question as to whether a linearization of the problem
is always permissible since we are all aware that there are
regions in the thermocline where the vertical temperature
gradient is relatively small and these are regions where
finite-amplitude variations could take place and steadiness
become less likely. Nevertheless, there is some evidence
indicating that the isothermal pattern observed in this figure
does tend to remain somewhat steady, at least relatively steady,
because there is some correlation of these eddies with the
shape of the ocean bottom. The coupling with the bottom, which
is 5 km deep, is weak allowing for lateral movements of rela-
tively steady streamlines.

LIST OF FIGURES

SECTION V   -   A General Circulation Theorem
Figure
V-1   Idealized Illustration of North-South Thermocline
             Variation in a Clockwise Eddy.

V-2   Vertical North-South Isotherm Section for Leg 3.

V-3   Illustration of Hypothetical Interwoven Laminar Flow
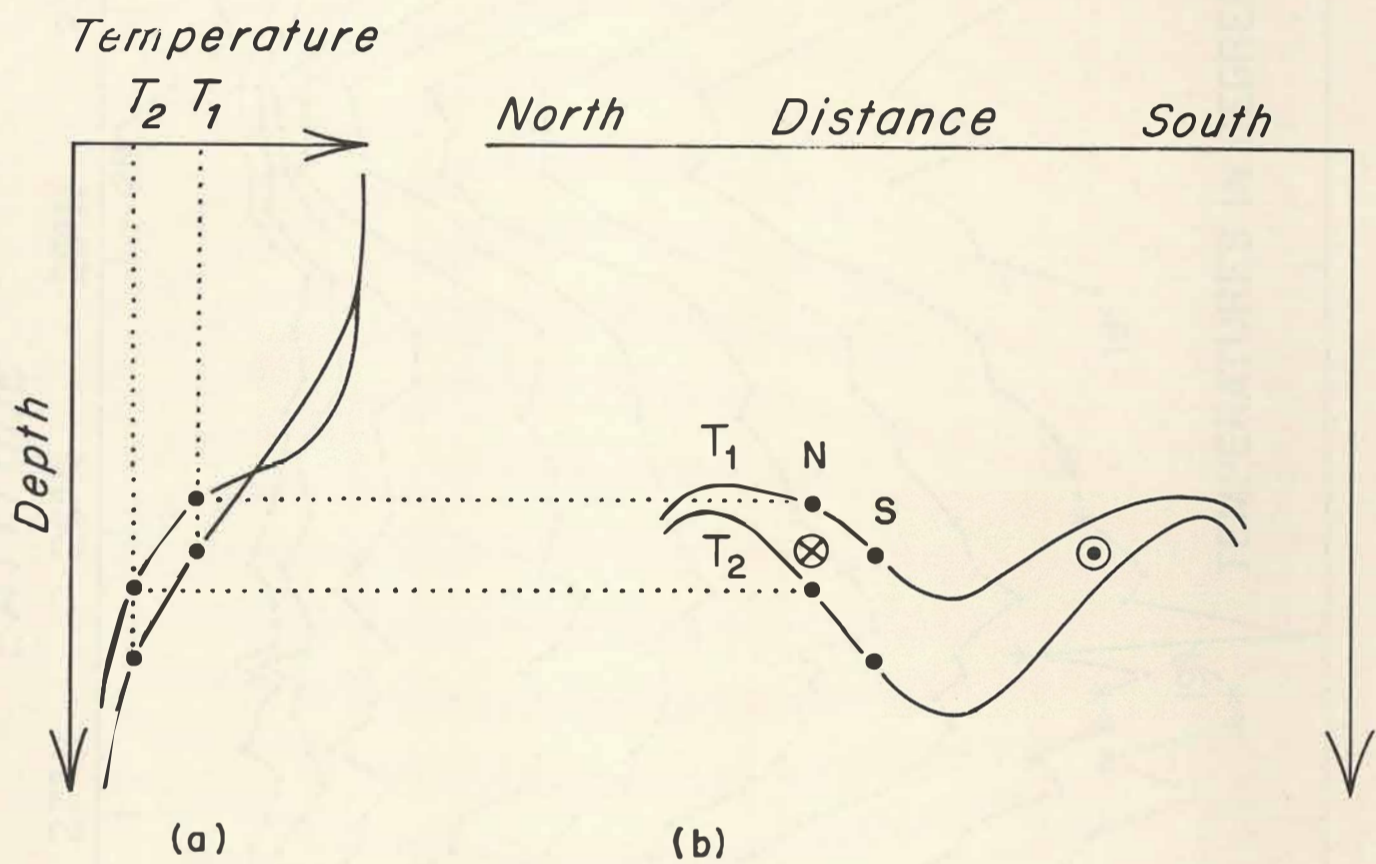   and Temperature Inversion.

Fig. V-1   Idealized Illustration of North-South Thermocline
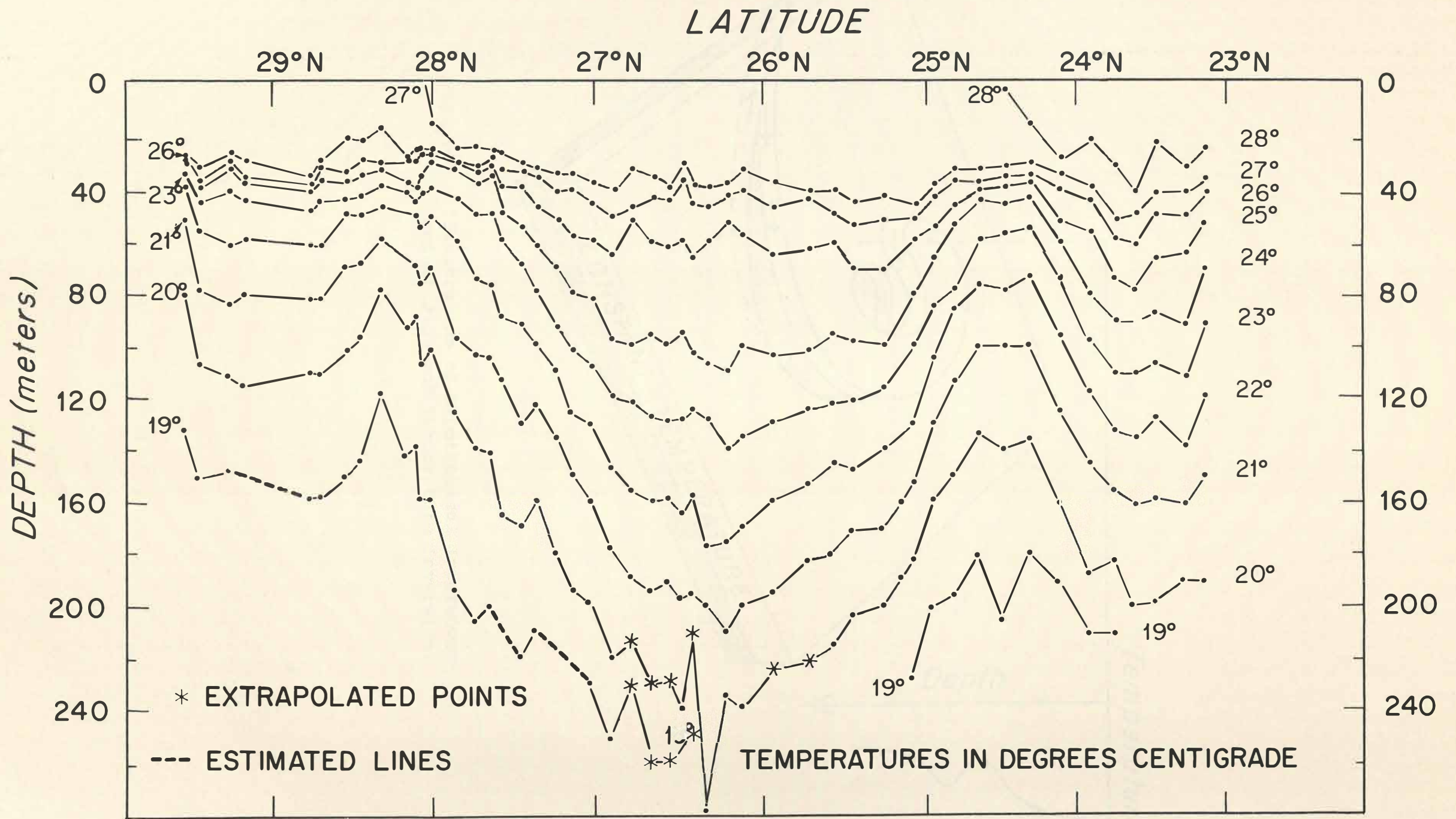   Variation in a Clockwise Eddy.

Fig. V-2   Vertical North-South Isotherm Section for Leg 3.
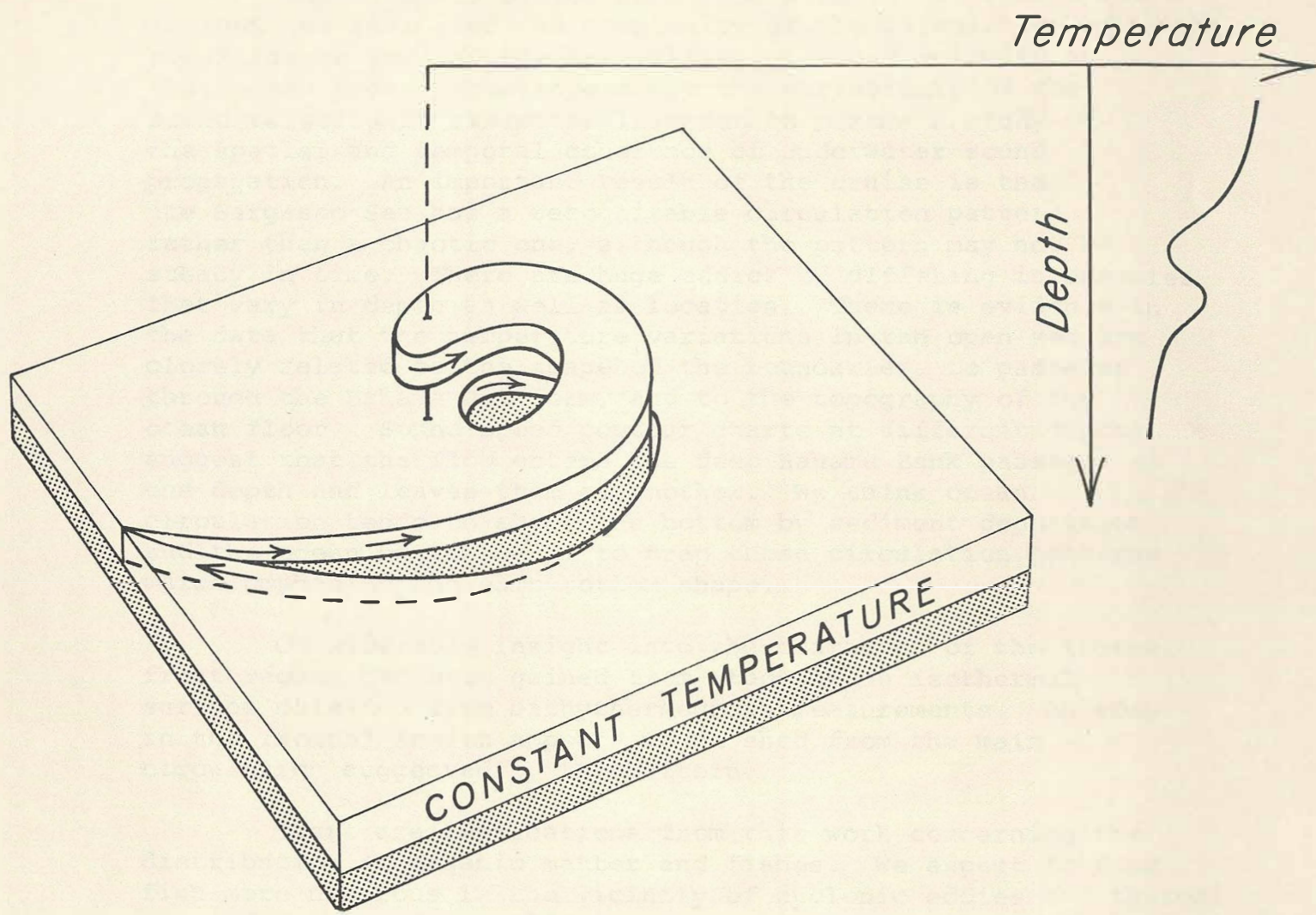
Fig. V-3   Illustration of Hypothetical Interwoven
            Laminar Flow and Temperature Inversion.

SECTION VI

SUMMARY AND RECOMMENDATIONS

The analysis of the data from ATLANTIS II Cruise #22
in 1966 has indicated the complexity of the circulation of
the Sargasso Sea and the variability of sound velocity in
that ocean area. Knowledge about the variability of the
sound velocity is essential in order to pursue a study of
the spatial and temporal coherence of underwater sound
propagation. An important result of the cruise is that
the Sargasso Sea has a recognizable circulation pattern
rather than a chaotic one, although the pattern may not be
steady in time. There are huge eddies of differing intensities
that vary in depth as well as location. There is evidence in
the data that the temperature variations in the open sea are
closely related to the shape of the boundaries, to passages
through the Bahama Platform, and to the topography of the
ocean floor. Sound speed contour charts at different depths
suggest that the flow enters the deep Bahama Bank passages at
one depth and leaves them at another. We think ocean
circulation tends to shape the bottom by sediment deposition
and the ocean bottom tends to trap those circulation patterns
which emphasize the same bottom shape.

Considerable insight into the character of the thermal
front region has been gained from studying an isothermal
surface obtained from bathythermograph measurements. An eddy
in the frontal region appears to be shed from the main
circulation suggested by the pattern.

There are implications from this work concerning the
distribution of organic matter and fishes. We expect to find
fish more numerous in the vicinity of cyclonic eddies and thermal
fronts (Backus et al., 1969) because of the upwelling of nutrients.
Consequently, we would want to learn how and where such eddies
move.

The analysis of the data led to application of an
assumption that the flow in the Sargasso Sea was isentropic,
namely, that we could neglect the vertical transfer of heat
from one layer to another for much of the discussion.
Accordingly, the flow was taken to be laminar along surfaces
of constant temperature. The vertical deformation of these
surfaces with horizontal co-ordinates and time could then be
related to the vorticity and hence to the circulation. In
this we made use of Ertel's circulation theorem. We think
this generalized theorem of Ertel's will have broad application
to ocean circulation and will have an influence on oceano-
graphy similar to that of the Rossby potential-vorticity
equation.

Although we have learned more about the Sargasso
Sea, many questions and hypotheses needing further research
have been generated. There are serious problems in oceanic
measurement. A typical question that confronts the scientist
on a cruise such as ATLANTIS II Cruise #22 is, should he take
extra time at each location where an anomalous SVP or similar
observation occurs in order to make a repeated measurement?
Another is, how should one determine the spacing of the profile
stations and their distribution in space and time, taking
into account the fact that the sampling must be interrupted
so that the ship can make port? Despite the large size of
the area covered by ATLANTIS II Cruise #22, it is still very
small compared to the Atlantic Ocean. It is only after wrestling
with the measurements of several cruises like ATLANTIS II
Cruise #22 that one appreciates the severe problems of sampling
a huge three-dimensional medium which is changing in time like
the ocean. If one stays entirely with standard methods,
then a multiship operation is necessary, augmented by a
distribution of deep-moored, instrumented buoys. A multiship
operation seems formidable, and the difficulties involved in
maintenance of many buoy installations are also formidable.
Moreover, both have their problems in analysis and interpretation
of the observations, since buoys allow observations only at
discrete points in a very large ocean and ships take a long
time to cover a reasonable area making synoptic measurements

difficult. Instrumented buoy installations might be widely
spaced in the ocean because ships were providing the spatial
and (to some extent) temporal information between them, but
first spatial information about ocean movements is needed
to permit adequate correlation and interpretation of the
long time series from pairs of widely spaced buoys. Indeed corre-
lations of measurements from deep-ocean moorings as a function
of spacing are in an early stage of research. The optimum
deployment of buoys and ship tracks for effective surveillance
of ocean movements would naturally depend on the ocean region
and its fluctuation characteristics. Such a long-range study
effort, both experimental and theoretical, needs to be
supported.

However, another approach to the problem also needs
support and this approach might best be labelled "Acoustical
Oceanography". The use of acoustic signals is a more natural
way to maintain surveillance on internal ocean movements in
real time. We use light to watch the movement of internal
waves in the sky as the nearly regular formations of clouds
pass by; it should be possible to monitor similar movements
within the ocean with acoustical signals. Mathematical models
indicate that monitoring the many sound-channel arrivals from
a fixed impulsive and repetitive acoustic signal would provide
information about the average vertical thermal gradient in the
main thermocline over a few hundred miles. Such information
obtained over different sectors simultaneously and continuously
should provide information about ocean circulation. A system
of this kind could monitor internal movements of large areas
of the ocean, particularly if joined with the more usual
oceanographic instruments and ship surveys.

ACKNOWLEDGEMENTS

Scientific Party ATLANTIS II - Cruise 22

John C. Beckerle (C)
Stanley V. Bergstrom
Paul R. Boutin
John H. Bradshaw (S)
Hugh Michael Byrne (S)
Victor E. Delnore (S)
Willard Dow
Diana Drucas*
Carlton W. Grant, Jr.
Frederic M. Herman (S)
Gordon B. Jacobs (S)
William F. Kean, Jr. (S)
Bruce A. Magnell (S)
Joseph L. McCallion (S)
Coert D. Olmsted (S)

Richard E. Payne (S) (C)
Thomas E. Pease (S)
Alan R. Rice (S)
Robert D. Sanders*
Robert J. Schlitz
Leonard F. Shodin
Robert J. Stanley
Stephen Stillman
Robert Tasko
James Teixeira*
Colin E. Walden
Kenneth Westlund*
Jackson E. Wood (S)
Jaques R. V. Zaneveld (S)

(S) Student Scientist   (C) Chief Scientist
 * ARL of Sylvania Electronics Products, who assisted in computer analysis aboard ship.

REFERENCES

Page Location

Backus, R.H., J.E. Craddock, R. L. Haedrich, and
    D.L. Shores, 1969. Mesopelagic Fishes and
    Thermal Fronts in the Western Sargasso Sea.   22
    Mar. Biol., Vol. 3, No. 2, pp. 87-106.   67

Barkley, R.A., 1968. The Kuroshio-Oyashio Front
    as a Compound Vortex Street. J. Mar. Res.,
    Vol. 26, No. 2, pp. 83-104.   35

Beckerle, J.C., 1965. "Sound Velocity Measurement
    South of Bermuda", in Summary of Investigations   22
    Conducted in 1964. W.H.O.I. Ref. No. 65-13,   24
    pp. 109-113.   27

Beckerle, J.C., 1966a. Detection of Internal Waves
    from Doppler-Shift Observations (Abstract).
    Trans. Amer. Geophys. Un., Vol. 47, No. 1,
    p. 110. (see also W.H.O.I. Ref. No. 68-19).   22

Beckerle, J.C., 1966b. Acoustical and Environmental
    Fluctuations. Proc. of the Symposium; Third
    U.S. Navy Symp. on Military Oceanography,   33
    Vol. I, pp. 331-339.   34

Beckerle, J.C., 1968a. The Dynamics of the Sargasso
    Sea as Revealed by Temperature and Sound
    Velocity Measurements. Proc. of the Symposium;
    Fifth U.S. Navy Symp. on Military Oceanography,
    Vol. I, pp. 364-382.   34

Beckerle, J.C., 1968b. A Report on ATLANTIS II
    Cruise 22. Part II - Sound Velocity Profiles.
    W.H.O.I. Ref. No. 68-67.   3

Beckerle, J.C., and S.W. Bergstrom, 1967. "Analysis
    of CHAIN 47 Sound Velocity Data", in Oceanogra-
    phic and Underwater Acoustics Research Conducted
    during the period 1 May 1966 - 31 October 1966.
    W.H.O.I. Ref. No. 67-3, pp. 22-24.   43

- 72 -

Page Location

Beckerle, J.C., J. S. Reitzel, R.E. Payne, and
J.B. Hersey, 1966. Variations in Sound
Velocity Profiles in the Ocean between
Bermuda and the Antilles (Abstract). Trans.
Amer. Geophys. Un., Vol. 47, No. 1, pp. 109-   33
110. (see also W.H.O.I. Ref. No. 68-19)   41

Byers, H.R., 1944. General Meteorology, McGraw-
Hill, New York, p. 432.   13

Carnvale, A., P. Bowen, M. Basileo, and J. Sprenke,
1968. Absolute Sound-Velocity Measurement
in Distilled Water. J. Acoust. Soc. Amer.,
Vol. 44, No. 4, pp. 1098-1102.   20

Defant, A., 1961. Physical Oceanography, Vols. I   33
and II, Pergamon Press, London.   36

Dow, W., and S.J. Stillman, 1961. Inverted Echo
Sounder. Mar. Sci. Inst., Vol. 1, pp. 263-271.
(see also W.H.O.I. Ref. No. 63-6).   20

Eckart, C., 1961. Internal Waves in the Ocean.   29
Physics of Fluids, Vol. 4, No. 7, pp. 791-799.   30

Eittreim, S.L., M. Ewing, and E.M. Thorndike, 1969.
Suspended Matter along the Continental Margin
of the North American Basin. Deep-Sea Res.,
Vol. 16, pp. 613-624.   45

Ertel, H., 1942. Ein neuer hydrodynamischer
wirbelsatz. Meteorol. Ztschr., Vol. 59,
No. 9, pp. 277-281.   58

Fomin, L.M., 1964. The Dynamic Method in Oceano-
graphy, trans. by Scripta Technica, T. Winter-
feld, ed., Elsevier, New York.   19

Fuglister, F.C., 1960. Atlantic Ocean Atlas of
Temperature and Salinity Profiles and Data from
the International Geophysical Year of 1957-1958,
Woods Hole Oceanographic Inst., Woods Hole, p.33
and Fig. 51.   44

Page Location

Godske, C.L., T. Bergeron, J. Bjerknes, and
    R.C. Bundgaard, 1957. Dynamic Meteoro-
    logy and Weather Forecasting, American
    Meteorological Soc. and Carnegie Inst.,   7
    Washington, Chap. 11.   55

Greenspan, M., and C.E. Tschiegg, 1957. Sing-
    around Ultrasonic Velocimeter for Liquids.
    Rev. Scient. Inst., Vol. 28, No. 11,
    pp. 897-902.   20

Haurwitz, B., 1935. The Height of Tropical Cyclones
    and of the "Eye" of the Storm. Mon. Weather
    Rev., Vol. 63, No. 2, pp. 45-49.   7

Howard, L.N., 1968. "Rotating and Continuously
    Stratified Fluids - Inviscid Flows" in
    Geophysical Fluid Dynamics, 1968, Vol. I,
    W.H.O.I. Ref. No. 68-72, pp. 80-97.   66

Hubbard, C.J., and W.S. Richardson, 1959. The
    Contouring Temperature Recorder. W.H.O.I.
    Ref. No. 59-16.   27

Hubert, P.J., 1967. The Hurricane Season of 1966.   6
    Weatherwise, Vol. 20, No. 1, pp. 16-23.   16

Katz, E.J., 1969. Further Study of a Front in the
    Sargasso Sea. Tellus, Vol. 21, No. 2,   34
    pp. 259-269.   54

Kochin, N.E., I.A. Kibel, and N.V. Roze, 1964.
    Theoretical Hydromechanics, trans. by
    D. Boyanovich, J.R.M. Radok, ed., Interscience,
    New York.   61

Kuo, H.-L., 1949. Dynamic Instability of Two-Dimen-
    sional Nondivergent Flow in a Barotropic
    Atmosphere. J. Meteor., Vol. 6, No. 2,
    pp. 105-122.   15

Page Location

LaFond, E.C., and K.G. LaFond, 1966. Vertical and
    Horizontal Thermal Structures in the Sea. U.S.
    Navy Electronics Lab., R. and D. Report 1395.   27

Lamb, H., 1932. Hydrodynamics, Dover Press, New
    York.   39

LaSeur, N.E., 1962. On the Role of Convection in
    Hurricanes. Proc. Second Technical Conf. on
    Hurricanes, Nat'l Hurricane Res. Proj. Report,
    No. 50, Part II, pp. 323-334.   8

Leipper, D.F., 1967. Observed Ocean Conditions and
    Hurricane Hilda, 1964. J. Atmos. Sci., Vol. 24,
    No. 2, pp. 182-196.   9

Longuet-Higgins, M.S., 1965. The Response of a
    Stratified Ocean to Stationary or Moving Wind-
    Systems. Deep-Sea Res., Vol. 12, pp. 923-973.   11

Lynn, R.J., and J.L. Reid, 1968. Characteristics and
    Circulation of Deep and Abyssal Waters. Deep-
    Sea Res., Vol. 15, No. 5, pp. 577-598.   59

Malkus, J.S., and H. Riehl, 1960. On the Dynamics
    and Energy Transformations in Steady-State
    Hurricanes. Tellus, Vol. 12, No. 1, pp. 1-20.   13

McSkimin, H.J., 1965. Velocity of Sound in Distilled
    Water for the Temperature Range 20°-75°C.
    J. Acoust. Soc. Amer., Vol. 37, No. 2,
    pp. 325-328.   20

Montgomery, R.B., 1938. Circulation in Upper Layers
    of Southern North Atlantic Deduced with use of
    Isentropic Analysis. Papers Phys. Oceano.
    Meteor., Vol. 6, No. 2, pp. 4-48.   59

Neumann, G., and W.J. Pierson, Jr., 1966. Principles
    of Physical Oceanography, Prentice-Hall, Engle-
    wood Cliffs, N.J., p. 169.   36

Page Location

O'Brien, J.J., and R.O. Reid, 1967. The Non-Linear
    Response of a Two-Layer Baroclinic Ocean to a
    Stationary, Axially-Symmetric Hurricane.   7
    Part I: Upwelling Induced by Momentum Transfer. 9
    J. Atmos. Sci., Vol. 24, No. 2, pp. 197-207.   10

Parr, A.E., 1936. On the Probable Relationship
    between Vertical Stability and Lateral Mixing
    Processes. J. du Conseil, Vol. 11, No. 4,
    pp. 308-313.   58

Payne, R.E., and J.C. Beckerle, 1966. Sound Velocity
    Structure of the Ocean between Bermuda and the
    Antilles. W.H.O.I. Ref. No. 66-52.   47

Petersen, D.P., and D. Middleton, 1962. Sampling and
    Reconstruction of Wave-Number-Limited Functions
    in N-Dimensional Euclidean Spaces. Information
    and Control, Vol. 5, No. 4, pp. 279-323.   19

Phillips, N.A., 1963. Geostrophic Motion. Rev.
    Geophys., Vol. 1, No. 2, p.123-176.   58

Phillips, O.M., 1966. The Dynamics of the Upper   16
    Ocean, Cambridge University Press, Cambridge.   30

Platzman, G.W., 1968. The Rossby Wave. Quart. J.
    Roy. Meteor. Soc., Vol. 94, No. 401, pp.225-248. 39

Prandtl, L., and D. Tietjens, 1931. Hydro-und Aero-
    mechanic, Vol. 2, Springer, Berlin, Plate 7,
    Figs. 10-16. (See also Modern Developments in
    Fluid Dynamics, S. Goldstein, ed., Clarendon
    Press, Oxford, 1938, Vol. 1, Plates 15-17).   54

Pratt, R.M., 1968. Atlantic Continental Shelf and
    Slope of the United States: Adjacent Deep-sea
    Physiography and Sediments. U.S.G.S. Prof. Paper
    529-B, Plate I.   40

Press, M., J. Teixeira, K. Westlund, and J. Storer,
    1966. A Real-Time Processing System for
    Oceanographic Velocity Profiles. Res. Report
    No. 578, Sylvania Electronic Products.   55

Page Location

Rhines, P.B., 1968. Quasigeostrophic waves in an
      Ocean of Varying Depth. Doctoral Thesis,
      Dept. of App. Math. and Theor. Phys.,
      Cambridge University.   39

Rhines, P.B., 1969a. Slow Oscillations in an Ocean
      of Varying Depth. Part 1: Abrupt Topography.
      J. Fluid Mech., Vol. 37, Part I, pp. 161-189.   59

Rhines, P.B., 1969b. Slow Oscillations in an Ocean
      of Varying Depth. Part 2: Islands and Sea-
      mounts. J. Fluid. Mech., Vol. 37, Part I,
      pp. 191-205.   59

Riehl, H., 1963. Some Relations between Wind and
      Thermal Structures of Steady-State Hurricanes.   8
      Nat'l Hurricane Res. Proj. Report No. 63.   13

Rossby, C.-G.A., 1939. Relation between Variations
      in the Intensity of Zonal Circulation of the
      Atmosphere and the Displacements of the Semi-
      Permanent Centers of Action. J. Mar. Res.,   39
      Vol. 2, No. 1, pp. 38-55.   59

Schroeder, E., and H. Stommel, 1969. How Represen-
      tative is the Series of PANULIRUS Stations of
      Monthly Mean Conditions off Bermuda? Progress
      in Oceanography, Vol. 5, Mary Sears, ed.,
      Pergamon Press, Oxford, pp. 31-40.   22

Snyder, R.M., 1961. A Progress Report on Environ-
      mental Studies in the Mediterranean Sea:
      Thermal Structure of the Surface Waters of the
      Mediterranean Sea. J. Underwater Acoust.,
      Vol. 11, No. 4, pp. 763-769.   27

Tabata, S., 1967. Circulation of the Northeast Pacific
      Ocean as Deduced from Isentropic Analysis.
      Speech Delivered at Int'l Oceanography Conf.   59

Page Location

Thompson, B., 1965. Automated Thermal-Structure
        Forecasting Techniques. Informal Manuscript
        Report No. 0-45-65, Mar. Sci. Dept., U.S.
        Naval Oceanographic Office.   41

Voorhis, A.D., 1965. "Thermal Fronts", in Summary
        of Investigations Conducted in 1964. W.H.O.I.
        Ref. No. 65-13, p. 172.   34

Voorhis, A.D., 1969. The Horizontal Extent and
        Persistence of Thermal Fronts in the Sargasso
        Sea. Deep-Sea Res., Vol. 16, Supplement,
        pp. 331-339.   54

Voorhis, A.D., and J.B. Hersey, 1964. Oceanic
        Thermal Fronts in the Sargasso Sea. J.   22
        Geophys. Res., Vol. 69, No. 18, pp. 3809-3814. 54

Warren, B., 1963. Topographic Influences on the Path
        of the Gulf Stream. Tellus, Vol. 15, No. 2,   39
        pp. 167-183.   57

Welander, P., 1955. Studies on the General Develop-
        ment of Motion in a Two-Dimensional, Ideal
        Fluid. Tellus, Vol. 7, No. 2, pp. 141-156.   59

Welander, P., 1968. Effects of Planetary Topography
        on the Deep-Sea Circulation, with an Appli-
        cation to the North Atlantic. Office of Naval 39
        Res. Tech. Report No. 25, WB-ESSA Tech. Report 40
        No. 28.   57

Wilson, J.A., Jr., and J. C. Beckerle, 1965. "Sound
        Velocity Contours Northeast of the Bahamas", in
        Summary of Investigations Conducted in 1964.
        W.H.O.I. Ref. No. 65-13, p. 109.   38

Wüst, G., 1963. On the Stratification and the
        Circulation in the Cold-Water Sphere of the
        Antillean-Caribbean Basins. Deep-Sea Res.,
        Vol. 10, pp. 165-187.   44

0205
DISTIRUBTION LIST

Office of Naval Research
Department of the Navy
Attn: Code 480   1
              466   1
              468   1
              414   1
              102-OS   1
Arlington, Virginia   22217

Chief of Naval Operations
Department of the Navy
Attn: OP 07   1
              71   1
              95   1
Washington, D. C.   20350

Director
Office of Naval Research   1
Branch Office
495 Summer Street
Boston, Massachusetts   02210

Director
Office of Naval Research   1
Branch Office
New York Area Office
207 West 24th Street
New York, New York   10011

Director, Naval Research Laboratory
Attn: Library, Code 2029 (ONRL)   6
          Technical Information Division 6
Washington, D. C.   20390

Commander
Naval Ship Systems Command
Department of the Navy
Attn: SHIPS 03   1
              00V1   1
              205   1
Washington, D. C.   20360

Commander
Naval Air Systems Command
Department of the Navy
Attn: AIR 370C   1
Washington, D. C.   20360

Chief of Naval Material
Department of the Navy
Attn: DCNM (Development)   1
Washington, D. C.   20360

Assistant Secretary of the Navy   1
   for Research and Development
Department of the Navy
Washington, D. C.   20350

Commander
U. S. Naval Oceanographic Office
Washington, D. C.   20390
Attn: Code 037-B   1
          Code 1640   1

Naval Research Laboratory   1
Underwater Sound Reference Div.
P. O. Box 8337
Orlando, Florida   32806

Commander
Navy Electronics Laboratory Center
Attn: Code 3060C   1
          Code 3102   1
San Diego, California   92152

Commander
Naval Ordnance Laboratory   1
White Oak
Silver Spring, Maryland   20910

Commanding Officer
Naval Underwater Systems Center   1
Newport, Rhode Island   02844

Commanding Officer   1
Naval Civil Engineering Laboratory
Port Hueneme, California   93401

Commander
Navy Air Development Center   1
Attn: NADC Library
Warminster, Pennsylvania   18974

Environmental Science Department   1
U.S. Naval Academy
Annapolis, Maryland   21402

Commanding Officer   1
Naval Ship Research and
  Development Laboratory
Annapolis, Maryland   21402

Commanding Officer and Director   1
Naval Underwater Systems Center
New London Laboratory
New London, Connecticut   06321

Commanding Officer   1
Naval Ship Research and
  Development Laboratory
Panama City, Florida   32401

Office Chief of Research and
  Development   1
Department of the Army
Washington, D.C.   20310

U.S. Army Beach Erosion Board   1
5201 Little Falls Rd., N.W.
Washington, D.C.   20016

Defense Documentation Center   20
Cameron Station
Alexandria, Virginia   22314

National Academy of Sciences
National Research Council
2101 Constitution Ave., N.W.
Attn: Committee on Undersea
          Warfare   1
          Committee on Oceanography   1
Washington, D.C.   20418

ESSA
U.S. Department of Commerce
Attn: Institute of Oceanography   1
          Institute of Atmospheric
             Sciences   1
Washington, D.C.   20235

Geological Division
Marine Geology Unit   1
U.S. Geological Survey
Washington, D.C.   20240

U.S. Geological Survey   1
Marine Geology and Hydrology
345 Middlefield Road
Attn: Dr. Rusnak
Menlo Park, California   94025

Director
Oceanography Museum of
  Natural History   1
Smithsonian Institution
Washington, D.C.   20560

Commander   1
Submarine Development Group TWO
U. S. Naval Submarine Base
Groton, Connecticut   06340

Mr. Theodore V. Ryan   1
Director
Pacific Oceanographic Research Laboratory
1801 Fairview Avenue East
Seattle, Washington   98102

Commander   1
Naval Weapons Center
Attn: Technical Library
China Lake, California   93555

Naval Post Graduate School
Attn: Librarian   1
          Dept. of Meteorology and
             Oceanography   2
Monterey, California   93940

Advanced Research Projects Agencies 1
Attn: Nuclear Test Detection Office
Washington, D.C.   20301

Director
Scripps Institution of Oceanography 1
La Jolla, California   92037

Ordnance Research Laboratory   1
Pennsylvania State University
University Park, Penn.   16801

Director
Marine Physical Laboratory   1
Scripps Institution of Oceano-
  graphy
San Diego, California   92152

Director
Marine Laboratory
University of Miami
#1 Rickenbacker Causeway
Miami, Florida   33149   1

Director
Department of Oceanography
  and Meteorology   1
Texas A & M University
College Station, Texas   77843

Head, Department of Oceanography   1
Oregon State University
Corvallis, Oregon   97331

Director
Arctic Research Laboratory   1
Point Barrow, Alaska   99723

Head, Department of Oceanography
University of Washington   1
Seattle, Washington   98105

Geophysical Institute of the
    University of Alaska   1
College, Alaska   99735

Applied Physics Laboratory
University of Washington   1
1013 NE Fortieth Street
Seattle, Washington   98105

Department of Geodesy and
    Geophysics   1
Cambridge University
Cambridge, England

Director
Institute of Geophysics   1
University of Hawaii
Honolulu, Hawaii   96825

Director
Applied Research Laboratories   1
University of Texas
Austin, Texas   78712

Bell Telephone Laboratories, Inc.
Attn: Dr. John Mayo, Div. 54
Whippany, New Jersey   07981   1

U.S. Naval Schools, Mine Warfare
U.S. Naval Base   1
Charleston, South Carolina   29408

Hawaii Technological Information Center
P.O. Box 2359
Honolulu, Hawaii   96813   1

National Institute of Oceanography
Wormley, Godalming
Surrey, England
Attn: Librarian   1

Lamont-Doherty Geological Observatory 1
Palisades, New York   10964

Woods Hole Oceanographic Institution
Reference No. 68-66

A REPORT ON ATLANTIS II CRUISE 22 JUNE, JULY, AND AUGUST 1966, PART I: The Dynamics of Ocean Movements in the Sargasso Sea Revealed by Sound Velocity and Temperature Measurements by John Beckerle. October 1970. 83 pages, plus 65 figures, 64 references. Contract Nonr - 4029(00); NR 260-101 and Nonr-2866(00); NR 287-004.

On Cruise #22 of R/V ATLANTIS II from June 10 to August 4, 1966, 115 sound velocity profiles WHOI SVP #371 - SVP #485, were measured with a sound velocity profiling system that incorporated an on-line PDP-5 computer. The cruise covered approximately 356,000 square miles of water between Bermuda and the Antilles. The main purpose of the cruise was to look for long-period internal Rossby waves expected from earlier cruises, ATLANTIS II #11 and CHAIN #47, and to improve our techniques in gathering oceanographic data. Part I of this report presents the observations of ATLANTIS II Cruise #22 with possible interpretations. On the way to the Sargasso Sea ATLANTIS II traversed the eye of hurricane ALMA and we obtained new information on the air-sea interaction. In the Sargasso Sea the temperature data and the sound veloctiy data suggest that the circulation is complicated with eddies of large size. Part II is separately bound and consists of figures of the sound velocity profiles with comments concerning their relia-bility where necessary.

1. Sargasso Sea
2. Circulation
3. Rossby Waves

I. Beckerle, John
II. Nonr-4029(00); NR 260-101
III. Nonr 2866(00); NR 287-004

This card is Unclassified

DOCUMENT CONTROL DATA - R&D

(Security classification of title, body of abstract and indexing annotation must be entered when the overall report is classified)

1. ORIGINATING ACTIVITY *(Corporate author)*	2a. REPORT SECURITY CLASSIFICATION
Woods Hole Oceanographic Institution Woods Hole, Massachusetts 02543	Unclassified
	2b. GROUP

3. REPORT TITLE

A REPORT ON ATLANTIS II CRUISE 22 JUNE, JULY, AUGUST 1966, PART I: The Dynamics of Ocean Movements in the Sargasso Sea Revealed by Sound Velocity and Temperature Measurements.

4. DESCRIPTIVE NOTES *(Type of report and inclusive dates)*

Technical Report

5. AUTHOR(S) *(Last name, first name, initial)*

Beckerle, John.

6. REPORT DATE	7a. TOTAL NO. OF PAGES	7b. NO. OF REFS
October 1970	83 pages, & 65 fig.	64

8a. CONTRACT OR GRANT NO.	9a. ORIGINATOR'S REPORT NUMBER(S)
Nonr 4029(00); NR 260-101 b. PROJECT NO. Nonr 2866(00); NR 287-004.	WHOI REF. NO. 68-66
c.	9b. OTHER REPORT NO(S) *(Any other numbers that may be assigned this report)*
d.	

10. AVAILABILITY/LIMITATION NOTICES

This document has been approved for public release and sale; its distribution is unlimited.

11. SUPPLEMENTARY NOTES	12. SPONSORING MILITARY ACTIVITY
	Office of Naval Research Ocean Science & Technology Division Arlington, Virginia 22217

13. ABSTRACT

On Cruise #22 of R/V ATLANTIS II from June 10 to August 4, 1966 115 sound velocity profiles WHOI SVP #371- SVP #485, were measured with a sound velocity profiling system that incorporated an on-line PDP-5 computer. The cruise covered approximately 356,000 square miles of water between Bermuda and the Antilles. The main purpose of the cruise was to look for long-period internal Rossby waves expected from earlier cruises, ATLANTIS II #11 and CHAIN #47, and to improve our techniques in gathering oceanographic data. Part I of this report presents the observations of ATLANTIS II Cruise #22 with possible interpretations. On the way to the Sargasso Sea ATLANTIS II traversed the eye of hurricane ALMA and we obtained new information on the air-sea interaction. In the Sargasso Sea the temperature data and the sound velocity data suggest that the circulation is complicated with eddies of large size. Part II is separately bound and consists of figures of the sound profiles with comments concerning their reliability where necessary.

DD FORM 1473
1 JAN 64

14.		LINK A		LINK B		LINK C	
KEY WORDS		ROLE	WT	ROLE	WT	ROLE	WT
1. Sargasso Sea							
2. Circulation							
3. Rossby Waves							

INSTRUCTIONS

1. **ORIGINATING ACTIVITY:** Enter the name and address of the contractor, subcontractor, grantee, Department of Defense activity or other organization *(corporate author)* issuing the report.

2a. **REPORT SECURITY CLASSIFICATION:** Enter the overall security classification of the report. Indicate whether "Restricted Data" is included. Marking is to be in accordance with appropriate security regulations.

2b. **GROUP:** Automatic downgrading is specified in DoD Directive 5200.10 and Armed Forces Industrial Manual. Enter the group number. Also, when applicable, show that optional markings have been used for Group 3 and Group 4 as authorized.

3. **REPORT TITLE:** Enter the complete report title in all capital letters. Titles in all cases should be unclassified. If a meaningful title cannot be selected without classification, show title classification in all capitals in parenthesis immediately following the title.

4. **DESCRIPTIVE NOTES:** If appropriate, enter the type of report, e.g., interim, progress, summary, annual, or final. Give the inclusive dates when a specific reporting period is covered.

5. **AUTHOR(S):** Enter the name(s) of author(s) as shown on or in the report. Enter last name, first name, middle initial. If military, show rank and branch of service. The name of the principal author is an absolute minimum requirement.

6. **REPORT DATE:** Enter the date of the report as day, month, year; or month, year. If more than one date appears on the report, use date of publication.

7a. **TOTAL NUMBER OF PAGES:** The total page count should follow normal pagination procedures, i.e., enter the number of pages containing information.

7b. **NUMBER OF REFERENCES:** Enter the total number of references cited in the report.

8a. **CONTRACT OR GRANT NUMBER:** If appropriate, enter the applicable number of the contract or grant under which the report was written.

8b, 8c, & 8d. **PROJECT NUMBER:** Enter the appropriate military department identification, such as project number, subproject number, system numbers, task number, etc.

9a. **ORIGINATOR'S REPORT NUMBER(S):** Enter the official report number by which the document will be identified and controlled by the originating activity. This number must be unique to this report.

9b. **OTHER REPORT NUMBER(S):** If the report has been assigned any other report numbers *(either by the originator or by the sponsor)*, also enter this number(s).

10. **AVAILABILITY/LIMITATION NOTICES:** Enter any limitations on further dissemination of the report, other than those imposed by security classification, using standard statements such as:

(1) "Qualified requesters may obtain copies of this report from DDC."

(2) "Foreign announcement and dissemination of this report by DDC is not authorized."

(3) "U. S. Government agencies may obtain copies of this report directly from DDC. Other qualified DDC users shall request through

_____."

(4) "U. S. military agencies may obtain copies of this report directly from DDC. Other qualified users shall request through

_____."

(5) "All distribution of this report is controlled. Qualified DDC users shall request through

_____."

If the report has been furnished to the Office of Technical Services, Department of Commerce, for sale to the public, indicate this fact and enter the price, if known.

11. **SUPPLEMENTARY NOTES:** Use for additional explanatory notes.

12. **SPONSORING MILITARY ACTIVITY:** Enter the name of the departmental project office or laboratory sponsoring *(paying for)* the research and development. Include address.

13. **ABSTRACT:** Enter an abstract giving a brief and factual summary of the document indicative of the report, even though it may also appear elsewhere in the body of the technical report. If additional space is required, a continuation sheet shall be attached.

It is highly desirable that the abstract of classified reports be unclassified. Each paragraph of the abstract shall end with an indication of the military security classification of the information in the paragraph, represented as *(TS)*, *(S)*, *(C)*, or *(U)*.

There is no limitation on the length of the abstract. However, the suggested length is from 150 to 225 words.

14. **KEY WORDS:** Key words are technically meaningful terms or short phrases that characterize a report and may be used as index entries for cataloging the report. Key words must be selected so that no security classification is required. Identifiers, such as equipment model designation, trade name, military project code name, geographic location, may be used as key words but will be followed by an indication of technical context. The assignment of links, roles, and weights is optional.